Vol. 103 No. 1 March 15, 1978
(Computer Techniques and Optimization, Vol. 2 No. 1)
ISSN 0378-4304

ANALYTICA CHIMICA ACTA

International journal devoted to all branches of analytical chemistry

COMPUTER TECHNIQUES AND OPTIMIZATION

EDITOR
J. T. CLERC (Zürich, Switzerland)

Associate Editor
E. ZIEGLER (Mülheim, Germany)

Editorial Advisers
R. E. Dessy, Blacksburg, Va.
J. W. Frazer, Livermore, Calif.
H. Günzler, Ludwigshafen
S. R. Heller, Washington, D.C.
J. F. K. Huber, Vienna
P. C. Jurs, University Park, Pa.
M. Knedel, Munich
D. L. Massart, Sint Genesius-Rhode
H. C. Smit, Amsterdam

ELSEVIER SCIENTIFIC PUBLISHING COMPANY

ANALYTICA CHIMICA ACTA

International journal devoted to all branches of analytical chemistry
Revue internationale consacrée à tous les domaines de la chimie analytique
Internationale Zeitschrift für alle Gebiete der analytischen Chemie

PUBLICATION SCHEDULE FOR 1978 (incorporating the section on Computer Techniques and Optimization).

	J	F	M	A	M	J	J	A	S	O	N	D
Analytica Chimica Acta	96/1	96/2	97/1	97/2	98/1	98/2	99/1	99/2	100	101/1	101/2	102
Section on Computer Techniques and Optimization			103/1			103/2			103/3			103/4

Scope. *Analytica Chimica Acta* publishes original papers, short communications, and reviews dealing with every aspect of modern chemical analysis, both fundamental and applied. The section on *Computer Techniques and Optimization* is devoted to new developments in chemical analysis by the application of computer techniques and by interdisciplinary approaches, including statistics, systems theory and operation research.

Submission of Papers. Manuscripts (three copies) should be submitted to:
for *Analytica Chimica Acta:* Dr. A. M. G. Macdonald, Department of Chemistry, The University, P.O. Box 363; Birmingham B15 2TT, England;
for the section on *Computer Techniques and Optimization:* Dr. J. T. Clerc, Laboratorium für Organische Chemie, Swiss Federal Institute of Technology, Universitätstrasse 16, CH-8092 Zürich, Switzerland.

Information for Authors. Papers in English, French and German are published. There are no page charges. Manuscripts should conform in layout and style to the papers published in this Volume. Authors should consult Vol. 93, p. 379 for detailed information. Reprints of this information are available from the Editors or from: Elsevier Editorial Services Ltd., Mayfield House, 256 Banbury Road, Oxford OX2 7DE (Great Britain).

Reprints. Fifty reprints will be supplied free of charge. Additional reprints (minimum 100) can be ordered. An order form containing price quotations will be sent to the authors together with the proofs of their article.

Advertisements. Advertisement rates are available from the publisher.

Subscriptions. Subscriptions should be sent to: Elsevier Scientific Publishing Company, P.O. Box 211, Amsterdam, The Netherlands. The section on *Computer Techniques and Optimization* can be subscribed to separately.

Publication. *Analytica Chimica Acta* (including the section on *Computer Techniques and Optimization*) appears in 8 volumes in 1978. The subscription for 1978 (Vols. 96–103) is Dfl. 1000.00 plus Dfl. 120.00 (postage) (Total approx. US $486.96). The subscription for the *Computer Techniques and Optimization* sections only (Vol. 103) is Dfl. 125 plus Dfl. 15.00 (postage) (Total approx. US $60.87). Journals are sent automatically by air mail to the U.S.A. and Canada at no extra cost and to Japan, Australia and New Zealand for a small additional postal charge. All earlier volumes (Vols. 1–87) are available at Dfl. 115.00 (plus postage).

Claims for issues not received should be made within three months of publication of the issue, otherwise they cannot be honoured free of charge.

ANALYTICA CHIMICA ACTA

VOL. 103 (1978)

(Computer Techniques and Optimization, Vol. 2)

ANALYTICA CHIMICA ACTA

International journal devoted to all branches of analytical chemistry

COMPUTER TECHNIQUES AND OPTIMIZATION

VOL. 2 1978

EDITOR:
J. T. CLERC (Zürich, Switzerland)

Associate Editor:
E. ZIEGLER (Mülheim, Germany)

Editorial Advisers:
R. E. Dessy, Blacksburg, Va.
J. W. Frazer, Livermore, Calif.
H. Günzler, Ludwigshafen
S. R. Heller, Washington, D.C.
J. F. K. Huber, Vienna
P. C. Jurs, University Park, Pa.
M. Knedel, Munich
D. L. Massart, Sint Genesius-Rhode
H. C. Smit, Amsterdam

ELSEVIER SCIENTIFIC PUBLISHING COMPANY

Anal. Chim. Acta, Vol. 103 (1978)

26 NOV 2021

© Elsevier Scientific Publishing Company, 1978.
All rights reserved. No part of this publication may be reproduced, stored in a retrieval system or transmitted in any form or by any means, electronic, mechanical, photocopying, recording or otherwise, without the prior written permission of the publisher, Elsevier Scientific Publishing Company, P.O. Box 330, Amsterdam, The Netherlands.

Submission to this journal of a paper entails the author's irrevocable and exclusive authorization of the publisher to collect any sums or considerations for copying or reproduction payable by third parties (as mentioned in article 17 paragraph 2 of the Dutch Copyright Act of 1912 and in the Royal Decree of June 20, 1974 (S. 351) pursuant to article 16 b of the Dutch Copyright Act of 1912) and/or to act in or out of Court in connection therewith.

Submission of an article for publication implies the transfer of the copyright from the author to the publisher and is also understood to imply that the article is not being considered for publication elsewhere.

Printed in The Netherlands

Analytica Chimica Acta, 103 (1978) 1—9
Computer Techniques and Optimization
©Elsevier Scientific Publishing Company, Amsterdam — Printed in The Netherlands

SAMPLING OF INTERNALLY CORRELATED LOTS. THE REPRODUCIBILITY OF GROSS SAMPLES AS A FUNCTION OF SAMPLE SIZE, LOT SIZE AND NUMBER OF SAMPLES
Part I. Theory

P. J. W. M. MÜSKENS and G. KATEMAN*

Catholic University of Nijmegen, Department of Analytical Chemistry, Faculty of Sciences, Toernooiveld, Nijmegen (The Netherlands)

(Received 17th July 1977)

SUMMARY

Sampling of lots which show internal correlation is different from lots with random composition. The relation between lot size, sample size and number of samples for lots with internal correlation has been derived.

One of the problems in analytical chemistry is the size of the sample necessary to describe a lot with sufficient accuracy. This problem is different from that of sampling a process stream in order to control the process, as described by many authors (e.g. [1]). A lot is a finite part of a process, e.g. a wagon load of product, a river during one year, the production of one batch.

A lot that shows random variation of the properties to be analyzed is a simple case. The variation (expressed as standard deviation) within the gross sample, composed of n samples, will decrease with $1/n^{1/2}$. The size of the samples, and thus the gross sample, is determined by the size of the quantity needed for analysis, bearing in mind that the standard deviation due to the variation in analytical results will decrease with $1/N^{1/2}$, N being the number of repeat analyses.

A different situation exists when the distribution of the property to be known shows a random variation within the sample, but only when a sufficiently large sample is taken. This is the case, e.g. in sampling inhomogeneous materials like ore, where the particle size of the components is finite and sometimes even quite large, the particles having different compositions. The size of the gross sample is not only set by the number of samples and the standard deviation of the method of analysis, but also by the composition of the particles and the particle size distribution. These problems have been covered by many authors, e.g. [2—4].

When dealing, however, with samples whose constituents are correlated with those of other samples of the same lot, the situation is different. Factors

causing this correlation include (a) diffusion or mixing within the lot, e.g. in mixing tanks, buffer hoppers, and rivers, and (b) changing properties of the producer of the lot, reactors, emitters, etc. The change in properties within a lot can be in space as well as in time, e.g. when sampling a river, pipe line, or conveyor at a fixed point. The space variation is usually in three dimensions though in practice two dimensions (e.g. in sampling a paint surface) and one dimension (e.g. a conveyor belt) also occur.

In order to design a sampling strategy for correlated samples, it is necessary to know to what extent the number of samples and their size is influenced by the degree of correlation within the lot.

THEORY

A one-dimensional lot, that can be thought of as a part of a process, which is continuous in time or space, is assumed. The investigations are restricted to gaussian stationary stochastic processes of the first order. Such processes can be described by a mean value μ, for convenience set equal to 0, a time constant T_x, and a variance σ_x^2.

For lots derived from processes with $T_x \to 0$, the usual statistics can be used. For lots derived from processes with $T_x \neq 0$ the mean composition of the lot can be expected to be different from the mean composition of the process, though the mean of many lots will equal the process mean. Assume the length of the lot to be P. The real mean of the lot is

$$\mu = (1/P) \int_0^P x(t)\mathrm{d}t$$

where $x(t)$ is the real composition at moment or position t of the component to be known. An estimate of the mean of the lot, m, can be obtained by taking n samples of size G, equally spaced with a distance A, so $P = nA$. As the total size of the gross sample nG cannot be more than the whole lot P, a condition is that $A \geqslant G$.

The estimated value of the composition of the lot is given by

$$m = (1/nG) \sum_{i=0}^{n-1} \int_0^G [x(iA + t)\mathrm{d}t]$$

The mean deviation between estimated and real value of the lot is $E[m - \mu] = 0$ the variance of the deviations is

$$E[m - \mu]^2 = E[m^2] + E[\mu^2] - 2E[m\mu]$$

or $\sigma_{\text{est}}^2 = \sigma_m^2 + \sigma_\mu^2 - 2\sigma_{m\mu}$.

Information is needed on the effect of the number of samples (n), their spacing (A) and the size of the sample (G) on the uncertainty (σ_{est}^2) in the composition of the gross sample (nG) compared with the real composition of lots showing different degrees of internal correlation.

(a) The variance in the composition of the gross sample

Where m is the mean of one gross sample taken from the process,

$$m = (1/nG) \sum_{i=0}^{n-1} \int_0^G x(iA + t)\mathrm{d}t$$

The mean value of m is

$$E[m] = (1/nG) \sum_{i=0}^{n-1} \int_0^G E[x(iA + t)]\mathrm{d}t = 0$$

The variance of m, σ_m^2 is

$$\sigma_m^2 = E[m - E(m)]^2 = E[m^2]$$

$$= (1/n^2G^2) \sum_{i=0}^{n-1} \sum_{j=0}^{n-1} \int_0^G \int_0^G E[x(iA + t_1)x(jA + t_2)]\mathrm{d}t_1\mathrm{d}t_2$$

By definition

$$E[x(t)x(t + \Delta t)] \equiv \sigma_x^2 \varphi(\Delta t)$$

where $\varphi(\Delta t)$ is the autocorrelation function of a time series with time constant T_x and variance σ_x^2. Then

$$\sigma_m^2 = (\sigma_x^2/n^2G^2) \sum_{i=0}^{n-1} \int_0^G \int_0^G \varphi(|t_1 - t_2|)\mathrm{d}t_1\mathrm{d}t_2$$

$$+ (\sigma_x^2/n^2G^2) \sum_{i=0}^{n-1} \sum_{j\neq i}^{n-1} \int_0^G \int_0^G \varphi\{|(i-j)A + t_1 - t_2|\}\mathrm{d}t_1\mathrm{d}t_2$$

In most cases the autocorrelation functions are approximately exponential, $\varphi(t) \simeq \exp(-|t|/T_x)$. According to Appendix A, the variance σ_m^2, will be

$$\sigma_m^2 = \frac{2\sigma_x^2T_x^2}{nG^2}\left[G/T_x - 1 + \exp(-G/T_x) + \{\exp(-G/T_x) + \exp(G/T_x) - 2\}\right.$$

$$\left.\left\{\frac{\exp(-A/T_x)}{1 - \exp(-A/T_x)} - \frac{\exp(-A/T_x).(1 - \exp(-P/T_x))}{n(1 - \exp(-A/T_x))^2}\right\}\right] \qquad \text{(I)}$$

(b) The variance in the composition of the whole lot

The real mean of the lot can be obtained by sampling the whole lot, so $n = 1$ and $G = P = nA$. The variance in the real mean is

$$\sigma_\mu^2 = (2\sigma_x^2T_x^2/P^2)\,[P/T_x - 1 + \exp(-P/T_x)] \qquad \text{(II)}$$

(c) The covariance between m and μ

The covariance can be derived from

$$\sigma_{m\mu} = E[m\mu] = E\left[\frac{1}{nGP} \sum_{i=0}^{n-1} \int_0^G x(iA + t_1)\mathrm{d}t_1 . \int_0^P x(t_2)\mathrm{d}t_2\right]$$

$$= \frac{\sigma_x^2}{nGP} \sum_{i=0}^{n-1} \int_0^G \int_0^P \varphi(|iA + t_1 - t_2|)\mathrm{d}t_1\mathrm{d}t_2$$

As is shown in Appendix B

$$\sigma_{m\mu} = \frac{\sigma_x^2 T_x^2}{nPG}\left[2nG/T_x + (\exp(-G/T_x) - 1)\cdot\frac{1-\exp(-P/T_x)}{1-\exp(-A/T_x)} + (\exp(G/T_x) - 1)\cdot\frac{1-\exp(-P/T_x)}{1-\exp(A/T_x)} \right] \quad \text{(III)}$$

(d) The reproducibility of the gross sample

The variance in the difference between the real composition of the lot and the composition, estimated from the gross sample, will be:

$$\sigma_{est}^2 = \text{(I)} + \text{(II)} - 2\cdot\text{(III)} \quad \text{(IV)}$$

A graphical form of this function is shown in Fig. 1. This figure can be used to determine which combination of number of samples n and sample size F, expressed as fractions of the lot size P, so that $F = G/P$, should be applied to obtain a ratio σ_{est}/σ_x of 0.1.

Special cases

(1) G = A. If the sample size is chosen such that the subsequent samples are taken without interruption, it can be shown that $\sigma_{est}^2 = 0$. This result is not surprising as now the whole lot has been sampled: $A = P/n$, and the gross sample size is $nG = P$.

(2) n = *1*. If only one sample is taken, with a sample size $G < P$, the following equation is obtained, with $A = P$:

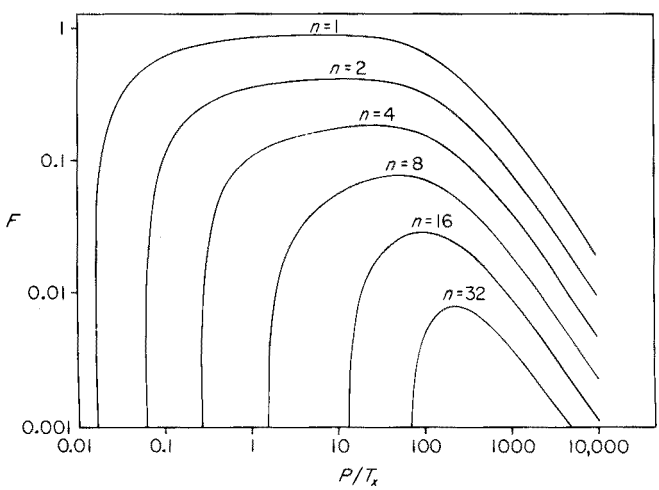

Fig. 1. Relationship between the relative lot size P/T_x and the relative sample size F for different values of the number of samples $n(\sigma_{est}/\sigma_x = 0.1)$.

$$\sigma^2_{est} = \frac{2\sigma_x^2 T_x^2}{P^2}[G/T_x - 1 + \exp(-G/T_x)] - \frac{2\sigma_x^2 T_x^2}{PG}\left[2G/T_x - 1 + \exp(-G/T_x) - \frac{1-\exp(-P/T_x)}{1-\exp(P/T_x)} \cdot (1-\exp(G/T_x))\right] + \frac{2\sigma_x^2 T_x^2}{P^2}[P/T_x - 1 + \exp(-P/T_x)] \quad (V)$$

(3) $G \to 0$. If the sample size G is diminished to very small values it can be shown that

$$\sigma^2_{est} = \frac{\sigma_x^2}{n}\left[1 + 2\left\{\frac{\exp(-A/T_x)}{1-\exp(-A/T_x)} - \frac{\exp(-A/T_x)\,(1-\exp(-P/T_x))}{n(1-\exp(-A/T_x))^2}\right\}\right] - \frac{2\sigma_x^2 T_x}{nP}\left[2n - \frac{1-\exp(-P/T_x)}{1-\exp(-A/T_x)} + \frac{1-\exp(-P/T_x)}{1-\exp(A/T_x)}\right] + \frac{2\sigma_x^2 T_x^2}{P^2}[P/T_x - 1 + \exp(-P/T_x)] \quad (VI)$$

(4) $T_x = 0$. For an uncorrelated process it can be shown that (I), (II) and (III) and consequently σ^2_{est} are all 0. If however $G = 0$, (I) is not equal to 0 but equals σ_x^2/n, so $\sigma^2_{est} = \sigma_x^2/n$ and the statistics of the normal uncorrelated case follow from (IV).

(5) $T_x \to \infty$. If a process is nearly totally correlated it can be shown that (I), (II) and (III) all approach the value of σ_x^2. Therefore σ^2_{est} will be 0.

Test

Although the derived function (IV) satisfies the extreme conditions for $nG = P$, $T_x = 0$ and $T_x \to \infty$, the theory was tested by comparison with discrete simulation. Discrete processes were simulated with a discrete white noise generator from the IBM library. The transformation in a discrete process with a time constant T_x was obtained by a procedure described previously [5].

TABLE 1

Comparison of the values of σ_{est}, calculated from eqn. (IV), with the values of s_{est}, obtained by simulation ($\sigma_x = 1$, $T_x = 120$, $P = 100$)

n	A	G	σ_{est} (calc)	s_{est} (sim)
1	100	50	0.321	0.318
1	100	10	0.579	0.571
1	100	5	0.611	0.598
1	100	1	0.637	0.621
2	50	10	0.259	0.257
2	50	5	0.291	0.291
2	50	1	0.317	0.318
10	10	5	0.0325	0.0324
10	10	1	0.0584	0.0606
20	5	1	0.0260	0.0281

Three different processes were simulated with $T_x = 120$, 10 and 1 and with $\sigma_x = 1$.

From each process 250 lots were taken with size $P = 100$. These lots were sampled with n samples of size G (Tables 1, 2, 3).

The value of σ_{est} was compared with the value

$$s_{est} = \left\{ \left[\sum_{i=1}^{250} (m_i^s - \mu_i^s)^2 \right] / 249 \right\}^{1/2}$$

where μ_i^s is the real mean and m_i^s is the estimated mean of lot i. The results (Tables 1—3) show that the theoretical values σ_{est} agree very well with the values s_{est} obtained by simulation. The differences occurring at small G-values are caused mainly by the fact that the theory is developed for continuous processes, whereas the simulated processes are discrete ones.

TABLE 2

Comparison of the values of σ_{est}, calculated from eqn. (IV), with the values of s_{est}, obtained by simulation ($\sigma_x = 1, T_x = 10, P = 100$)

n	A	G	σ_{est} (calc)	s_{est} (sim)
1	100	50	0.375	0.387
1	100	10	0.801	0.852
1	100	5	0.889	0.915
1	100	1	0.968	0.944
2	50	10	0.465	0.464
2	50	5	0.538	0.533
2	50	1	0.603	0.599
10	10	5	0.0726	0.0712
10	10	1	0.131	0.131
20	5	1	0.0587	0.0680

TABLE 3

Comparison of the values of σ_{est}, calculated from eqn. (IV), with the values of s_{est}, obtained by simulation ($\sigma_x = 1, T_x = 1, P = 100$)

n	A	G	σ_{est} (calc)	s_{est} (sim)
1	100	50	0.139	0.138
1	100	10	0.402	0.408
1	100	5	0.552	0.585
1	100	1	0.853	1.017
2	50	10	0.266	0.266
2	50	5	0.377	0.374
2	50	1	0.595	0.701
10	10	5	0.111	0.120
10	10	1	0.234	0.294
20	5	1	0.134	0.173

CONCLUSION

On the basis of the theory of first-order stochastic processes, a formula is derived for the estimation of the mean composition of a lot. It is shown that if the lots are not internally correlated the traditional statistical laws apply. If the lot is internally totally correlated, i.e. there is no variation in the composition, the mean composition is exactly known by taking one sample. However, more interesting are the lots which show correlated variation in the composition. For these cases it is not possible to simplify formula (IV). The simulation and the graphical presentation do not show results that disagree with expectations.

In the following paper (Part II) the theory will be applied to practical situations.

APPENDIX A

The symbols used are as follows:

A = distance between the middle of two adjacent samples, $A = P/n$
F = relative sample size as fraction of the lot size, $F = G/P$
$\varphi(\Delta t)$ = autocorrelation function of process variable $x(t)$
G = sample size
m = mean composition of gross sample taken from lot P
μ = mean composition of the lot P
n = number of samples taken equally spaced from lot P
N = number of repeat analyses performed on gross sample
P = lot size
s^2_{est} = estimate of variance of the difference between composition of lot and gross sample, obtained by discrete simulation
σ^2_{est} = reproducibility of the gross sample
σ^2_m = variance of composition of gross samples
σ^2_μ = variance of composition of lots
$\sigma_{m\mu}$ = covariance of composition of lot and gross sample
σ^2_x = variance of process
T_x = time constant of process
$x(t)$ = process variable; composition of process at moment or position t

The variance is

$$\sigma^2_m = \frac{\sigma^2_x}{n^2G^2} \sum_{i=0}^{n-1} \int_0^G \int_0^G \varphi\,(|t_1 - t_2|)\,dt_1 dt_2$$

$$+ \frac{\sigma^2_x}{n^2G^2} \sum_{i=0}^{n-1} \sum_{j\neq i}^{n-1} \int_0^G \int_0^G \varphi\,\{|(i-j)A + t_1 - t_2|\}dt_1 dt_2$$

as $\varphi(|\Delta t|) = \exp\{-|\Delta t|/T_x\}$ the first term of the right hand side will be:

$$\frac{\sigma_x^2}{nG^2}\int_0^G\int_0^G \exp\{-|t_1-t_2|/T_x\}\,dt_1dt_2$$

$$=\frac{\sigma_x^2}{nG^2}\int_0^G\left[\int_0^{t_2}\exp\{-(t_2-t_1)/T_x\}dt_1+\int_{t_2}^G\exp\{-(t_1-t_2)/T_x\}dt_1\right]dt_2$$

$$=\frac{\sigma_x^2T_x}{nG^2}\int_0^G\left[2-\exp(-t_2/T_x)-\exp\{(-G-t_2)/T_x\}\right]dt_2$$

$$=\frac{2\,\sigma_x^2T_x^2}{nG^2}[G/T_x-1+\exp(-G/T_x)]$$

the second term is:

$$\frac{\sigma_x^2}{n^2G^2}\sum_{i=0}^{n-1}\sum_{j\neq i}^{n-1}\exp\{-|i-j|A/T_x\}\cdot\int_0^G\int_0^G\exp\{-(t_1-t_2)/T_x\}dt_1dt_2$$

$$=-\frac{T_x\sigma_x^2}{n^2G^2}\sum_{i=0}^{n-1}\sum_{j\neq 1}^{n-1}\exp\{-|i-j|A/T_x\}\cdot\int_0^G\{\exp(-G/T_x)-1\}\cdot\exp(-t_2/T_x)dt$$

$$=+\frac{T_x^2\sigma_x^2}{n^2G^2}\sum_{i=0}^{n-1}\sum_{j\neq i}^{n-1}\exp\{-|i-j|A/T_x\}\cdot\{\exp(-G/T_x)+\exp(+G/T_x)-2\}$$

$$=+\frac{2T_x^2\sigma_x^2}{nG^2}\sum_{k=1}^{n-1}(1-k/n)\exp(-kA/T_x)\{\exp(-G/T_x)+\exp(+G/T_x)-2\}$$

$$=\frac{2T_x^2\sigma_x^2}{nG^2}\left[\{\exp(-G/T_x)+\exp(+G/T_x)-2\}\cdot\left\{\frac{\exp(-A/T_x)}{1-\exp(-A/T_x)}\right.\right.$$

$$\left.\left.-\frac{\exp(-A/T_x)\,(1-\exp(-nA/T_x))}{n(1-\exp(-A/T_x))^2}\right\}\right]$$

APPENDIX B

$$\sigma_{m\mu}=\frac{1}{nGP}\sum_{i=0}^{n-1}\int_0^G\int_0^P\varphi(|iA+t_1-t_2|)dt_1dt_2$$

as $\varphi(|\Delta t|) = \exp\{-|\Delta t|/T_x\}$:

$$=\frac{\sigma_x^2}{nGP}\sum_{i=0}^{n-1}\int_0^G\int_0^P\exp\{-|iA+t_1-t_2|/T_x\}dt_1dt_2$$

$$=\frac{\sigma_x^2}{nGP}\sum_{i=0}^{n-1}\int_0^G\left[\int_0^{iA+t_1}\exp\{-(iA+t_1-t_2)/T_x\}dt_2\right.$$

$$\left.+\int_{iA+t_1}^P\exp\{-(t_2-iA-t_1)/T_x\}dt_2\right]dt_1$$

$$= \frac{\sigma_x^2 T_x}{nGP} \sum_{i=0}^{n-1} \int_0^G [2 - \exp\{-(iA + t_1)/T_x\} - \exp\{-(P - iA - t_1)/T_x\}]\,dt_1$$

$$= \frac{\sigma_x^2 T_x^2}{nGP} \left[\frac{2nG}{T_x} + \{\exp(-G/T_x) - 1\} \sum_{i=0}^{n-1} \exp(-iA/T_x) \right.$$

$$\left. - \{\exp(G/T_x) - 1\} \exp(-nA/T_x) \sum_{i=0}^{n-1} \exp(iA/T_x) \right]$$

REFERENCES

1 F. A. Leemans, Anal. Chem., 43(11) (1971) 36A.
2 B. Baule and A. Benedetti-Pichler, Z. Anal. Chem., 74 (1928) 442.
3 A. L. v. d. Mooren, thesis, Delft, 1967.
4 J. Visman, Mater. Res. Stand., 9 (11) (1969) 9; Mater. Res. Stand., 11(8) (1971) 32.
5 A. Gelb and P. Palosky, IEEE Trans. Aut. Contr., (1966) 148.

Analytica Chimica Acta, 103 (1978) 11—20
Computer Techniques and Optimization
©Elsevier Scientific Publishing Company, Amsterdam — Printed in The Netherlands

SAMPLING OF INTERNALLY CORRELATED LOTS. THE REPRODUCIBILITY OF GROSS SAMPLES AS A FUNCTION OF SAMPLE SIZE, LOT SIZE AND NUMBER OF SAMPLES [1]
Part II. Implications for Practical Sampling and Analysis

G. KATEMAN* and P. J. W. M. MÜSKENS

Catholic University of Nijmegen, Department of Analytical Chemistry, Faculty of Sciences, Toernooiveld, Nijmegen (The Netherlands)

(Received 17th July 1977)

SUMMARY

Sampling of internally correlated lots is different from sampling lots with random composition. The relation between lot size and number of samples for lots with internal correlation is given. The practical implications in reaching a required accuracy in the composition of a gross sample, compared with the lot it is derived from, are described. When the internal correlation is taken into account considerable benefits can be achieved in practical situations.

The sampling of internally correlated lots is a neglected part of sampling theory. Only a special case, the sampling of particulate material, has been treated by many authors, e.g. [2—4]. Many lots to be analysed are internally correlated, e.g. a lot of manufactured product, the contents of a container, warehouse or storage tank, the composition of a river during a year. This means that samples taken at finite intervals are not fully independent and that the normally used statistical rules may not be applied. A practical aspect of this internal- or auto-correlation is that, as a rule, fewer samples are needed to determine the mean composition of the lot with the required accuracy, compared with a random distribution of the component in the lot. Furthermore, the sample size has a considerable influence on the number of samples needed. Also the size of the combined samples, called the gross sample, varies considerably depending on the characteristics of lot and sampling.

If for the internally correlated lot of size P the variance σ_x^2, the time constant T_x, the sample size G and the number of samples n, are known, the reproducibility σ_{est} of the gross sample can be calculated by eqn. (1), in part I of this series [1].

The number of samples n and their size G can be calculated by approximation if the required reproducibility σ_{est} and the other properties of the lot (P, T_x, σ_x) are known.

$$\sigma^2_{est} = \frac{2\sigma_x^2 T_x^2}{nG^2}\left[G/T_x - 1 + \exp(-G/T_x) + \{\exp(-G/T_x) + \exp(G/T_x) - 2\}\cdot\right.$$
$$\left.\left\{\frac{\exp(-A/T_x)}{1-\exp(-A/T_x)} - \frac{\exp(-A/T_x)\cdot(1-\exp(-P/T_x))}{n(1-\exp(-A/T_x))^2}\right\}\right]$$
$$+ \frac{2\sigma_x^2 T_x^2}{P^2}\cdot\{P/T_x - 1 + \exp(-P/T_x)\}$$
$$- \frac{2\sigma_x^2 T_x^2}{nPG}\cdot\left[2nG/T_x + \{1-\exp(-P/T_x)\}\cdot\right.$$
$$\left.\left\{\frac{\exp(-G/T_x)-1}{1-\exp(-A/T_x)} + \frac{\exp(G/T_x)-1}{1-\exp(A/T_x)}\right\}\right] \qquad (1)$$

(The symbols used in this paper are defined in Table 1.)

Simplification of this formula is not possible, since it describes the situation between the extreme $T_x \to 0$ (random) with $\sigma^2_{est} = \sigma_x^2/n$ (for $G = 0$) and $T_x \to 0$ with $\sigma^2_{est} = 0$. Some practical applications of this formula are given.

Estimation of parameters

T_x, the time- or space-constant, is used as a parameter for the internal correlation of the lot. An estimate of T_x can be obtained in several ways. When it is possible to do an experiment, T_x can be estimated by introducing a sudden disturbance in the composition. The distance between the first sign of disturbance in the output and the moment that 63% of the total disturbance is reached can be taken as the time constant T_x. When measuring

TABLE 1

List of symbols

A	= distance between the middle of two adjacent samples, $A = P/n$
Δ_{est}	= error in the estimation of the mean composition of the lot
F	= relative sample size as fraction of the lot size, $F = G/P$
G	= sample size
n	= number of samples taken equally spaced from lot P
N	= number of repeat analyses performed on gross sample
p	= lot size expressed in units of T_x
P	= lot size
σ_a^2	= variance of the method of analysis
σ^2_{est}	= reproducibility of the gross sample
σ_L^2	= combined variance of σ^2_{est} and σ_a^2
σ_x^2	= variance of process
t_n	= value of Student's t for 95% confidence level and n observations
T	= length of time series x_t
T_x	= time constant of process
Δt	= time lag
x_t	= process variable; composition of process at moment t
$\bar{x}$	= mean composition of process during time period T
$\psi(\Delta t)$	= autocovariance function of process variable x_t

the distance in other units, e.g. length or objects, T_x is expressed in these units (Fig. 1).

When experimentation is not possible, an estimate of T_x can be obtained by calculating $\psi(\Delta t)$, the autocovariance function of the process variable x_t, i.e. the composition at moment or position t [5].

$$\psi(\Delta t) = \frac{1}{T} \sum_{t=0}^{T-\Delta t} \{(x_t - \bar{x})\,(x_{t+\Delta t} - \bar{x})\}$$

The use of an absolute time scale for the values x_t enables the calculation of the autocovariance, even when fragments of the process x are missing [6]. As a rough approximation, $\psi(\Delta t) = \psi(0) \cdot \exp(-|\Delta t|/T_x)$ so that the value of Δt, where $\psi(\Delta t) = 0.37\ \psi(0)$, is an estimate of T_x (Fig. 2). Note that $\psi(0)$ is an estimate of σ_x^2.

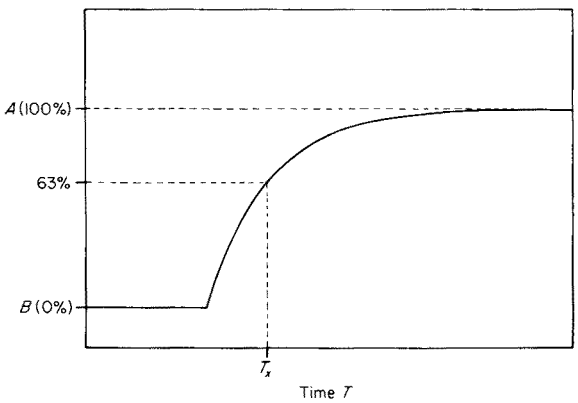

Fig. 1. Relationship between the speed of recovery of a process and the time constant T_x. A and B are the levels after and before disturbance, respectively.

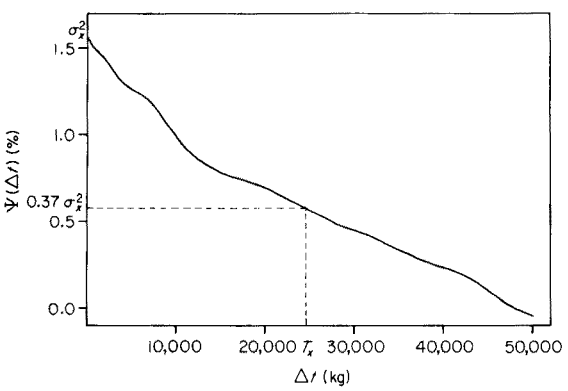

Fig. 2. Autocovariance function of a product stream.

As the lot size P is expressed in the same units as T_x, this parameter can be made dimensionless by dividing by T_x. Now $p = P/T_x$ is a parameter that describes the lot size in correlation constants. A low value of p denotes a high degree of autocorrelation. The sample size G can also be expressed as $g = G/T_x$ but it is more convenient to use $F = G/P$, the sample size expressed as a fraction of the lot size. For convenience the reproducibility of the gross sample σ^2_{est}, which is in fact the variance in the difference between the compositions of the lot and the gross sample, is divided by the process variance σ^2_x. When an ideal method of analysis is available, $\sigma^2_{est}/\sigma^2_x$ should equal zero, but as smaller variations are not detectable by the variance of the method of analysis, in practice a finite value of $\sigma^2_{est}/\sigma^2_x$ suffices.

Properties of internally correlated lots

In Fig. 3, the relation of p, F and n for a constant value of $\sigma_{est}/\sigma_x = 0.1$ is given as calculated from eqn. (1). At low values of p both a small sample size fraction F and a small number of samples n are needed to obtain this value. This means that in highly autocorrelated lots only one small sample is needed to describe the lot with sufficient accuracy. In fact a low value of p means that the lot is homogeneous in composition and that no changes of composition within the lot may be expected. Other lots, however, may have different compositions.

For higher values of p the change of composition within the lot tends to become random; now only the size of the gross sample nF is determining. Therefore it is unimportant whether nF is obtained by taking many small samples or one larger sample. The size of the gross sample decreases linearly with larger lot sizes p or less autocorrelated lots. The most interesting parts of Fig. 3 are the medium lot sizes p. In this region the smallest gross sample needed to obtain a certain value σ_{est}/σ_x, is one made up from many small samples. When fewer but larger samples are taken, the size of the gross

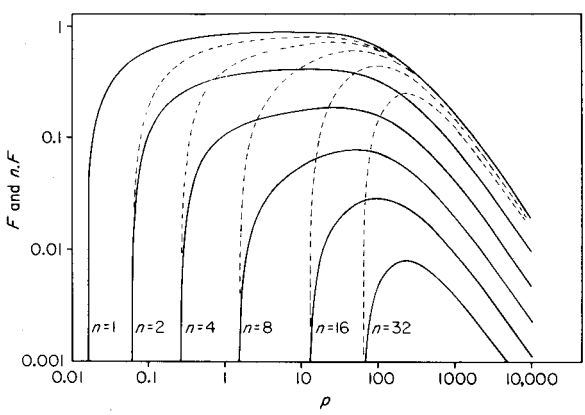

Fig. 3. The relative sample size F (——) and the relative gross sample size nF (— — —) plotted versus the relative lot size p for different numbers of samples ($\sigma_{est}/\sigma_x = 0.1$).

sample increases. For $F = 0$ and a given value of n, σ_{est}/σ_x can only be equal to 0.1 for values of p larger than those indicated in Table 2. If p is less than these values, σ_{est}/σ_x is less than 0.1. For large values of p and σ_{est}/σ_x is constant, $\log F$ is directly proportional to $\log p$. At $p \to \infty$ (uncorrelated process) and $F = 0$, $\sigma_{est}/\sigma_x = 0.1$ for $n = 100$.

The rather unexpected maxima in Fig. 3 can be explained by two effects. For highly correlated processes the composition within limited intervals hardly changes. This means that small samples, which do not differ considerably from their surroundings, allow a precise estimation of the mean composition of the lot. For uncorrelated processes the composition changes rather abruptly. However in the mean composition of a sample with size $G > 0$, the variations are smoothed, so that the sample composition gives a good estimate of the mean of the process and consequently of the lot. By introducing the cost of sampling and sampling material the optimal sampling strategy can be obtained.

In Fig. 4, the relation between n, G and σ_{est}/σ_x for some values of T_x and a fixed value of P is given as calculated from eqn. (1).

It is possible to reach lower values of σ_{est}/σ_x for medium values of T_x in two ways: by increasing the number of samples n or by increasing the sample size G. Over certain values of G increasing n is impossible as nG, the size of the gross sample, cannot exceed the lot size, P. For lower values of T_x an increase in sample size F causes a larger improvement in the precision than for higher values of T_x. Table 3 shows the relative sample size F needed for one sample to reach the same precision as is reached by 32 samples of size $F = 0.01$. From this table and Figs. 3 and 4 it can be concluded that for lots with $p < 1000$ it is better to use a large number of small samples than a small number of large samples.

Influence of the variance of the method of analysis

When the samples are combined to a gross sample, the ultimate accuracy σ_L^2 is determined by $\sigma_L^2 = \sigma_{est}^2 + \sigma_a^2/N$ with σ_a the standard deviation of the analytical method and N the number of repeat analyses. For certain problems, however, it is not possible to combine the samples, e.g. when the samples are liable to decompose within the time required to sample the whole lot. In this case, each sampling action is followed by an analysis and the ultimate accuracy is determined by $\sigma_L^2 = \sigma_{est}^2 + \sigma_a^2/n$. Taking into account the appropriate values for the cost of sampling and analysis, an optimization of total costs of analysis and sampling is possible.

TABLE 2

Minimal values of p to obtain $\sigma_{est}/\sigma_x = 0.1$ ($F = 0$)

n	1	2	4	8	16	32	64	100
p	0.0151	0.0614	0.2640	1.508	12.54	62.34	342.0	∞

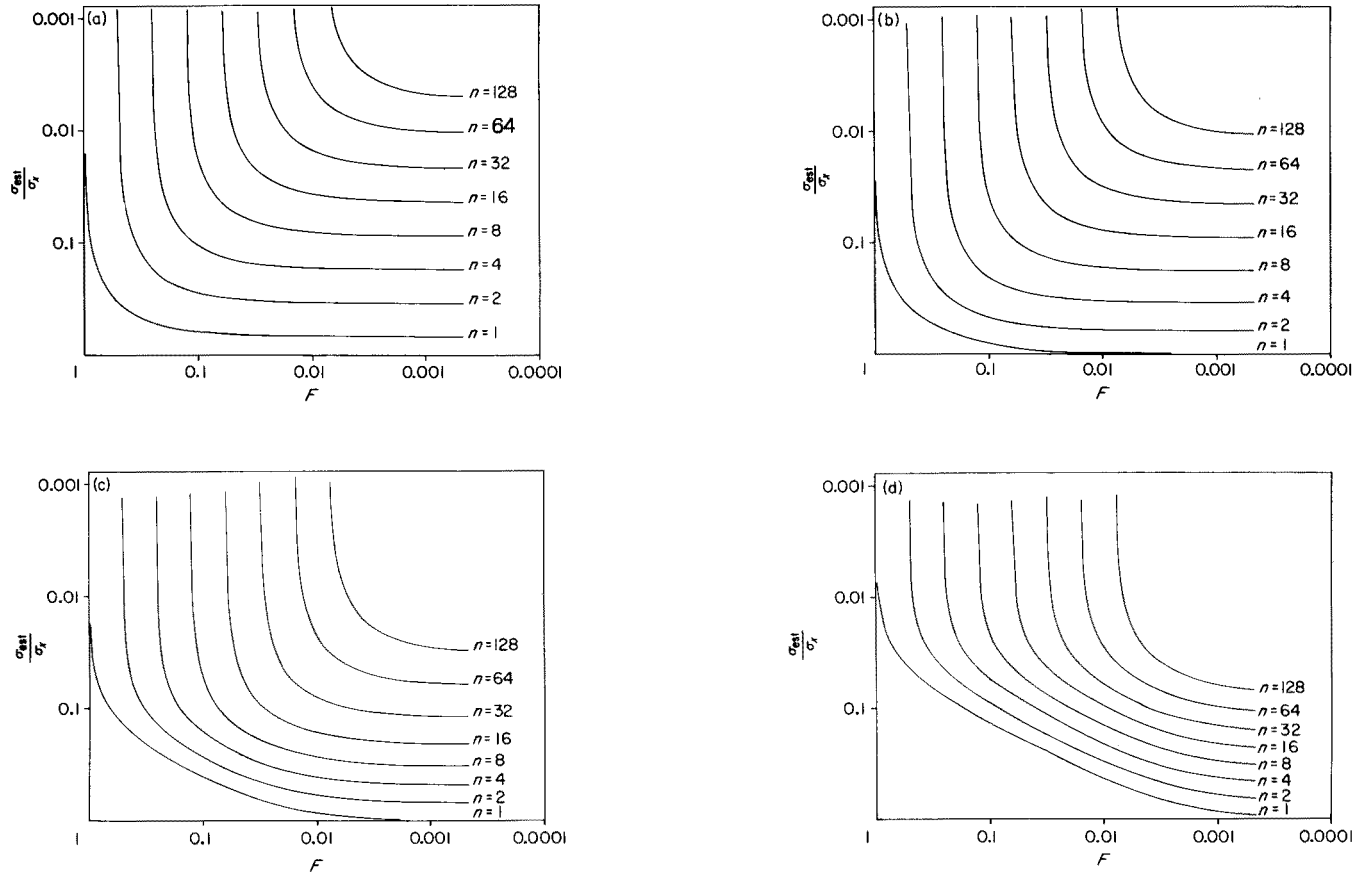

Fig. 4. Relationship between σ_{est}/σ_x and the sample size G for a given lot size and time constant and for different numbers of samples. (a) ($P = 1000$, $T_x = 1000$, $p = 1$) (b) ($P = 1000$, $T_x = 100$, $p = 10$) (c) ($P = 1000$, $T_x = 10$, $p = 100$) (d) ($P = 1000$, $T_x = 1$, $P = 1000$).

TABLE 3

Comparison of different nF combinations which yield the same ratio σ_{est}/σ_x

p	n	F	σ_{est}/σ_x	n	F
1000	32	0.01	0.060	1	0.350
100	32	0.01	0.079	1	0.730
10	32	0.01	0.031	1	0.960
1	32	0.01	0.015	1	0.980

PRACTICAL APPLICATIONS

Sampling a lot of correlated items

A certain bulk chemical is sold in lots of 10,000 bags of 25 kg each. By sampling the product stream during production, the autocovariance function was calculated and the parameters σ_x and T_x were estimated (Fig. 2). As the product is sold under the condition that the analysis of the whole lot will not deviate by more than 0.3% from the specified composition, a 95% confidence level is adopted. The standard deviation of the gross sample should not exceed 0.1%, accounting for the standard deviation of the method of analysis. The sampling scheme of Table 4 can be computed from eqn. (1). Note that a sample size G of less than 1 bag still requires 1 sampling action. It is clear that, in this case, sampling 19 bags is the method of choice. When it is assumed that the lot is not internally correlated, the data of Table 5 are valid. It is clear that in this case more samples are needed. The incorporation of the time constant T_x in the calculations can decrease the number of samples from 150 to 19.

Sampling a river

For estimation of the annual mean of a component in a river, a certain number of samples must be taken. If the internal correlation of the component is considered, the precision will be higher than if this autocorrelation

TABLE 4

Size of gross sample as a function of the number of samples for a specified value of $\sigma_{est}/\sigma_x = 0.08$
($\sigma_x = 1.25\%$; $\sigma_{est} = 0.1\%$; $T_x = 24{,}600$ kg = 984 bags; $P = 10{,}000$ bags; $p = 10{,}000/984 = 10.2$)

No. of samples n	Sample size F	Sample size $G = PF$ bags	Gross sample nG bags
1	0.91	9100	9100
10	0.045	450	4500
18	0.0014	14	252
19	0	1	19
20	0	1	20
40	0	1	40

TABLE 5

Size of gross sample as a function of the number of samples for a specified value of $\sigma_{est}/\sigma_x = 0.08$, assuming $T_x = 1$ (bag).
($\sigma_x = 1.25\%$; $\sigma_{est} = 0.1\%$; $P = 10{,}000$ bags; $p = 10{,}000/1 = 10{,}000$)

No. of samples n	Sample size F	Sample size $G = PF$ bags	Gross sample nG bags
1	0.03	300	300
10	0.0029	29	290
20	0.0014	14	280
50	0.00048	5	250
100	0.00014	2	200
150	0	1	150
200	0	1	200

is neglected. Otherwise, an accepted precision can be obtained with less samples. For the concentration and load of some components of the river Rhine at Bimmen (B.R.D.)* σ_x, σ_a and T_x were estimated from the auto-covariance function (Table 6) [7].

The error of the determination of the mean value of a component during one year, Δ_{est}, depends on the values of σ_{est} and σ_a, the precision of the method of analysis. Assuming that each sampling is followed by an analysis, the ultimate precision is $\sigma_L^2 = \sigma_{est}^2 + \sigma_a^2/n$. For a confidence level of 0.05, $\Delta_{est} = t_n \sigma_L$ where t_n is Student's t for a confidence level of 0.05 and n determinations. The calculations are performed for two sample sizes: $G = 0$ (in this case the samples are called momentary) and $G = A$, if the samples are integrated between the sampling actions. In the latter case, with $nG = P$, the value $\Delta_{est} = t_n \sigma_a / n^{1/4}$ is to be expected. For both cases the relationship between Δ_{est} and the sampling interval A or the number of samples n, calculated for the concentration of ammonia in the river Rhine, is shown in Fig. 5. The same relationship is also shown for $G = 0$ and with neglect of the autocorrelation ($T_x = 0$). If the number of samples n is

TABLE 6

Parameters of the River Rhine for the concentration and load values of two components. Estimated from data measured in the period 1971—1975

Variable		$\bar{x}$ mg l^{-1}	σ_x mg l^{-1}	σ_a mg l^{-1}	T_x days
Concentration	NH_4^+	3.07	1.87	0.62	120
Load	NH_4^+	4.91	2.07	0.93	50
Concentration	NO_3^-	13.43	4.79	1.47	90
Load	NO_3^-	24.22	11.71	2.67	30

*The measurements, upon which the data are based, were kindly furnished by the "Landesanstalt für Wasser und Abfall, Nordrhein-Westfalen".

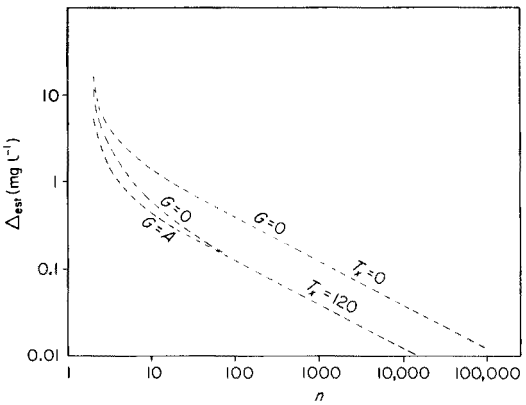

Fig. 5. The error in the estimation of the annual average, Δ_{est}, as function of the number of samples n (NH_4^+-concentration, data from Table 6).

larger than 130 the results for $G = 0$ and $G = A$ are practically identical. Furthermore, it can be shown that samples collected over 1 day ($G = 1$) barely give a better estimation of the annual average than the momentary samples ($G = 0$).

From this graph conclusions can be drawn about the sampling strategy. The best strategy (with the lowest value of Δ_{est}) is to take a sample collected over the whole period P, which should be analyzed afterwards by a very precise method. However, if a precise method is not available, or if the samples cannot be conserved over the whole period, more samples have to be taken and analyzed. The number of samples needed to obtain a certain value of Δ_{est} can be deduced from Fig. 5.

Frequently, a relative error $\Delta_{est}/\bar{x}$, where $\bar{x}$ is the mean value of the variable, is required. Table 7 shows how many samples are needed to obtain the ratio $\Delta_{est}/\bar{x} = 0.1$, 0.5, 0.01 or 0.005. These calculations were performed for the estimation of the annual average of the variables of Table 6. The results are much lower than those suggested by Schippers et al. [8], who did not take into account the internal correlation of the river. The values of n, assuming no internal correlation ($T_x = 0$), are given in Table 8.

TABLE 7

Number of samples n needed to obtain a certain ratio $\Delta_{est}/\bar{x}$ in estimating the annual average of a variable investigated in the River Rhine ($G = 0$; other data in Table 6.)

Variable	Ratio $\Delta_{est}/\bar{x}$			
	0.1	0.05	0.01	0.005
Concentration NH_4^+	24	73	1600	6300
Load NH_4^+	22	65	1400	5500
Concentration NO_3^-	12	29	480	1900
Load NO_3^-	19	43	510	1900

TABLE 8

Number of samples n needed to obtain a certain ratio $\Delta_{est}/\bar{x}$ in estimating the annual average of a variable investigated in the River Rhine, if autocorrelation were neglected ($T_x = 0$; $G = 0$; other data in Table 6.)

Variable	Ratio $\Delta_{est}/\bar{x}$			
	0.1	0.05	0.01	0.005
Concentration NH_4^+	160	640	16000	63000
Load NH_4^+	85	330	8200	33000
Concentration NO_3^-	56	220	5400	21000
Load NO_3^-	97	380	9500	38000

Conclusions

For certain kinds of lots, internally correlated within diffuse boundaries of time- or space-constant, the number and size of samples are different from those in the extreme situations, i.e. totally homogeneous lots and randomly composed lots.

Optimization is possible when costs of sampling and samples are known. As a rule it is better to use a large number of small samples than a small number of large samples as the size of the gross sample decreases and the variation obtainable in the gross sample is lower.

A few examples show that application of the theory allows considerable savings in sampling.

REFERENCES

1 P. J. W. M. Müskens and G. Kateman, Anal. Chim. Acta (Comp. Tech. Opt.), 103 (1978) 1.
2 B. Baule and A. Benedetti-Pichler, Z. anal. Chem., 74 (1928) 442.
3 J. Visman, Mater. Res. Stand., 9(11) (1969) 9.
4 J. Visman, Mater. Res. Stand., 11(8) (1969) 32.
5 G. E. P. Box and G. M. Jenkins, Time Series Analysis, Holden-Day, San Francisco, 1970, p. 23.
6 C. B. G. Limonard, submitted for publication.
7 P. J. W. M. Müskens and W. G. J. Hensgens, Water Res., 11 (1977) 509.
8 J. C. Schippers, H. Hofman and J. Roelands, H_2O, 10 (1977) 70.

Analytica Chimica Acta, 103 (1978) 21—27
Computer Techniques and Optimization
©Elsevier Scientific Publishing Company, Amsterdam — Printed in The Netherlands

COMPILATION OF COMPUTER-READABLE SPECTRA LIBRARIES: GENERAL CONCEPTS

R. BÜCHI, J. T. CLERC*, Ch. JOST, H. KOENITZER and D. WEGMANN
Laboratorium für Organische Chemie, Eidgen. Technische Hochschule, Zürich (Switzerland)
(Received 10th October 1977)

SUMMARY

Compiling spectroscopic reference data in computer-readable form comprises five unit operations: selection, digitization, completion, formatting, and verification. General problems related to these five steps are discussed, and results arising from compiling m.s., ^{13}C-n.m.r., i.r. and u.v. spectra are reported.

The identification of organic compounds by means of spectroscopic methods relies heavily on reference data. Therefore, easy access to data sets in large data collections is essential, and this can be economically provided only with computer-readable files. Data sets in a reference data collection must be reliable and comprehensive, and access to individual data items must be rapid and easy. Furthermore, to insure relevance to potential users, a wide variety of spectra of suitable model compounds is necessary. High reliability and relevance necessitate a careful selection, as well as a thorough verification, of the data sets included in the collection. For rapid and easy access a suitably formatted file is indispensable. Thus, in building up spectroscopic reference data collections, five basic operations can be identified, namely selection, digitization, completion, formatting, and verification. This paper reports some experience in executing these steps on various collections of spectroscopic data, namely from ^{13}C-n.m.r. spectroscopy, mass spectrometry, infrared spectroscopy, and ultraviolet spectroscopy.

SELECTION

When spectra of appropriate compounds have to be selected for inclusion in a data collection, the field of interest of the users must be considered. Furthermore, only essentially complete data sets should be accepted and unnecessary duplication must be prevented. To provide reference data for a broad range of problems with a library of limited size, it is therefore necessary primarily to select simple model compounds rather than highly complex molecules. Furthermore, large series of homologous compounds are not included; the data collection is restricted to a few representative examples.

Where a choice is possible, a compound already documented in one or more of our spectral data collections is preferred. The selection process is obviously highly subjective. It is guided by experience accumulated through many years of practice in the field of structure elucidation and identification of organic compounds by spectroscopic methods.

DIGITIZATION

For inclusion in a computer-readable data collection the spectral data must be provided in digital form. If the instrument used for recording the spectral data is equipped with suitable hardware for direct digital output, no specific action is needed; otherwise, off-line digitization is necessary. Recent trends in instrument design indicate that modern spectrometric instruments will include the option of direct digital output, so that in future off-line digitization will probably be of limited importance. For the time being, however, off-line digitization of data previously accumulated in analog form is probably the most feasible way of starting a computer-readable data collection of reasonable size and quality.

The digitization step is critical to the quality of the data collection. Every piece of information lost during this step is lost for good and can never be recovered except by recording the spectra again. Therefore, it is desirable to acquire the spectroscopic data with the highest resolution possible. However, for economy reasons, the number of data points to be digitally recorded should be kept as low as possible by eliminating all irrelevant data. Accordingly, it is necessary to specify exactly which data items will be relevant to the solution of future, still undefined problems. This is extremely difficult, if not impossible. It is, however, possible to check if an abbreviated spectrum still contains all the information necessary for analytical applications. This is most easily done by reconstructing the original from the digitized data. If an experienced analyst considers this reconstructed curve trace as virtually identical to the original one, it can safely be assumed that no relevant information has been lost. However, this test gives no indication of the amount of irrelevant information still contained within the data.

There are many methods of digitization of analog data, featuring widely varying degrees of speed, user comfort, accuracy, precision, and cost. Which method is most appropriate depends primarily on the form of the raw data, but external factors such as budgetary considerations and manpower may also be decisive. Thus, full automation of the digitization step, giving the highest possible user comfort is not necessarily the most favored solution to the problem.

To digitize manually, i.e. reading data from a printed output and punching it directly into cards, is adequate only if there are relatively few data items per set. In this laboratory, this approach is used for recording compound names, instrument parameters, and other supplemental (non-spectroscopic)

information of relevance. Furthermore, ^{13}C-n.m.r. spectra taken from the literature, and in some instances mass spectra, are digitized manually.

However, if the number of data items per set becomes high, manual digitization is no longer feasible. Thus, for the digitization of curve traces, automatic or semiautomatic methods have to be used. Automated optical encoding [1] gives the highest user comfort, but it also implies relatively high investment, which can be justified only if a large number of curves of the same type have to be processed. In this laboratory, after acquisition of the spectra selected for inclusion in the first version of the data collections, digitization of analog curves will only rarely be needed. Thus, a fully automated approach would be too expensive, and the rather simple semiautomated method used is based on a DEC Writing Tablet Type VW 01 (Digital Equipment Corporation, Maynard, Mass.) linked to a PDP 8/e minicomputer equipped with a 4K core memory. The writing tablet consists essentially of a special pen and a tablet; the position of the pen on the tablet may be sensed under computer control either continuously or at selected moments. Here, the spectra are digitized by manually following the registered curve trace with the pen and sensing the pen position in the continuous mode. The data acquired are then output on a teletype punch. For identification and calibration, the spectrum number and the coordinates of a given number of calibration points (e.g. the four corners of the recording area) are also output. With this hardware, the resolution is about 0.3 mm per digit. Accuracy and precision are highly dependent on the care of the operator. Experience has shown that after a short introduction period, an untrained operator will very rarely depart from the curve by more than 5 digitization steps [2]. Defective data sets may result from shifting the original during digitization or from spikes.

COMPLETION

Spectroscopic data and supplementary non-spectrometric information about the compounds involved are often recorded at different times at different sites and on different data carriers. Merging the two data streams is quite simple in theory. In practice, however, organizational problems can make this troublesome and even frustrating. Instrument parameters should be set to some agreed standard values, or at least should be recorded. Solvents used must be encoded in a standard code, and the compound structure has to be recorded unambiguously. Practical chemists tend to apply the rules for generating systematic chemical names unsystematically, or develop trivial or semi-trivial names which carry little meaning to the outsider. Furthermore, simple arithmetical errors in calculating molecular mass and empirical formula are not uncommon. This very often results in inconsistencies between various data items that have to be resolved by further enquiries.

An important advantage of conversational computer programs for on-line acquisition of spectroscopic data is that the operating system can be programmed to insist on input of the supplementary non-spectroscopic information simultaneously with the spectral data. Even then the result depends critically on good cooperation between sample supplier, instrument operator, and data bank manager.

Various methods may be used to identify a sample structure. Two conditions must be satisfied unconditionally: encoding any sample structure must result in a unique code, and any code must correspond to only one structure. The best known and most widely used structure encoding systems include the connectivity table, the DARC code [3], and the Wiswesser Line Notation [4]. The first two systems are well suited to computer processing of chemical structures, the DARC system being specially optimized for the perception of substructural elements. However, the codes are voluminous and extremely hard to read and interpret by humans. In contrast, the Wiswesser code is very hard to manipulate, but is compact and comparatively easy to interpret. As excessive manipulation of the chemical structures stored in the data collections is not expected to be necessary here, the Wiswesser notation was selected. This allows for the preparation of directly interpretable structure indexes on a line printer. With these indexes, even some limited substructure search capabilities are realized. These distinct advantages of the Wiswesser code are reduced considerably by the fact that encoding a chemical structure with the WLN system generally is intellectually demanding and can be done only by trained personnel. Even with experienced encoders the process is time-consuming and error-prone. For the time being, however, the WLN code appears to be adequate.

FORMATTING

The raw data resulting from the digital acquisition of spectral data as well as the corresponding supplementary information for identification of the sample compound and for recording instrument parameters, will generally accumulate in a format which is determined predominantly by the data source. However, for easy and efficient processing, a standard format has to be matched to the often conflicting needs of the various processing steps. Furthermore, the format must be appropriate for data from all the different spectroscopic methods. For storage economy, a sequentially organized file is preferable. Each record in this file contains the data for one spectrum, and is divided into three segments. The first holds all non-spectroscopic information about the compound as well as a description of the third segment. This first segment is of fixed length and comprises all the data items needed to establish the identity of the sample, including identification number, compound name, molecular formula, and structure code. The second segment is also of fixed length; it contains the data items relating to instrumental parameters and sample preparation, their definition being different

for the different spectroscopic methods. The third segment, holding the spectroscopic data, is of variable length and structure, depending on the type of spectroscopic data. For each individual record, the length of this third segment is specified in the first segment. A file header, placed in front of the first data record, identifies the type of spectroscopic data documented, and gives the number of data records in the file. With this data structure, each segment contains the information necessary to process and interpret correctly the data items in the following segments. Design considerations and a more detailed description of the formats used will be reported later [5].

Normally, the raw data are converted to standard format at the earliest possible time. Thus, only simple re-formatting programs have to be adapted to the various data sources; all subsequent processing can be done with just one set of standard programs.

VERIFICATION

Spectroscopic reference data are used predominantly to resolve ambiguities in spectral interpretation. It is therefore of paramount importance that they be trustworthy. Users generally consult the reference data collection when in doubt about the values and significance of spectroscopic parameters, and so will normally not be in a position to judge the quality of the relevant reference data sets. Therefore, credibility of the data becomes the central factor governing user acceptance. Thorough and careful verification of all data included is extremely important.

The verification of spectroscopic reference data for a file has three main facets. The first is related to the recording of the spectroscopic data. The sample has to be identified and its purity assessed. The necessary checking for spectrometer malfunctions and for technical artefacts is best done during or immediately after recording of the spectrum, and requires close cooperation between the sample supplier and well trained, experienced instrument operators. Any inconsistencies between expected and observed values must be carefully and completely resolved. If the quality of the recorded spectrum is not beyond reasonable doubt, it should not be considered for inclusion in a reference data collection.

The second verification step deals with digitization and transformation of the acquired data. Any data set defective because of errors during transformation of raw data to the standardized digital representation must be marked and put aside for later correction. Elimination of duplicates and of spectra from samples belonging to compound classes which are already adequately documented is done at the beginning of this second step.

The last operation checks for loss of relevant information. The fully processed data set is transformed to a representation corresponding to the original input to the digitizer. For spectroscopic data, this is usually a replotted curve, whereas non-spectroscopic supplementary information is

output as text. These reconstructions are then compared to the source documents holding the original input. If from a spectroscopic point of view the two data sets are identical, it can safely be assumed that no relevant information has been lost during the whole process, and that no digitization errors have been overlooked. There is however no safeguard against most errors undetected in the first step.

RESULTS

Current efforts in this laboratory are directed mainly to extension of the various computer-readable collections of spectroscopic data. These files now include about 600 infrared spectra and 1700 ^{13}C-n.m.r. spectra, collected at this Institute. About 1000 ultraviolet spectra have also been digitized, but are not yet completely processed. A collection of mass spectra [6] containing about 9000 entries is also available. These collections form the data base for library search systems for the identification of organic compounds. Search systems for mass spectra [7] and for ^{13}C-n.m.r. spectra [8] are already in use.

The set of infrared spectra to be included initially in the file has been selected from the DMS collection [9]. About 2300 curve traces have been acquired and completely processed; in the initial phase, the various quality requirements were only loosely defined or unknown, hence 1700 data sets are now considered unacceptable. Around 100 data sets per week may be acquired. About 25% of the time is spent on selecting the compounds to be processed, 15% on digitization of the curves recorded, 10% on digitization of supplemental information, 5% on checking the spectroscopic information, and 5% on checking the supplementary information; overhead time is about 40%. On average, roughly 15% of the data sets acquired are found to be defective and have to be redigitized or corrected.

As the mass spectra collection [7] was available in computer-readable form, reformatting was assumed to be the only operation required. However, experience has shown that verification of the data is advantageous. Initially, duplicates were removed; these were identified by manually scanning the molecular formula index. Among the 9256 entries, 3265 duplicates were retrieved, representing 1400 compounds. For each multiply documented compound, all data sets were output in tabular and graphical form. For duplicates, the selection of the data set to be retained generally presents few problems. If the spectra exhibit large differences, errors and/or impurities are normally easily identified. If the data sets are largely identical, either may be selected. For about 50 compounds, it was impossible to identify the sample structure unambiguously. In these cases, all the relevant data sets were eliminated.

In conclusion, experience indicates that in creating, maintaining, and extending computer-readable spectra collections, expenditure of time and money tends to increase disproportionately with increasing quality require-

ments, and are therefore often underestimated. However, in the long run trading quality for quantity must be a bad bargain. Thus, very high quality criteria should be applied and rigorously enforced.

This work was supported by the Schweizerische Nationalfonds zur Förderung der wissenschaftlichen Forschung and by the Kommission der Europäischen Gemeinschaften, Aktion COST 64b.

REFERENCES

1 J. A. de Haseth, W. S. Woodward and T. L. Isenhour, Anal. Chem., 48 (1976) 1513.
2 J. T. Clerc, R. Knutti, H. Koenitzer and J. Zupan, Z. Anal. Chem., 283 (1977) 177.
3 J. E. Dubois, in W. T. Wipke, S. R. Heller, R. J. Feldmann and E. Hyde (Eds.), Computer Representation and Manipulation of Chemical Information, J. Wiley, New York, 1974, p. 239.
4 E. G. Smith and P. A. Baker, The Wiswesser Line-Formula Chemical Notation, Chemical Information Management, Inc., Cherry Hill, New Jersey, 1975.
5 H. Koenitzer et al., in preparation.
6 UKAEA, AWRE, Mass Spectrometry Data Centre, Aldermaston, Reading, RG7 4PR, U.K.
7 P. R. Nägeli and J. T. Clerc, Anal. Chem., 46 (1974) 739A.
8 R. Schwarzenbach, J. Meili, H. Koenitzer and J. T. Clerc, Org. Magn. Reson., 8 (1976) 11.
9 DMS Documentation of Molecular Spectroscopy, Verlag Chemie, Weinheim, B.R.D. and Butterworth, London, 1975.

Analytica Chimica Acta, 103 (1978) 29—42
Computer Techniques and Optimization
©Elsevier Scientific Publishing Company, Amsterdam — Printed in The Netherlands

DATEN-ERFASSUNG UND -VERARBEITUNG EINES MIKROWELLENPLASMADETEKTORS FÜR DIE GAS-CHROMATOGRAPHIE

J. BONNEKESSEL* und M. KLIER

BASF Aktiengesellschaft, D-6700 Ludwigshafen (B.R.D.)

(Eingegangen den 17. Juli 1977)

ZUSAMMENFASSUNG

Ein Helium-Mikrowellenplasma wird als Emissionsquelle für elementspezifische Detektion in der Gas-Chromatographie genutzt (MPD 850). Die von einem Spektrometer gleichzeitig gemessenen Signale von vier Elementen werden in analoger Form zwischengespeichert (sample-and-hold) und dann seriell von einem Datenerfassungssystem übernommen. Durch Einfügung eines sogenannten "SYNC"-Signals kann die Vollständigkeit eines jeden Meßzyklus kontrolliert werden. Die Auswertung erfolgt in einem Großrechner. Es stehen Programme zur Querempfindlichkeitsunterdrückung und zur Bestimmung der relativen Empfindlichkeit unter Berücksichtigung von Linearitätsabweichungen zur Verfügung. Als Ergebnis können die Elementverhältnisse für jeden Meßpunkt entlang eines Peakprofils angegeben werden. Arbeitsaufwand und Fehlerbreite dieser Methode sind im Vergleich zur herkömmlichen Auswertemethode deutlich verringert. Andere Programme erlauben die Ermittlung von Peakflächen, Retentionszeiten und Retentionsindices simultan für vier Kanäle.

SUMMARY

Data acquisition and processing of a microwave plasma detector in gas chromatography

A helium microwave plasma emission source is used as an elemental analyzer for gas chromatography (MPD 850). The signals of four elements are measured simultaneously with a spectrometer, added by a "SYNC"-signal, and stored with a sample-and-hold technique for later treatment. The data are read in series by a data acquisition computer. The programs for interpretation are designed for a large computer. Programs are available for selectivity improvement and for the adjustment of relative sensitivity with any necessary corrections for deviations from linearity. The result is the ratio of elements for each data point along a peak profile. Compared with the conventional method, the working time is reduced significantly and the accuracy is improved. Other programs allow the calculation of peak areas, retention times and retention indices simultaneously for four channels.

In den letzten Jahren hat die Emissionsspektroskopie unter Verwendung von Mikrowellenenergie Eingang in die Gas-Chromatographie (GC) gefunden. Das Eluat einer GC-Säule wird in ein Mikrowellenplasma geleitet und die in der elektrischen Entladung entstehende Atomemission zum analytischen Nachweis genutzt. In der Literatur sind mit Argon oder mit Helium betriebene Mikrowellenplasmadetektoren für die GC beschrieben [1—5].

Bei dem von uns verwendeten Mikrowellenplasmadetektor Modell MPD 850 (Applied Chromatography Systems Ltd.; früher Applied Research Laboratories Ltd.) wird nachgereinigtes Helium verwendet. Das Helium dient zunächst als Trägergas für die chromatographische Trennung (Abb. 1). Das Eluat der GC-Säule wird im Verhältnis 1:1 geteilt; so kann parallel neben dem MPD ein Flammenionisationsdetektor (FID) eingesetzt werden. Da der Helium-Plasmadetektor bei vermindertem Druck betrieben wird, ist für die Funktion des FID die Einstellung eines geringen Überdruckes gegen Atmosphäre am Ende der GC-Säule nötig. Dieser überdruck ist durch "He-Tail" und die beiden nachgeschalteten Strömungswiderstände unter Berücksichtigung des Säulendurchflusses festgelegt. Das zum MPD abgezweigte Eluat wird mit einem "Scavengergas", das aus Helium und Sauerstoff oder aus Helium und Stickstoff zusammengesetzt ist, vermischt und gelangt dann in die Plasmazone [5—7]. Der Zusatz von etwa 0,2% Sauerstoff oder Stickstoff unterdrückt weitgehend eine Kontinuumsemission, die hauptsächlich auf die Bildung von Kohlenstoffpartikeln im Plasma zurückzuführen ist [5]. Durch Betätigung eines Bypassventils ist es möglich, größere Substanzmengen wie beispielweise Lösungsmittelanteile am Plasmarohr vorbei zu leiten. Die Energie für die Plasmafackel wird einem Mikrowellengenerator (2,45 GHz, max. 200 W) entnommen und in einen Hohlraumresonator eingekoppelt. Die Emission der unteren Hälfte des Plasmas [5] wird mit einem Gitterspektrometer verfolgt. Für die Elemente C, H, D, N, O, F, Cl, Br, J, S und P ist jeweils eine güngstige Linie aus ihren Atomemissionsspektren ausgewählt. Auf diese Linien ist je ein Sekundärspalt und ein Photomultiplier justiert. Es ist also die simultane Verfolgung der Atomemission aller aufgeführten

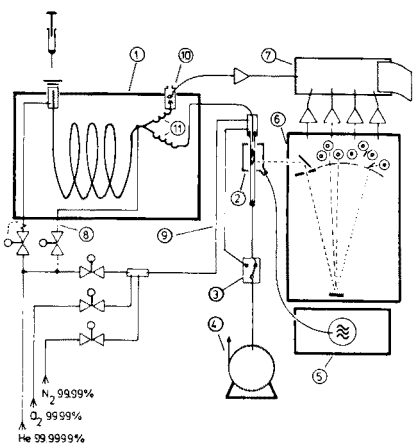

Abb. 1. Schematische Darstellung der Kopplung eines Gas-Chromatographen mit einem Mikrowellenplasmadetektor. (1) Gas-Chromatograph, (2) Hohlraumresonator und Quarzkapillare, (3) Bypassventil, (4) Vakuumpumpe, (5) Mikrowellengenerator, (6) Gitterspektrometer, (7) Registriersysteme, (8) "He-Tail", (9) Scavengergas, (10) FID, (11) Strömungswiderstände.

Elemente möglich. Praktisch haben wir uns auf die gleichzeitige Registrierung des FID-Signals und von vier frei wählbaren Elementsignalen beschränkt.

ANWENDUNG DES MIKROWELLENPLASMADETEKTORS

Einsatzbereiche des MPD

Der MPD wird von uns hauptsächlich zur qualitativen Charakterisierung von Komponenten in der Gas-Chromatographie eingesetzt. In Kombination mit GC-spezifischen Daten wie beispielsweise Retentionsindex bietet die Ermittlung der Elementverhältnisse einer Komponente eine zusätzliche Information zur Identifizierung. Selbstverständlich vermag diese Methode nicht die Möglichkeiten einer Kopplung der Gas-Chromatographie mit der Massenspektrometrie zu ersetzen. Bisherige Erfahrungen zeigen aber, daß die Kenntnis der Elementverhältnisse eine große Hilfe bei der Deutung der Massenspektren unbekannter Verbindungen sein kann. In Zweifelsfällen ist eine Interpretation von Massenspektren manchmal erst nach Einsatz eines hochauflösenden Massenspektrometers oder des MPD möglich; in der Regel wird dann eine GC/MPD-Kopplung wegen des geringeren Aufwandes durchgeführt.

Konventionelle Auswertemethode

Die konventionelle Auswertung von MPD-Messungen geht von den mit Kompensationsschreibern erfaßten Meßdaten aus. Der Schreiberausschlag ist proportional der Elementkonzentration im Plasma. Unter der Voraussetzung einer guten chromatographischen Trennung ist damit die Berechnung der Elementverhältnisse einer Komponente möglich. Allerdings bedarf es dazu noch einer Eichung der relativen Empfindlichkeit der Detektorkanäle an Hand einer geeigneten Verbindung.

Beispiel für Kohlenstoff und Wasserstoff. Die relative Empfindlichkeit für Wasserstoff gegenüber Kohlenstoff ($RE_{H/C}$) gibt an, um welchen Faktor sich die Meßeffekte (z.B. Schreiberausschlag) für H und C unterscheiden, wenn von beiden Elementen gleich viele Atome im Plasma sind. Es seien nun beispielsweise für die Eichsubstanz C_2H_6 folgende Peakhöhen gemessen: h_C = 220 mm (C-Kanal) und h_H = 118 mm (H-Kanal). Dann errechnet sich $RE_{H/C}$ wie folgt:

$$RE_{H/C} = h_H n_C / h_C n_H = 118 \times 2/220 \times 6 = 0{,}179$$

Es bedeuten n_H und n_C die Anzahl der Wasserstoff- bzw. Kohlenstoffatome im Molekül der Eichsubstanz.

Die Meßwerte für eine Komponente seien: h'_C = 185 mm und h'_H = 72 mm. Nun errechnet sich das Elementverhältnis ($EV_{H/C}$) für diese Komponente wie folgt

$$EV_{H/C} = h'_H / h'_C \, RE_{H/C} = 72/185 \times 0.179 = 2.17$$

Grundsätzlich lassen sich zur Datenerfassung auch Integratoren einsetzen. Bei der Auswertung werden dann an Stelle der Peakhöhen die Peakflächen genommen.

Vor- und Nachteile der konventionellen Auswertemethode

Die oben geschilderte Auswertemethode ist relativ einfach und führt rasch zu brauchbaren Ergebnissen. Schwierigkeiten ergeben sich aber bei der Auswertung komponentenreicher Gemische, da die obige Methode sich dann als zeitraubend erweist. Bei Peakhöhenauswertung stellt der geringe dynamische Bereich der Schreiber eine weitere Schwierigkeit dar. Integratoren und Schreiber versagen als Rohdatenerfassungssysteme bei nicht vollständiger chromatographischer Trennung. Schon die rein qualitative Zuordnung von Peakspitzen und Schultern bei schlecht getrennten Komponenten ist häufig nur dann möglich, wenn während der Messung durch Beobachtung der Schreiber die Zugehörigkeit der Peakspitzen bzw. Schultern zu den vier Kanälen kontrolliert und entsprechend notiert wird. Eine quantitative Auswertung nach der konventionellen Methode ist hier nicht meht sinnvoll.

MÖGLICHKEITEN EINER RECHNERGESTÜTZTEN AUSWERTUNG

Um obigen Schwierigkeiten begegnen zu können, diskutierten wir die Vorteile eines Anschlusses des MPD an ein vorhandenes Rechnersystem. Die rechnergestützte Datenerfassung und Auswertung sollte folgende Verbesserungen und Möglichkeiten bieten: (a) Sicherung der Meßdaten über einen großen dynamischen Bereich unter Beachtung der Synchronität der vier Kanäle; (b) Reduzierung des Eichaufwandes. Zur Berücksichtigung von Linearitätsabweichungen über einen großen dynamischen Bereich waren bisher mehrere Eichmessungen nötig; (c) Rechnergestützte Verbesserung der Selektivität; (d) Bestimmung der Elementverhältnisse auch bei teilweise überlappten Peaks; (e) Verringerung des Arbeitsaufwandes bei umfangreichen Messungen; (f) optimale Nutzung schon vorhandener GC-Programme nach geringer Anpassung. Daneben sind neue Programme zur Ermittlung der Elementverhältnisse erforderlich.

ANSCHLUß DES MPD AN EIN RECHNER-SATELLITENSYSTEM

Anschlußmöglichkeiten

Vorversuche zum off-line-Anschluß von vier einzelnen Magnetbandgeräten zur Datenerfassung schlugen fehl, da die Zuordnung der synchron anfallenden analogen Meßwerte — trotz Markierung der Zeitachsen mit synchronen Testsignalen — nach Einlesen in einen Rechner (IBM/7) nicht sicher genug feststellbar war. Da ein Vierspurmagnetbandsystem nicht zur Verfügung stand, wurden verschiedene Möglichkeiten eines on-line-Anschlusses an das vorhandene Satelliten-Rechnersystem der BASF [8] diskutiert.

Möglichkeit 1. Vier GC-on-line-Anschlüsse sind mit den vier Verstärkerausgängen des MPD verbunden. Mit jedem Interrupt vom Taktgeber — dies ist die Aufforderung an den Erfassungsrechner, einen Meßwert zu übernehmen [8] — werden unmittelbar nacheinander die vier Kanäle eingelesen. Für einen Einlesezyklus sollten maximal 15 ms Zeit nötig sein.

Möglichkeit 2. Nur ein GC-on-line-Anschluß wird über einen vierpoligen Umschalter, der mit jedem Interrupt eine Stufe weitergeschaltet wird, nacheinander mit allen vier Verstärkerausgängen des MPD verbunden. Die Abtastfrequenz beträgt mindestens 10 Hz je Kanal. Die zeitverschobene Datenerfassung der vier Kanäle kann softwaremäßig durch Interpolation berücksichtigt werden.

Möglichkeit 3. Die Daten werden simultan erfaßt und analog gespeichert (sample-and-hold) und dann seriell vom Rechner wie bei Möglichkeit 2 gelesen. Die Abtastfrequenz kann zwischen 1 und 5 Hz je Kanal liegen.

Die begrenzte Anzahl der noch zur Verfügung stehenden Anschlüsse sprach gegen Lösung 1. Die zeitlich versetzte Erfassung nach Vorschlag 2 erschien trotz hoher Abtastrate riskant, da mit einer Einbuße an "Gleichzeitigkeit" bei der Rohdatenerfassung eine deutliche Verschlechterung bei der Elementverhältnisberechnung zu erwarten war. Zusätzlich hat die erhöhte Abtastrate zwangsläufig einen deutlich höheren Speicherbedarf und damit höhere Auswertekosten zur Folge.

Anschluß des MPD an einen Rechner IBM/7

Die Anschlußversion nach Möglichkeit 3 wurde realisiert (Abb. 2). In einem Interface zwischen MPD und dem Datenerfassungsrechner (IBM/7) befinden sich vier Analogspeicher, ein 5-Kanal-Multiplexer und ein sog. SYNC-Signalgeber mit einer Bypass-Automatik. Gesteuert von der Logik des Interfaces wird mit jedem Interrupt des Taktgebers [8] ein analog gespeicherter

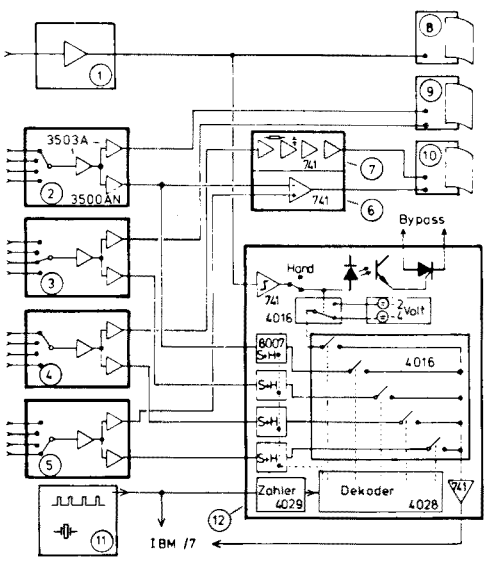

Abb. 2. Vereinfachte Darstellung der Rohdatenerfassung des MPD. (1) Parametrischer FID-Verstärker, (2—5) vier MPD-Verstärker, (6) Subtraktionsverstärker, (7) aktives Tiefpaßfilter (Butterworth-Filter 8. Ordnung), (8) Einkanalschreiber, (9 u. 10) Zweikanalschreiber, (11) Taktgeber, (12) Interface.

Wert eingelesen; nach dem seriellen Einlesen der vier MPD-Werte wird mit jedem fünften Interrupt dem Rechner ein großer, negativer Spannungswert (SYNC-Signal) übermittelt und gleichzeitig werden neue Meßwerte der vier MPD-Kanäle in die Analogspeicher übernommen. Dies ist der Beginn eines neuen Einlesezyklus. Im Normalfall beträgt der Sync-Wert −4,00 V; die MPD-Meßwerte liegen im positiven Spannungsbereich. Mit Hilfe der Sync-Signale kann später vom Auswerterechner die Vollständigkeit und der Anfang eines Einlesezyklus festgestellt werden. Bei Tätigkeit des Bypass-ventils, von Hand oder durch eine vom FID angesteuerte Automatik im Interface bewirkt, beträgt das SYNC-Signal nur −2,00 V. Das SYNC-Signal dient also gleichzeitig zur Datenkontrolle und zur Kontrolle der Bypasstätigkeit.

Auch bei rechnergesteuerter Auswertung werden weiterhin drei Schreiber (1 Einkanalschreiber für den FID und 2 Zweikanalschreiber für den MPD) zur Registrierung benutzt. Zwischen MPD und den Schreibern kann ein Subtraktionsverstärker für die "Geistersignal"-Korrektur eingesetzt werden. Mit diesem Gerät kann von einem Elementsignal ein dem Kohlenstoffsignal proportionaler Anteil abgezogen werden. Bei Bedarf kann der Subtraktionsverstärker auch zwischen MPD und Interface geschaltet werden.

Zur Verbesserung des Signal/Rausch-Verhältnisses sind teilweise zwischen MPD und den Schreibern passive oder aktive Filter eingefügt. Diese Maßnahmen finden bei der on-line-Datenerfassung nur begrenzte Anwendung, da schon sehr geringe Unterschiede der Zeitkonstanten dieser Filter zu untragbaren Zeitverschiebungen führen.

Datenfluß im Rechnersystem

Der Beginn und das Ende der Datenerfassung werden durch Betätigung einer "START/STOP"-Taste am Taktgebergerät festgelegt (Abb. 3). Die Umwandlung der vom Interface zwischengespeicherten Analogwerte erfolgt mit einem 14 bit "autoranging" ADU; dabei kann ein Bereich von etwa ±5,12 V bei einer Auflösung von 0,6 μV in der empfindlichsten Stufe überstrichen werden. Die nur für kurze Zeit im Erfassungsrechner (IBM/7) zwischengespeicherten Werte werden von einem Prozeßrechner (IBM 1800) übernommen und auf Plattenspeicher überschrieben. Zur Auswertung der Messung (M-Satz) gibt man über eine Fernschreibmaschine im Labor mehrere Parameter ein. In einem festformatierten "Kennsatz" (K-Satz) gibt man nach einer Kennziffer (die bei Beginn der Messung vom Prozeßrechner ausgegeben wurde) eine Probenbezeichnung ein; weitere Angaben können je nach gewünschter Auswertemethode beispielsweise Bruttoretentionszeiten von Referenzpeaks oder Elementverhältnisse von Eichkomponenten betreffen. In einem "Informationssatz" (I-Satz) sind der "Auswertetyp", die Elementbezeichnungen für jeden Kanal sowie Angaben zur Basislinienlegung zu definieren; je nach Auswertetyp sind verschiedene weitere Angaben notwendig, die aber erst weiter unten erörtert werden sollen. Bei einer Serie von M-Sätzen genügt die Eingabe eines I-Satzes; Voraussetzung ist hier, daß alle

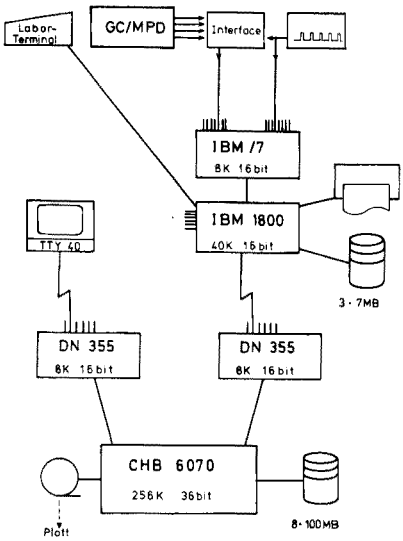

Abb. 3. Satelliten-Rechner-System.

Kennziffern dieser M-Sätze eine lückenlose Reihe bilden. Wenn alle M-, K- und I-Sätze vorhanden sind, werden alle Daten automatisch vom Prozeßrechner über eine Standleitung zum Rechenzentrum geschickt. Dort übergibt ein Datenvermittlungsrechner die Informationen an den Rechner CHB 6070. Hier erfolgt im Batchbetrieb nach formalen Prüfungen der K- und I-Satz-Eingaben die Auswertung. K- und M-Sätze werden nach Angaben im I-Satz für einen Zeitraum von wahlweise 1 bis 30 Tagen abgespeichert. Durch Eingabe eines neuen I-Satzes oder neuer K- und I-Sätze ist eine Wiederholung der Auswertung nach der gleichen Auswertemethode oder nach einer anderen Methode möglich. Die Ergebnisse gelangen auf dem gleichen Weg wie oben beschrieben zum Prozeßrechner IBM 1800 zurück und werden von einem Schnelldrucker ausgegeben.

AUSWERTEMETHODEN

Für die Auswertung von MPD-Messungen stehen zwei Gruppen von Auswertemethoden zur Verfügung: (a) die "MPD-orientierten"Auswertungen dienen zur Feststellung von Elementverhältnissen unter Berücksichtigung von Querempfindlichkeiten (MPD-GC-1, 2 und 3); (b) die "GC-orientierten" Programme ermöglichen die Ermittlung von Flächenanteilen und Retentionsindices mit der Möglichkeit der automatischen "Tabellensuche" (MPD-GC-9 und 4*3). Schließlich besteht noch die Möglichkeit, die im Rechenzentrum abgespeicherten Rohdaten plotten zu lassen (MPD-GC-7).

Zu Beginn einer jeden Auswertung werden alle Einlesezyklen auf Vollständigkeit kontrolliert; werden zwischen zwei SYNC-Signalen mehr oder weniger

als vier Meßpunkte festgestellt, so hat dieser Einlesezyklus nur noch zur Bildung der Abszisse Bedeutung. Solche Fehlstellen werden im Analysenbefund protokolliert. Einlesefehler dieser Art treten relativ selten auf.

In den beiden nächsten Schritten erfolgt — für jeden Kanal getrennt — die Durchführung einer Rauschanalyse und die Eliminierung von Spikes; weitere Details hierzu kann man der Literatur entnehmen [9]. Auch die Konstruktion der Basislinie ist bei [9] beschrieben.

MPD-GC-1

Mit diesem Programm können Querempfindlichkeiten zwischen verschiedenen Kanälen bestimmt werden. Beispielsweise macht sich die Kohlenstoff-Kontinuums-Emission auf dem Chlorkanal als "Geistersignal"bemerkbar. Diese Querempfindlichkeit kann man an Hand einer chlorfreien Verbindung feststellen. Es wird das von der Signalhöhe des "störenden" Elements abhängige Geistersignal des "gestörten" Elements "von Meßpunkt zu Meßpunkt" bei der Eluierung der Testkomponente ermittelt. Aus den Wertepaaren wird eine Ausgleichsgerade* errechnet und abgespeichert. Dazu ist im K-Satz der Anfang und das Ende des Eichpeaks zu definieren und im I-Satz sind störendes und gestörtes Element zu benennen. Es können für 2 gestörte Elemente je 2 Störelemente berücksichtigt werden. Als Ergebnis wird die Ausgleichsgerade angegeben, eine Tabelle der Wertepaare ($h_{C,abs}$ und h_X/h_C) mit der Kennzeichnung, ob der Meßpunkt auf der auf- oder absteigenden Peakflanke liegt, und ein "Plott" aus den Wertepaaren ausgedruckt.

Anmerkung. Die Signalhöhe des Störelements ist hier die Differenz zwischen dem Spannungswert im Meßpunkt und dem Spannungswert zu Beginn des Chromatogramms (= Grundwert); so kann auch bei Temperaturprogrammierung eine angehobene Basislinie berücksichtigt werden; das ist wichtig, weil die Querempfindlichkeit vom absoluten Signal des störenden Elements abhängig ist und nicht nur von seiner Konzentration (Abb. 4).

MPD-GC-2

Dieses Programm dient zur Messung der relativen Empfindlichkeit des Detektors. "Entlang des Peakprofils" einer bekannten Verbindung wird das Verhältnis der Meßeffekte für ein Element X und für das Bezugselement (üblicherweise Kohlenstoff) in Abhängigkeit von der absoluten Signalhöhe des Bezugselements ermittelt. Wiederum wird im Ergebnisprotokoll die

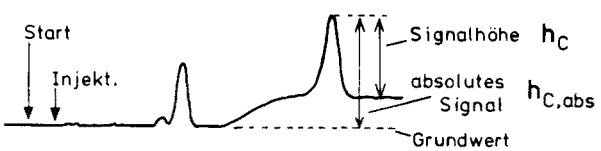

Abb. 4. Erläuterung s. Text.

*In vielen Fällen gibt eine Ausgleichsgerade nur eine mangelhafte Annäherung. Z. Zt. wird an einer verbesserten Approximation gearbeitet.

Ausgleichsgerade angegeben und die Tabelle der Wertepaare ($h_{C,abs}$ und h_X/h_C) ausgedruckt mit der Kennzeichnung, ob der Meßpunkt auf der auf- oder absteigenden Peakflanke liegt.

MPD-GC-3

Dies ist das "eigentliche" MPD-Auswerteprogramm. Hier wird unter der Berücksichtigung der Angaben im I-Satz von bis zu zwei Elementkanälen der Anteil der Geistersignale abgezogen; dann wird mit Hilfe der abgespeicherten Geradenfunktionen für die relativen Empfindlichkeiten (s. oben) ein Elementverhältnis für jedes der drei Elemente gegenüber dem Bezugskanal angegeben. Für den Bezugskanal werden die Signalhöhen (von der Basislinie an) ausgedruckt und für jeden Kanal die Maxima festgestellt. Überschreitet die Signalhöhe des Bezugskanals einen Schwellwert, der um einen vorgebenen Wert über der Basislinie liegt, so werden Elementverhältnisse ausgegeben. Die Schwellwertgröße ergibt sich aus der Rauschbreite und einem im I-Satz anzugebenden Faktor. Um die Protokollänge sinnvoll begrenzen zu können, ist im I-Satz eine Schrittweite anzugeben; bei einer Schrittweite von $n = 3$ beispielsweise wird nur jeder dritte Wert ausgedruckt.

MPD-GC-9

Die Daten eines jeden Kanals werden wie einzelne GC-Meßsätze behandelt. Nach Rohdatenglättung, Spikeunterdrückung und Basislinienlegung folgt die Detektion von Peaks und Schultern.

Im Ergebnisausdruck erscheinen neben der Bruttoretentionszeit in vier Spalten Angaben über Rohflächen und Höhen von Peaks und Schultern.

*MPD-GC-4*3*

Aus den abgespeicherten Daten der MPD-GC-9-Auswertung oder direkt aus den Rohdaten kann unter Einschaltung des MPD-GC-9-Programmes für jede Bruttoretentionszeit der Retentionsindex berechnet werden; dazu sind im K-Satz die Bruttoretentionszeiten von Referenzpeaks des Bezugskanals notwendig. Im I-Satz sind die Indices der Referenzpeaks anzugeben. Im Analysenausdruck sind neben Bruttoretentionszeit und Retentionsindex die Flächenanteile der Peaks der Kanäle in vier Spalten angegeben. Zusätzlich besteht die Möglichkeit, für alle von einem Kanal gefundenen Komponenten aus einer abgespeicherten Tabelle an Hand der Indices Identifizierungsvorschläge zu machen. Dazu müssen im I-Satz die Tabellennummer, die Torbreite in Indexeinheiten für die Tabellensuche und der abzuarbeitende Kanal definiert werden.

MPD-GC-7

Dieses Programm dient zur Vorbereitung des Plottens eines Meßsatzes. Über eine Laborschreibmaschine werden ein I- und ein K-Satz sowie weitere Parameter im Time-sharing-Betrieb eingegeben.

BEISPIEL, DISKUSSION

Die Möglichkeiten der rechnergestützten Auswertung der Daten einer GC/MPD-Kopplung sollen an einem Test-Chromatogramm gezeigt werden (Abb. 5). Die Ergebnisse der Querempfindlichkeitsbestimmung (MPD-GC-1) und der Bestimmung der relativen Empfindlichkeit (MPD-GC-2) sind in Abb. 6(a—d) zusammengefaßt; aus Platzgründen und zur besseren Übersicht sind die Ergebnisse in Diagrammform wiedergegeben. Schließlich sind in Tabelle 1 die Ergebnisse der Elementverhältnisermittlung (MPD-GC-3) und der Retentionsindexbestimmung (MPD-GC-4*3) zusammengefaßt. Zum besseren Vergleich sind hier die aus den gefundenen Elementverhältnissen errechneten Summenformeln angegeben; die Werte sind an den Peakmaxima der einzelnen Kanäle gefunden. Bei einigen Peaks stimmen die gefundenen Werte mit der Theorie nicht überein, da sich offensichtlich zwei Komponenten, die eine verschiedene Elementzusammensetzung haben, stark überlagern (Komp. 7 + 8 und Komp. 17 + 18). Hier kann eine Interpretation der Elementverhältnisse an den Peakflanken weiterhelfen. Bei 1639 s findet man einen deutlichen Hinweis auf eine wasserstoffreiche Verbindung; trotz "Verschmelzung" der Peakspitzen von Komp. 7 + 8 auf dem C-Kanal ist eine Retentionszeitbestimmung der Komp. 7 (H-Kanal) und der Komp. 8 (Cl-Kanal) hinreichend genau möglich. Auch die Elementverhältnisermittlung für Komp. 8 an der Peakflanke (1651 s) führt zu einem brauchbaren Ergebnis. Die Komponenten 17 und 18 sind wegen ähnlicher Elementzusammensetzung bei vermutlich ähnlichen Retentionszeitunterschieden wie bei den Komponenten 7 und 8 auf keinem der Kanäle als angetrennte Peaks wiederzufinden. Eine Untersuchung der Elementverhältnisse an den Peakflanken führt zu dem Schluß, daß wahrscheinlich $C_7H_4N_2O_4Cl$ etwas früher als $C_6H_3NO_2Cl_2$ eluiert (s. Tab. 1).

Das gezeigte Beispiel demonstriert, daß eine rechnergestützte Auswertung von GC/MPD-Rohdaten eine rasche Aussage über Elementverhältnisse und Retentionszeiten ermöglicht. Die konventionelle Auswertemethode über Peakhöhenvergleich würde hier unter hohem Zeitaufwand nur bei getrennten Komponenten zu gut verwertbaren Ergebnissen führen; zur Erreichung einer Genauigkeit wie bei der Rechnerauswertung ist bei der konventionellen Methode zur Erstellung einer Eichkurve nochmals ein vielfacher Zeitaufwand nötig. Erst mit Hilfe des Rechners können jetzt auch entlang des Peakprofils Elementverhältnisse ermittelt werden: Eine fast vollständige Peaküberlappung, wie sie beispielsweise bei der Detektion mit einem FID erst nach einigen Änderungen (Temperaturänderung, Gasflußänderung, Säulenwechsel) unter Zeitaufwand beherrscht werden kann, stellt bei Detektion mit dem MPD in Verbindung mit dem Rechner häufig kein großes Hindernis zur präzisen Bestimmung von Retentionszeit und -index dar.

Es soll hier aber auch auf noch bestehende Schwierigkeiten hingewiesen werden. Das ungünstige Signal/Rausch-Verhältnis der Kanäle für Stickstoff und Sauerstoff begrenzt für diese Elemente den Anwendungsbereich erheblich.

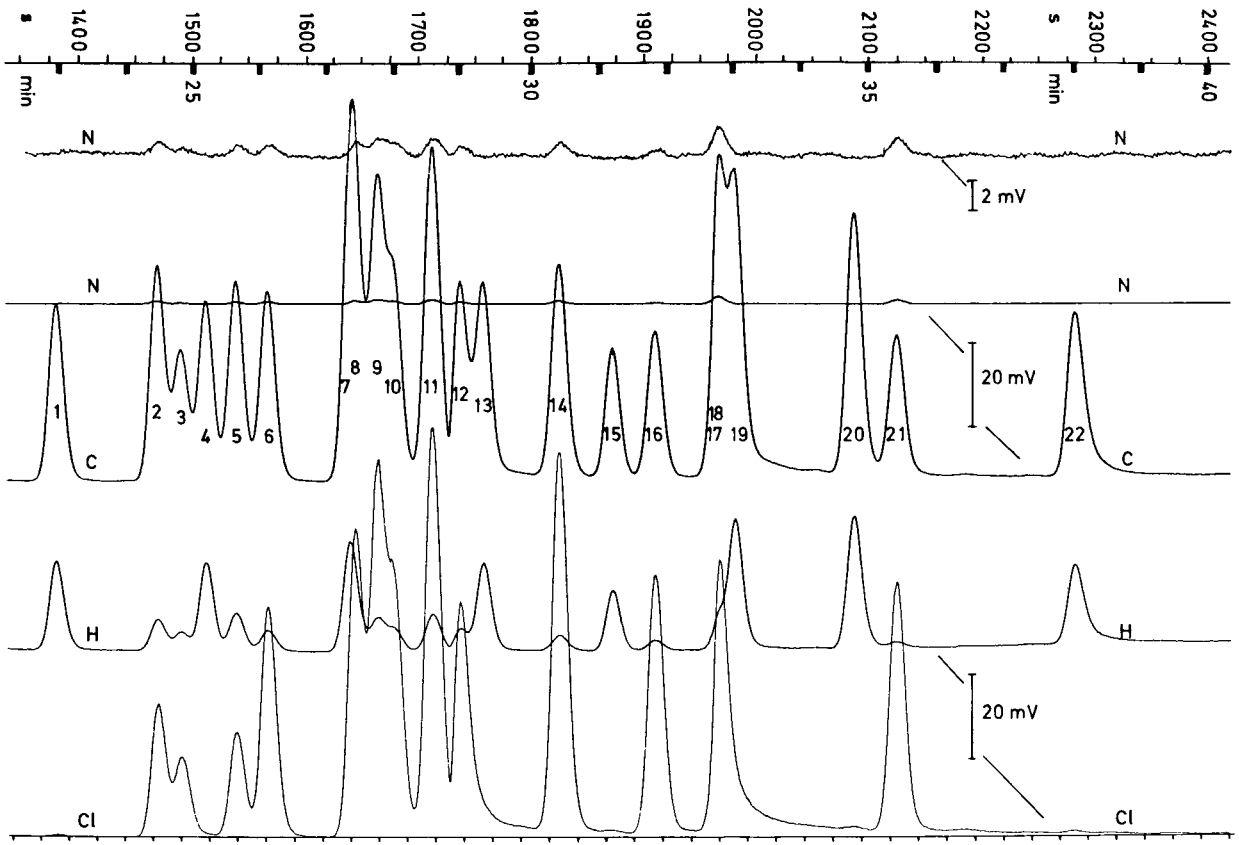

Abb. 5. Plott eines Teils eines Test-Chromatogramms (der N-Kanal wurde zweimal geplottet). Die Probe besteht aus *n*-Paraffinen und aus chlorierten und nitrierten Derivaten von Benzol, Toluol und Phenol (je etwa 0,1%) in Toluol. GC-Bedingungen: 2-m Glassäule, 15% OV-17 auf Chromosorb W; Temperaturprogramm, 5 min 60°C. Temperaturrate 6°C min^{-1}. Temperatur-Ende 260°C. Dosiert, 0,3 μl.

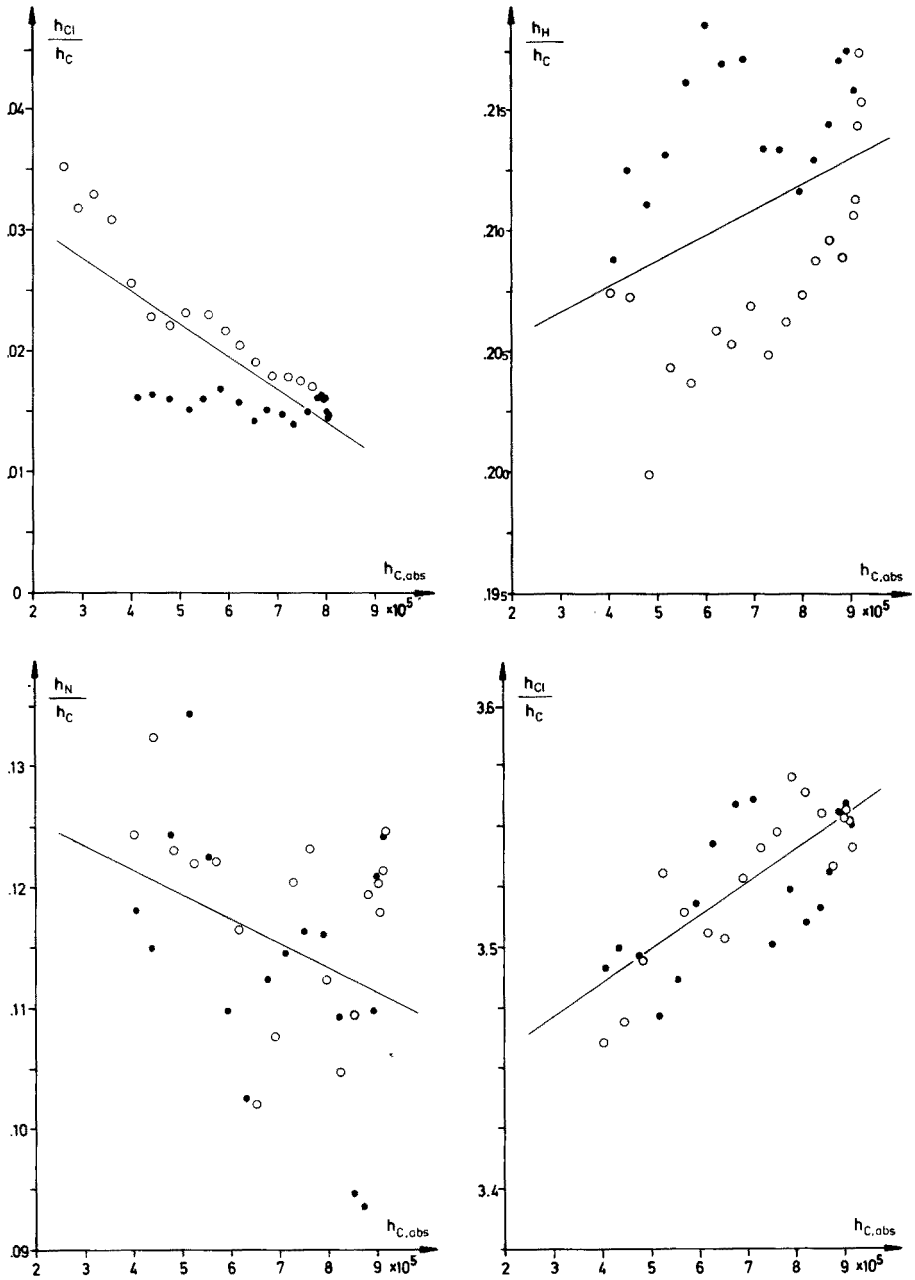

Abb. 6. Darstellung der Ergebnisse der Eichprogramme. Die eingezeichneten Ausgleichsgeraden geben die vom Rechner ermittelte Eichgerade wieder. (a) Bestimmung der Störung des Cl-Kanals durch den C-Kanal (MPD-GC-1). (b—d) Messung der relativen Empfindlichkeit für H/C, N/C und Cl/C (MPD-GC-2). ○ Meßpunkt von aufsteigender Peakflanke. • Meßpunkt von absteigender Peakflanke. 10^5 Skalenteile der Abszisse entsprechen ca. 6.1 mV.

TABELLE 1

Zusammenfassung der wichtigsten Ergebnisse von den Programmen MPD-GC-3 und MPD-GC-4*3
(Die mit "*" bezeichneten Indices sind die gewählten Stützstellen. Komp. Nr. 14 diente zur Erstellung der Eichgeraden für die relative Empfindlichkeit.)

Komp. Nr.	Retentions-		Summenformel				
	Zeit (s)	Index	der Test-substanz	aus gefundenem Elementverhältnis berechnet			
				C	H	N	Cl
1	1379	1400,0*	$C_{14}H_{30}$	14	33,15	—	—
2	1470	1467,5	$C_6H_4NO_2Cl$	6	4,098	0,936	1,026
3	1490	1482,8	$C_6H_4NO_2Cl$	6	4,080	0,888	1,026
4	1512	1500,0*	$C_{15}H_{32}$	15	34,80	—	0,029
5	1539	1520,9	$C_7H_6NO_2Cl$	7	6,209	0,979	1,013
6	1567	1543,0	$C_6H_3NO_2Cl_2$	6	3,127	0,894	2,026
	1628			16	28,96	—	0,918
7	1639	1601,3	$C_{16}H_{34}$	16	22,47	1,220	2,810
8	1644	1605,5	$C_6H_3NO_2Cl_2$	6	6,447	0,648	1,386
	1651			6	4,600	0,671	1,735
9	1665	1622,2	$C_6H_3NO_2Cl_2$	6	3,036	0,914	2,023
10	1676	1631,7	$C_6H_3NO_2Cl_2$	6	3,081	0,906	2,050
11	1713	1662,3	$C_6H_3NO_2Cl_2$	6	3,019	0,931	2,019
12	1737	1682,6	$C_6H_3NO_3Cl_2$	6	3,181	0,867	1,972
13	1757	1700,0*	$C_{17}H_{36}$	17	35,77	—	0,738
14	1824	1758,7	$C_6H_2NO_2Cl_3$	6	2,025	1,094	2,987
15	1870	1800.0*	$C_{18}H_{38}$	18	39,56	—	0,154
16	1908	1834,8	$C_6H_2NO_2Cl_3$	6	1,958	1,036	2,995
	1957			7	3,459	1,983	1,330
				6	2,965	1,700	1,140
17 + 18	1965	1887,9	$C_7H_4N_2O_4Cl$	7	3,984	1,714	1,608
			$C_6H_3NO_2Cl_2$	6	3,415	1,492	1,378
19	1978	1900,0*	$C_{19}H_{40}$	19	35,48	0,838	1,483
20	2083	2000.0*	$C_{20}H_{42}$	20	46,09	—	0,184
21	2121	2037,2	$C_6HN_2O_4Cl_3$	6	1,229	1,916	2,999
22	2278	2200,0*	$C_{22}H_{46}$	22	50,73	—	0,070

Die Methode der Ausgleichsgeraden bei den Eichungen erlaubt nur innerhalb eines relativ kleinen dynamischen Bereiche eine hinreichend genaue Bestimmung der Elementverhältnisse (s. oben).

Für Konstruktion und Bau des Interfaces danken wir Herrn Becker, Frau Larsen und Frau Berkemeier haben wir für umsichtige Konzeption und sorgfältige Detailausarbeitung der erforderlichen Programme zu danken, der BASF Aktiengesellschaft, Ludwigshafen, für die Erlaubnis zur Veröffentlichung der Arbeit.

LITERATUR

1 A. J. McCormack, S. S. C. Tong und W. D. Cooke, Anal. Chem., 37 (1965) 1470.
2 C. A. Bache und D. J. Lisk, Anal. Chem., 39 (1967) 786.
3 W. R. McLean, D. L. Stanton und G. E. Penketh, Analyst, 98 (1973) 432.
4 R. M. Dagnall, T. S. West und P. Whitehead, Analyst, 98 (1973) 647.
5 W. R. McLean, The Microwave Plasma Detector System, aus D. R. Hodges (Ed.), Recent Analytical Developments in the Petroleum Industry, Applied Science Publishers Ltd., 1974, p. 139.
6 F. A. Serravallo und T. H. Risby, Anal. Chem., 47 (1975) 2141.
7 P. Brassem und F. J. M. J. Maessen, Spectrochimica Acta Part B, 30 (1975) 547.
8 H. Günzler, Chemie-Ing.-Techn., 42 (1970) 877.
9 F. Caesar und M. Klier, Chromatographia, 7 (1974) 525.

Analytica Chimica Acta, 103 (1978) 43—60
Computer Techniques and Optimization
©Elsevier Scientific Publishing Company, Amsterdam — Printed in The Netherlands

A USER-ORIENTED SOFTWARE FOURIER SPECTRUM DISPLAY FOR ANALYTICAL PURPOSES

H. L. WALG and H. C. SMIT*

Laboratory for Analytical Chemistry, University of Amsterdam, Nieuwe Achtergracht 166, Amsterdam (The Netherlands)

(Received 1st June 1977)

SUMMARY

A multipurpose Fourier spectral analysis program is presented. The particular features are: great flexibility with respect to the input data and output possibilities; optimum performance without pre-knowledge of Fourier spectral theory; confidence limits are supplied wherever possible. The program is based on profound theoretical considerations and has been tested extensively. It is an inexpensive but valuable tool in analytical data analysis, determination of detection limits, optimization, detector development and many other fields.

One of the main objects in analytical research is to specify and, above all, to minimize systematic and random errors in analytical methods. Many analytical techniques deliver dynamic (time-varying) signals containing the desired information, e.g. chromatography, flameless atomic absorption, electroanalytical methods, etc. Optimum information processing and error calculations are only feasible after signal and noise parameters in both time and frequency have been specified, e.g. the detection limit in chromatography can be computed [1] from the power spectrum of the base-line noise, and the random error in other dynamic analytical methods can be calculated.

The study of detectors in analytical chemistry is very important, especially in chromatography; the merits of detectors cannot be assessed without determining the dynamic (systems-theoretical) properties by means of auto-covariance functions (a.c.v.f.), cross-covariance functions (c.c.v.f.), and transfer functions.

Analysis in the frequency domain by Fourier transforms of a.c.v.f., c.c.v.f., and time series is an important aid. This applies especially to the frequency power spectrum, but often the phase information cannot be neglected.

Electronics and digital computers have created the possibility of new techniques, e.g. correlation chromatography [2], lock-in amplifiers as a part of a g.l.c. detector [3], signal enhancement, signal averaging, etc. Again signal and noise analysis in the time and frequency domain are essential.

The automation of several analytical techniques also makes frequent use of Fourier transforms of signals. To prevent distortion and aliasing in digitizing of signals in on-line micro- or minicomputer applications, an accurate signal analysis is necessary. Correct sample frequencies as well as optimum and matched filter characteristics can be determined.

Another field of interest is laboratory optimization. Studies can be made of series of analytical measurements to check for periodicities, most probable trends in concentration, etc., by Fourier transformation; these examples of the use of Fourier transformation offer a wide variety of either time series, sampled mostly from low frequency signals, or a.c.v. and c.c.v. functions. The latter can be obtained by means of a hardwired device (Hewlett-Packard, PAR) or by separate computer calculation from time series.

All possible data formats can occur. Off-line processing is satisfactory and of universal applicability. Both stochastic and deterministic signals can be present. Power spectra, amplitude spectra and phase spectra, both unsmoothed and smoothed, have to be determined. The calculation of statistical confidence levels of spectra is useful; the Fourier transform output should be available as a table and/or a plot.

To a certain extent some hardwired Fourier transformers (Hewlett-Packard, Spectral Dynamics) come up to these requirements and are of reasonably universal applicability. Some analytical techniques (n.m.r., i.r.) use dedicated instruments for Fourier transformation; these instruments are not available for the universal applications mentioned. Certain limitations (limited number of data points, no calculation of the confidence levels) and the relatively high price for an instrument that is used infrequently prevent general use of the universal hardware devices, even in research.

The software solution, as presented in this paper, is intended as a contribution to statistical and deterministic signal analysis. It can be an inexpensive and useful tool for every analyst with access to a digital computer, but the main application will probably be limited for the present to research and education.

The lack of experience of many analysts in (mathematical) signal analysis is taken into account in developing the program.

Required properties of a software solution

Although numerous fast Fourier transform (FFT) algorithms and source texts in several programming languages are available [4], the FFT should be pre- and post-processed to achieve a complete and universal spectrum analysis program.

The few existing commercial packages are strongly dependent on the type of computer; published programs still require a lot of knowledge and work to be usable in practice.

The object of the authors has been to develop for analytical use a user-oriented Fourier spectral analysis program with similar features to a hardwired

spectral analyser, but without the disadvantages already mentioned. The demands were as follows.

(1) The program should be able to process a.c.v.f., c.c.v.f., and time series.

(2) Program output: power-, amplitude- and phase-spectra, unsmoothed as well as smoothed: spectra with confidence levels available as a table and/or a plot, presented so as to avoid interpretation troubles. Results must be correct with respect to the qualities obtained.

(3) The program has to be usable by chemists without a profound knowledge and experience of Fourier techniques, and safeguarded against misuse; any occurrence has to be flagged.

(4) Universal implementation on any type of computer, if not too small, must be possible. Program language: highly standardized, ANSI FORTRAN.

(5) Versatile input/output structure:
input devices: magtape, cards, papertape and diskfiles.
output devices: line printer, tapepunch, terminal and plotter.

These demands imply an excessive I/O procedure (interactive mode of operation), that consumes the greater part of computational time. Thus it is meaningless to improve existing FFT routines.

THEORY

A description of the complete theoretical basis and of all considerations is beyond the scope of this paper. However, sometimes more than one definition is adopted in the literature. To avoid wrong interpretation of the results, a description of the essential definitions and formulae used in the program is necessary. No new theory is given; an extensive theoretical treatment can be found in the literature.

Autospectra

The power-spectral density (p.s.d.) $G_x(f)$ of a time function $x(t)$ is defined as [5]:

$$G_x(f) = \lim_{\Delta f \to 0} \frac{P_x(f, f + \Delta f)}{\Delta f} = \lim_{T \to \infty} \frac{2}{T} |F(f)|^2$$

where T = sample record length, and $x(t) \overset{\text{f.t.}}{\longleftrightarrow} F(f)$.

The power spectrum P_x is defined as:

$$P_x(f, f + \Delta f) = \lim_{T \to \infty} \int_0^T x^2(t, f, \Delta f)\, dt \qquad (2)$$

$G_x(f)$ can be determined either directly from the time series or via the covariance function (Wiener-Khintchine).

In both cases only a sample of $x(t)$ of finite duration can be processed. The results will be a distorted version of the true p.s.d.: the sample power-spectral density. A proper choice of the sample record length T can shift the distortion to uninteresting frequency ranges.

The obligatory discretization of x(t) is a periodicity operation: consequently, a periodical and distorted version $F(f)_{per}$ of the desired Fourier Transform F(f) of x(t) is determined. A proper choice of the sample time Δt prevents alias distortion (Shannon sample theorem). In digital computers the best attainable result will be a Fourier pair relationship between two possibly aliased periodic functions $x(n\Delta t)_{per}$ and $F(k\Delta f)_{per}$; $x(n\Delta t)_{per}$ and $F(k\Delta f)_{per}$ are the periodically repeated versions of x(t) and F(f).

A mapping from the frequency domain to the time domain can be achieved by means of the infinite but discrete Fourier series:

$$x(t) = \sum_{k=-\infty}^{\infty} c(kf_0)\, e^{j2\pi k f_0 t} \tag{3}$$

where $f_0 = 1/T$. The spectral properties can be determined from the complex Fourier coefficients, because of the simple relationship between Fourier coefficients and the Fourier transform of a periodic function. The Fourier coefficients are defined as:

$$c(kf_0) = \frac{1}{T} \int_{-T/2}^{T/2} x(t)\, e^{-j2\pi k f_0 t}\, dt \tag{4}$$

An approximate estimate of eqn. (4) can be obtained with the aid of the trapezoid rule for sampled data:

$$\begin{aligned} c(kf_0) &= \frac{1}{N\Delta t} \int_{0}^{(N-1)\Delta t} x(n\Delta t)_{per} \cdot e^{-j2\pi n \Delta t k \Delta f}\, dt \\ &= \frac{1}{N\Delta t} \sum_{n=0}^{N-1} x_s(n\Delta t)_{per} \cdot e^{-j2\pi n \Delta t k \Delta f}\, \Delta t \\ &= \frac{1}{N} \sum_{n=0}^{N-1} x_s(n\Delta t)_{per} \cdot e^{-j2\pi k/N} = c(k\Delta f)_{per} = DFT\{x(n\Delta t)_{per}\} \end{aligned} \tag{5}$$

where $n = 0, 1, \ldots N-1$, $k = 0, 1, \ldots N-1$, x_s is the sample from x(t) at $t = n\Delta t$, and DFT is the discrete Fourier transform. The consequences of the application of the DFT to the various kinds of time functions (periodic, non-periodic, even, odd, etc.) can be found in the literature [6--8].

The use of the DFT as a signal processing tool has been made attractive in practice by the development of fast Fourier transform (FFT) algorithms, calculating

$$a_k = \sum_{n=0}^{N-1} x_n e^{-j2\pi nk/N} = N.DFT(x_n) \tag{6}$$

by only about $N.\log_2 N$ operations instead of about N^2 necessary for the straightforward computation of eqn. (6).

The Fourier coefficients can be affected by leakage of the spectral estimates [4, 8]. Leakage is caused by a sine wave that is non-periodic in the rectangular analysing window. The remedy is a multiplication of x(t) by a certain time-function (window) before transforming [8—11]. A Tukey window with a full cosine-bell shape is the most favourable one in many cases [10].

In the case of stochastic time series, the p.s.d. is commonly determined by means of the a.c.v.f.

Use of the aperiodic linear sample a.c.v.f. estimate:

$$R_{xx}(\tau) = \frac{1}{T}\int_0^{T-\tau} \{x(t) - \bar{x}\}\{x(t+\tau) - \bar{x}\}dt; \qquad (-T \leqslant \tau \leqslant T)$$
$$= 0 \qquad (|\tau| > T) \tag{7}$$

is more favourable than the use of the circular a.c.v.f. estimate, only if no window is applied; otherwise both linear and circular a.c.v.f. can be used equally.

In the linear estimate (eqn. 7), the theoretical a.c.v.f. is multiplied by a triangular lag window.

Cross-spectra

The definition of the linear sample cross-covariance function estimate (c.c.v.f.) is:

$$R_{xy}(\tau) = \frac{1}{T}\int_0^{T-\tau} \{x_1(t) - \bar{x}_1\}\{x_2(t+\tau) - \bar{x}_2\}dt; \qquad (0 \leqslant \tau \leqslant T)$$
$$R_{xy}(-\tau) = \frac{1}{T}\int_0^{T-\tau} \{x_1(t+\tau) - \bar{x}_1\}\{x_2(t) - \bar{x}_2\}dt; \qquad (0 \leqslant \tau \leqslant T) \tag{8}$$

The complex sample cross-spectrum is defined as:

$$C_{xy}(f) = \int_{-T}^{T} R_{xy}(\tau) \cdot e^{-2j\pi f\tau} d\tau \tag{9}$$

The complex quantity $C_{xy}(f)$ can be written as:

$$C_{xy}(f) = |C_{xy}(f)| \cdot e^{j\theta_{xy}(f)} \tag{10}$$

where $|C_{xy}(f)|$ is called the cross amplitude spectrum.

The variability is treated in the computational section.

THE PROGRAM*

The program meets the stated requirements. The excessively large I/O procedure implies the necessity of overlays.

In the program, consisting of one main overlay and eight primary overlays, every set of data is submitted to both an unsmoothed and a smoothed transform: the first and second pass (Fig. 1). Two input procedures are available, one for fixed format decimal or octal integers, and one for free-format reals or decimal integers. Interactively the user can make a selection of the output if no lineprinter is present. Plotter output is available, but always on request. All non-numerical information input should be supplied on the computer request; a yes/no reply is sufficient except for the output-identification code. (Examples are the choice from the I/O-device possibilities in the computer configuration, the type of data (a.c.v.f., c.c.v.f. or time series), the desired amount of lineprinter output, the desirability of plotter output, and the alphanumerical identification code.) Computer requests for numerical input are in free format. (Examples are the time-scale factor, the amplitude-scale factor, the expected number of data points, and possibly the total number of points from which an average (a.c.v.f. and c.c.v.f.) has been determined.) Data input validity checks for both alpha input and numerical input are present. Finally, there are extensive possibilities for data input corrections.

The intention of the fixed format integer data input procedure is to collect octal or decimal integers from multichannel devices with a fixed number of channels (maximum 1000).

A data set might consist of 10 ASCII characters. Reading is performed in blocks of 7 data points at each logical record, with subsequently close-packed writing on disk. Reader errors, parity errors and data length errors (more than 1000 points) are considered as end-of-tape conditions.

After rewinding, the data are analysed by an error-detecting subroutine, building-up numerical data from the ASCII characters. The size of the data expected by the subroutine can be modified by a single data statement.

Erroneous data are displayed with the matching channel number and can be corrected by the user. The total number of data is compared with the expected number; if a difference is found, the user can decide to continue or to abort the program.

The requirements for the free-format real/integer data input procedure, collecting data from digital voltmeters or similar devices, are rather different. First, the number of data points is free (up to 1000) and depends on the record length and the sampling interval. Secondly, data points may appear in an integer format of arbitrary length, or in an E- or F format with arbitrary length of the integer and fractional parts of the mantissa. Also the exponent part of E-format numbers may have an arbitrary length, while fractional exponents in E-format numbers can occur. Thirdly, erroneous

*Listings of either a CDC 6500 version or a Varian V-70 version are available at copy costs.

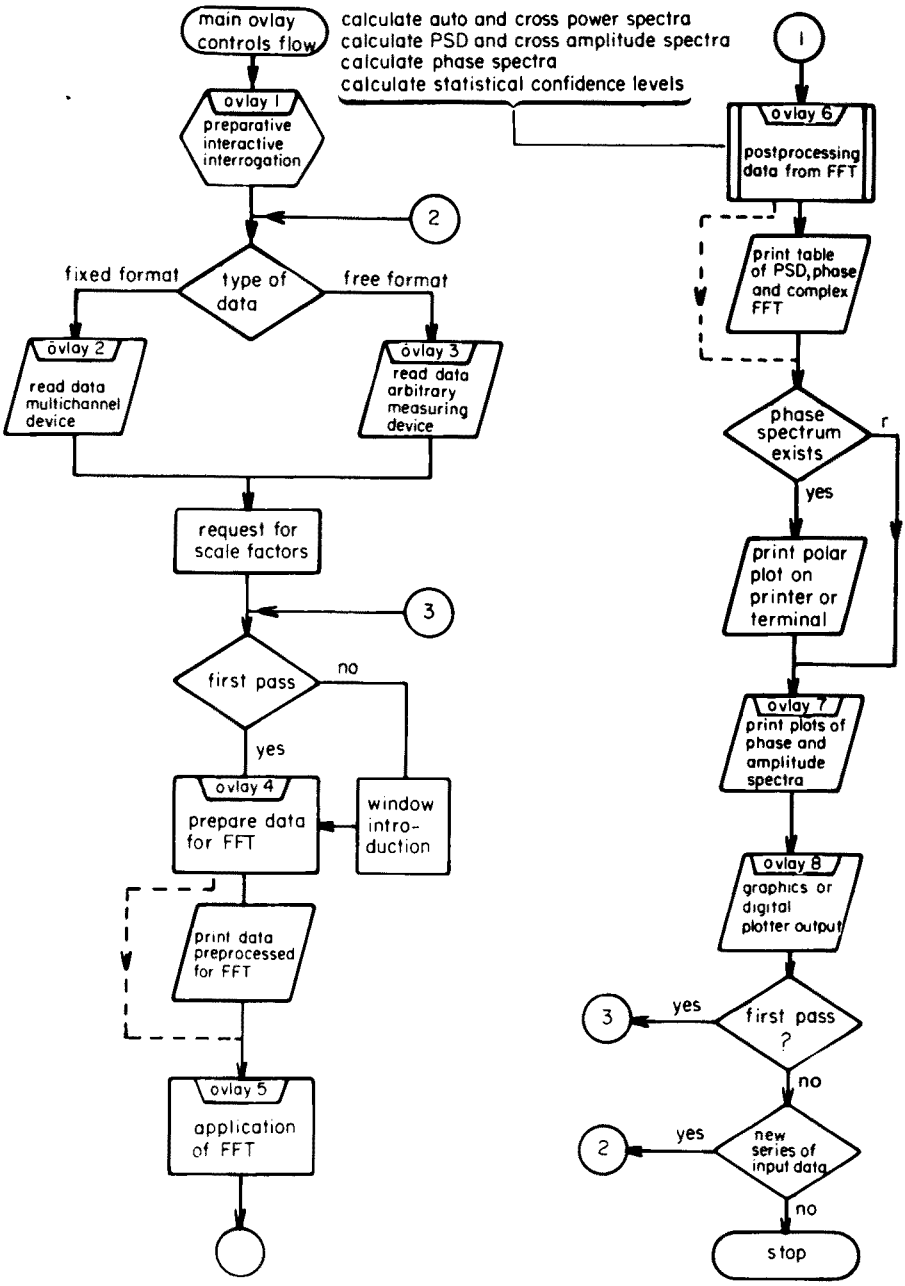

Fig. 1. System flow of the general purpose program.

data points should be dropped, because generally the correct value is unknown. For the rest, the procedure is about the same: the number of data points is restricted to 1000 because of the required memory in the f.f.t. routine. Finally, the usable number of data points is displayed.

COMPUTATIONAL PROCEDURES

The mixed-radix FFT subroutine from Singleton [11] is used. The auxiliary array length in this subroutine has been chosen in such a way that factorization of the input data length may yield primes up to 97. To avoid higher primes occurring, an algorithm is used, manipulating the data length by means of a truncation or extension by, at most, 1%. Thus any input data length up to 1000 can be directly transformed without array-space difficulties. The error in the frequency domain can be neglected. This procedure will be referred to as adjusting the array length.

The prime factor algorithm is preferred to the radix-2 algorithm, because the zero-appending or circular continuation can be avoided. The latter gives reliable results if the circular a.c.v.f. is a better estimate than the linear one. This is the case for a deterministic periodic time series, in contrast to a stochast where the linear a.c.v.f. is preferred. In the last case, zero-appending would be preferable [12]; the results for a deterministic periodic time phenomenon are however inferior. Hence, the demands are conflicting; it is better to use the prime factor method in a general-purpose program.

It is advisable, however, to use the information that is available. If, for instance, one half of an even function has been measured, the complete even function may be used as the input for the FFT-routine.

THE AUTOCOVARIANCE FUNCTION

Unsmoothed pass

The adjusted length of the a.c.v.f. is extended by even continuation at negative τ-values, as discussed in detail in the c.c.v.f.-transform section. The resolution is doubled, retaining the same Nyquist-frequency (N points in, N points out). The memory requirements of the FFT subroutine will turn out to be completely determined by the cross-covariance function transform. The I/O procedures are by far the most time-consuming. So none of the special algorithms are applied to reduce the core-size requirements for the DFT of a real function. The imaginary time data array is filled with 2N zeroes.

The p.s.d. estimator, in this case, is:

$$C_{xx}(k\Delta f) = 2\Delta t\,\{FFT(R_{xx}(l\Delta t))\} \tag{11}$$

where $l = 0, 1, 2, \ldots, 2N-1$; $k = 0, 1, 2, \ldots, N-1$; and $\Delta f = 1/(2N\Delta t)$. The phase relationship is absent.

Smoothed pass

After re-reading and adjusting the array length, the a.c.v.f. is multiplied by the window coefficients, depending on the chosen window type and intersection point. The user can select a Bartlett, a Tukey, a Parzen or a rectangular window. Also the quantity

$$I = 2 \sum_{l=0}^{M-1} w(l\Delta t)^2/(M) \tag{12}$$

is calculated. This is the discrete equivalent of

$$\frac{1}{T_m} \int_{-T_m}^{T_m} w^2(\tau)d\tau \tag{13}$$

$w(l\Delta t)$ and $w(\tau)$ are window values; T_m is the intersection point (last non-zero lag value in continuous time); and $M - 1$ is the index of the point corresponding to T_m in discrete time. I is used in statistical post-processing. When the same procedures as in the unsmoothed pass are used (doubling etc.), the smoothed p.s.d. is estimated by means of

$$\bar{C}_{xx}(k\Delta f) = 2\Delta t\{FFT(R_{xx}(l\Delta t) \cdot w(l\Delta t))\}, \tag{14}$$

where $l = 0, 1, 2, \ldots, 2N - 1$; $k = 0, 1, 2, \ldots, N - 1$; and $\Delta f = 1/(2N\Delta t)$.

TIME SERIES TRANSFORM

Unsmoothed pass

Only time series with mainly non-stochastic (periodic) components give reliable spectrum estimators.

Apart from a data length adjustment, no further manipulation, either by appending zeroes or circular continuation, is performed. Corresponding to Dirichlet's conditions, the first data point is replaced by the averaged value of the first and the last data point. The space for the imaginary part of the time data is filled with zeroes.

The raw periodogram is computed from

$$C_{xx}(k\Delta f) = \frac{2\Delta t}{N} |FFT(x_n)|^2 \tag{15}$$

where $x_n = x(n\Delta t)$, $n = 0, 1, \ldots, N - 1$; $k = 0, 1, \ldots [N/2] - 1$; and $\Delta f = 1/(N\Delta t)$.

The phase spectrum is given by:

$$\theta(k\Delta f) = \arctan\left[\frac{Im\{FFT(x_n)\}}{Re\{FFT(x_n)\}}\right] \tag{16}$$

Only 1/2 N usable spectral estimators are obtained. No hanning is implemented because the type of data in analytical chemistry generally does not lead to leaked spectra. Moreover, either optional or built-in hanning

would cause disadvantages: too slow program execution, too gross program flow, and an excessive amount of output. Also a certain pre-knowledge about the resulting spectrum is required for a proper use of hanning.

If, nevertheless, a user persists on the hanning periodogram transform, the authors suggest that it is performed in the sense switch mode, depending on the computer type. The window correction term [13] should then be introduced. In any event, drift and offset have to be recognised in a time series before the hanning coefficients may be applied. Generally this problem is yet unsolved.

Smoothed pass

In the smoothed pass, mainly usable for stochastic time series, the array length is readjusted after re-reading. The offset is corrected by subtraction of the average of the time series.

Computation of the circular a.c.v.f. with subsequent introduction of the window coefficients is the most important step. The window width or maximum lag (τ_{max}) can be controlled by the user if the default value is unacceptable.

The circular a.c.v.f. is computed over M points ($M \leqslant N$) from

$$R_{xx}(\tau)_{circ} = R_{xx}(l\Delta t)_{circ} =$$

$$= \frac{1}{N} \sum_{n=0}^{N-1} \{x_{per}(n\Delta t) - \bar{x}\} \{x_{per}((n + l)\Delta t) - \bar{x}\} \qquad (17)$$

where $l = 0, 1, 2, \ldots, M - 1$; x_{per} is the circularly repeated time series; $(M - 1)\Delta t$ is the maximum lag at which $w(l\Delta t) \neq 0$; and $M \leqslant N/2$, because the circular a.c.v.f. is used. Nevertheless, to maintain N points as the input for the f.f.t. zeroes are appended up to N points.

The quantity I from eqn. (12) is computed (user-supplied window type) or substituted (program-supplied window type). The continued processing, including the appending of the negative τ-half, is identical to the smoothed a.c.v.f. transform.

CROSS-COVARIANCE FUNCTION TRANSFORM

Under laboratory conditions the c.c.v.f. generally represents an impulse response of a system. Because all real systems are causal, the c.c.v.f. is identical to zero at negative τ-values. If the input data are N-points from a correlator, encompassing completely or partially the non-zero range of the c.c.v.f. at positive τ-values, the total data length is extended with zeroes to 2N, causing a spectral resolution proportional to 1/2N.

The (real) c.c.v.f. is resolved into a real even and a real odd function after a slight data length adjustment. Both functions are transformed pseudo-separately.

Unsmoothed pass

The c.c.v.f. estimate, measured in N points with N − 1 appended zeroes, is defined as:

$$R_l^{xy} \equiv R_{xy}(l\Delta t) \approx R_{xy}(\tau); \qquad l = 0, 1, 2, \ldots, N-1$$
$$\equiv R_{xy}\{[(l.\ \text{modulo}\ N) - (N-1)]\Delta t\} = R_{xy}(-\tau) = 0;$$
$$l = N, N+1, \ldots, 2N-2 \tag{18}$$

The f.f.t. subroutine considers these 2N − 1 points as one complete period of the circular repetition of R_l^{xy}.

The even function is obtained by processing only half of the c.c.v.f. at positive τ-values:

$$E_l^{xy} = E_{xy}(l\Delta t) = 1/2\ R_l^{xy}; \qquad l = 0, 1, \ldots N-1$$
$$E_N^{xy} = E_{xy}(N\Delta t) = E_{xy}\{(N-1)\Delta t\}; \qquad l = N \tag{19}$$
$$E_l^{xy} \equiv E_{xy}\{[(l.\text{modulo}\ N) - N].\Delta t\} = 1/2\ R_{xy}\{[(2N-1) - (l-1)].\Delta t\};$$
$$l = N+1, \ldots, 2N-1$$

The function consists of N points measured, one auxiliary point to make the sequence length even, as is preferable for the FFT, and N − 1 points obtained by mirroring. The auxiliary point causes a negligible shift of the τ-values of the c.c.v.f.-estimate (maximum $1/2\Delta t$).

A similar procedure gives the odd function O_l^{xy}:

$$O_l^{xy} = 0; \qquad l = 0 \text{ (Dirichlet)}$$
$$O_l^{xy} = E_l^{xy}; \qquad l = 1, 2, \ldots, N-1 \tag{20}$$
$$O_l^{xy} = -E_l^{xy}; \qquad l = N, N+1, \ldots, 2N-1$$

The cospectrum and quadrature spectrum estimators $L_{12}(k\Delta f)$ and $Q_{12}(k\Delta f)$ are obtained by a separate Fourier transformation of E_l^{xy} and O_l^{xy}.

$$L_{12}(k\Delta f) = 2\Delta t\{FFT(E_l^{xy})\}$$
$$Q_{12}(k\Delta f) = 2\Delta t\{FFT(0_l^{xy})\} \tag{21}$$

where $l = 0, 1, \ldots, 2N-1$; $k = 0, 1, \ldots, N-1$; and $\Delta f = 1/(2N\Delta t)$.

The complex cross-spectrum can now be derived:

$$C_{xy}(k\Delta f) = L_{12}(k\Delta f) - jQ_{12}(k\Delta f) \tag{22}$$

The cross-amplitude spectrum estimator

$$|C_{xy}(k\Delta f)| = (L_{12}^2(k\Delta f) + Q_{12}^2(k\Delta f))^{\frac{1}{2}} \tag{23}$$

and the phase spectrum estimator, both widely used, can be calculated.

$$\theta_{xy}(k\Delta f) = \arctan\left\{\frac{-Q_{12}(k\Delta f)}{L_{12}(k\Delta f)}\right\} \tag{24}$$

Smoothed transform

The splitting-up into even and odd functions allows for the use of lag windows, symmetrical with respect to zero τ value. Hence, the procedure for the smoothed c.c.v.f. transform can be similar to the previously described smoothed a.c.v.f. transform, resulting in the smoothed cross-spectrum estimators:

$$\bar{C}_{xy}(k\Delta f) = FFT(2\Delta t\bar{E}_l^{xy}, 2\Delta t\bar{O}_l^{xy}) = \bar{L}_{12}(k\Delta f) - j\bar{Q}_{12}(k\Delta f) \tag{25}$$

where $l = 0, 1, \ldots, 2N-1$; $k = 0, 1, \ldots, N-1$; and $\Delta f = 1/(2N\Delta t)$, with

$$\bar{E}_l^{xy} \equiv E_{xy}(l\Delta t).w(l\Delta t) = 1/2\ R_{xy}(l\Delta t).w(l\Delta t) \tag{26}$$

and

$$\bar{O}_l^{xy} = 0; \bar{O}_l^{xy} = \bar{E}_l^{xy}; \bar{O}_l^{xy} = -\bar{E}_l^{xy} \tag{27}$$

analogously to eqn. (20). The smoothed cross-amplitude spectrum estimator:

$$|\bar{C}_{xy}(k\Delta f)| = (\bar{L}_{12}^2(k\Delta f) + \bar{Q}_{12}^2(k\Delta f))^{\frac{1}{2}} \tag{28}$$

and the smoothed phase spectrum estimator:

$$\bar{\theta}_{xy}(k\Delta f) = \arctan\left\{\frac{-\bar{Q}_{12}(k\Delta f)}{\bar{L}_{12}(k\Delta f)}\right\} \tag{29}$$

can then be calculated.

VARIABILITY OF SPECTRAL ESTIMATORS

It is useless to determine the confidence limits in the unsmoothed pass, because it gives usable results for deterministic signals only.

A.c.v.f. and time series transforms, smoothed by lag windows symmetrical around zero lag and satisfying certain conditions [10], give an expression for the normalized variance:

$$\frac{Var[\bar{C}_{xx}(k\Delta f)]}{G_{xx}^2(k\Delta f)} \approx \frac{1}{K}\,IM/N \tag{30}$$

where K is the number of segments used for averaging; M/N is the window closing ratio; and I is the quantity computed from eqn. (12). The use of a window can cause serious bias and a compromise between bias and variance reduction is necessary. In the case of an a.c.v.f., K is large and M/N = 1; for time series M/N = 1/3 because K = 1. All smoothed autospectral estimators have the same statistical distribution independent of frequency.

The random variable $Z_{xx}(f)$ satisfies:

$$Z_{xx}(f) = \frac{\nu\bar{C}_{xx}(k\Delta f)}{G_{xx}(k\Delta f)}\ DIS\ \chi_\nu^2,\ \nu \geqslant 2 \tag{31}$$

ν can be evaluated:

$$\nu = \frac{2G_{xx}^2(k\Delta f)}{Var[\bar{C}_{xx}(k\Delta f)]} = \frac{2.KN}{IM} \tag{32}$$

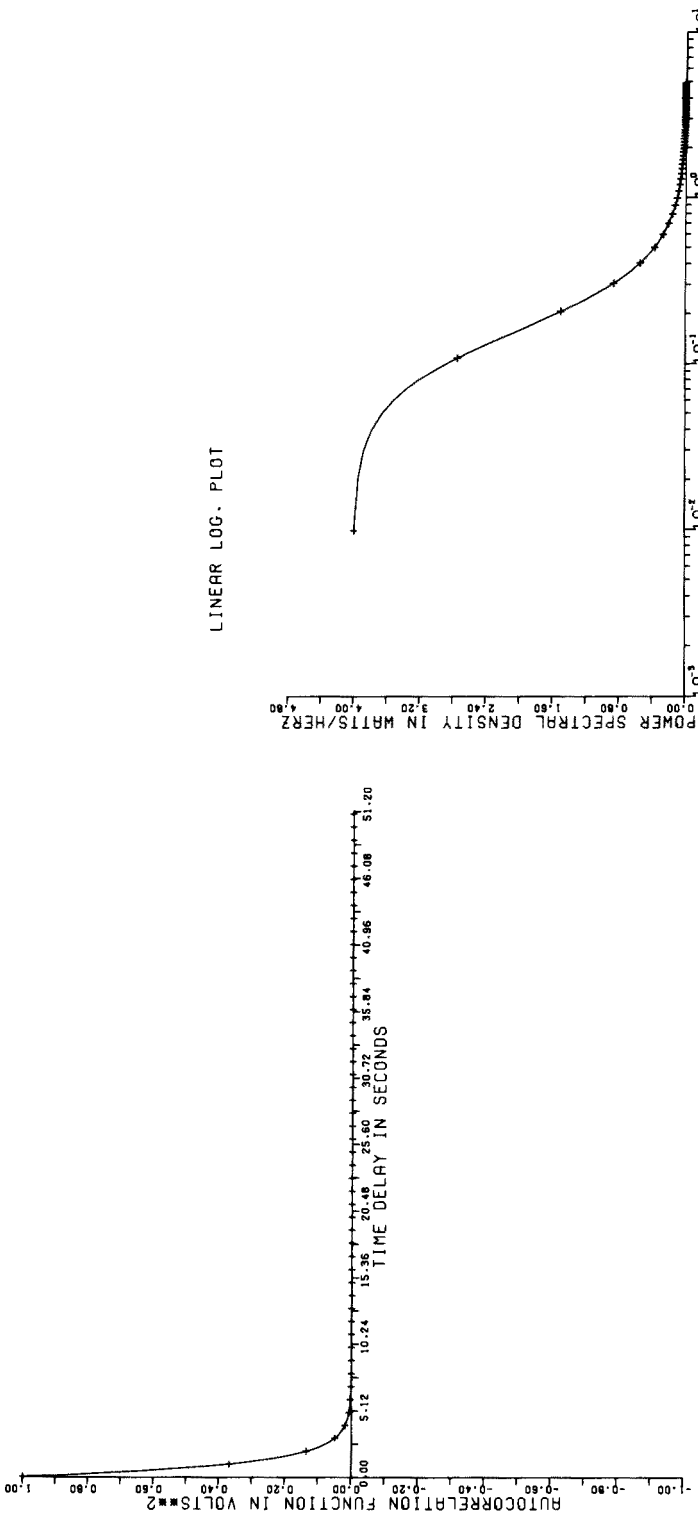

Fig. 2. Simulated a.c.v.f. $e^{-|\tau|}$ from first-order, band-limited white noise. $\Delta\tau = 0.1$ s.

Fig. 3. Unsmoothed p.s.d.-plot, obtained by transforming the a.c.v.f. from Fig. 2.

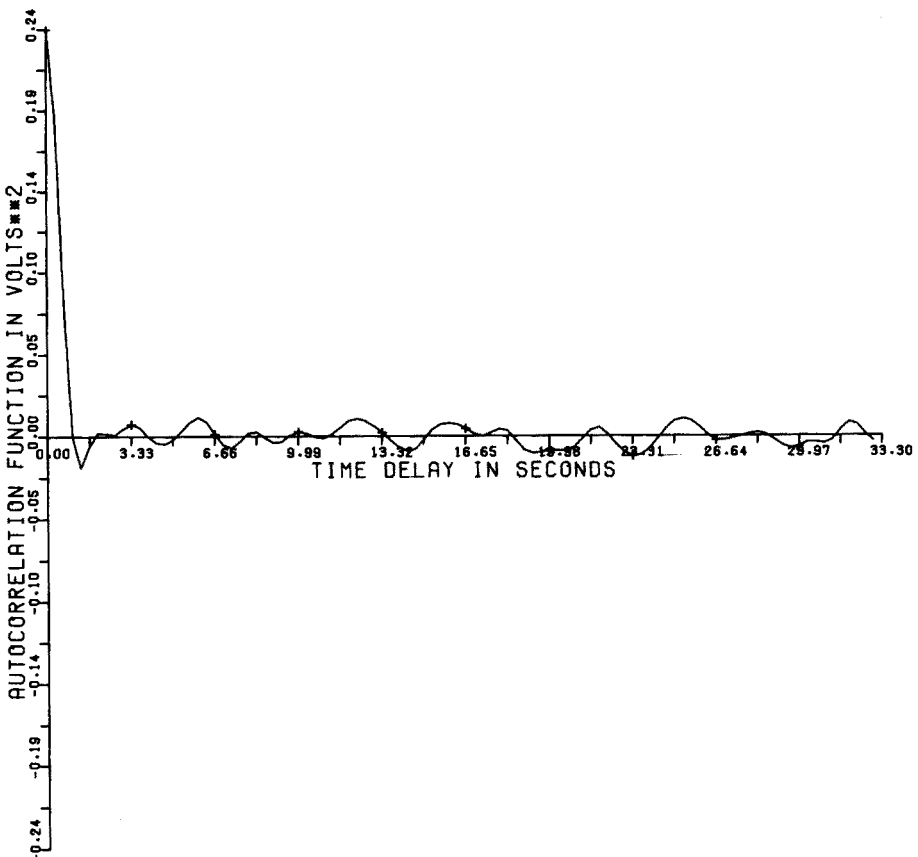

Fig. 4. Sample a.c.v.f. of higher-order, band-limited white noise, determined as an average of 40 segments of 100 points. $\Delta\tau$ = 0.333 s.

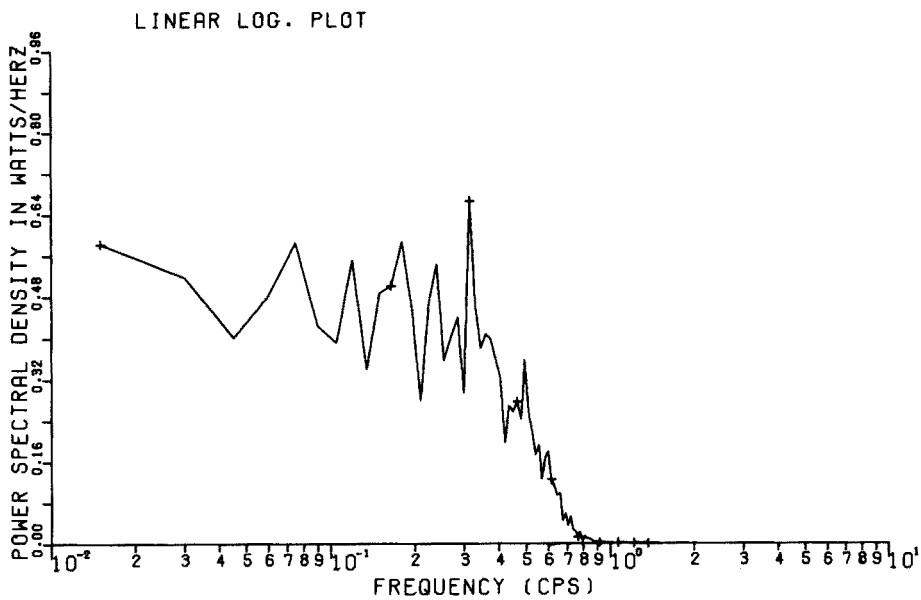

Fig. 5. Unsmoothed p.s.d. plot of higher-order, band-limited white noise, obtained by transforming the a.c.v.f. of Fig. 4.

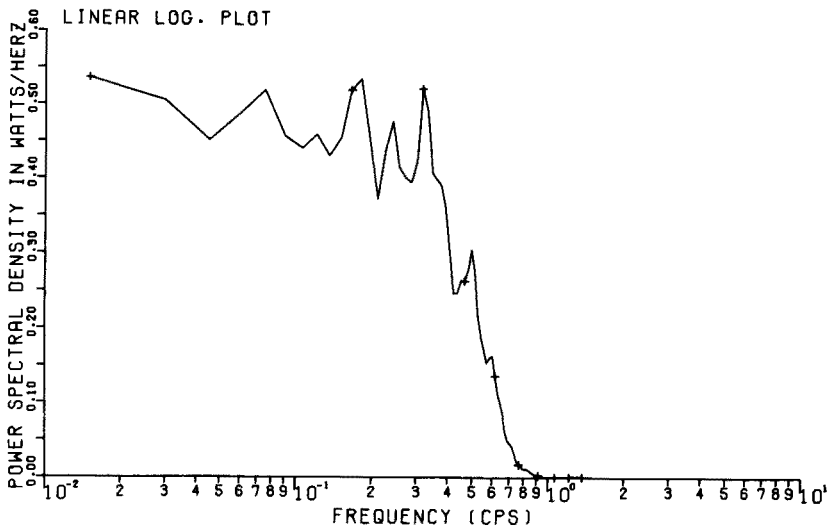

Fig. 6. Smoothed p.s.d. plot of higher-order, band-limited white noise, obtained by a windowed transform of the a.c.v.f. of Fig. 4.

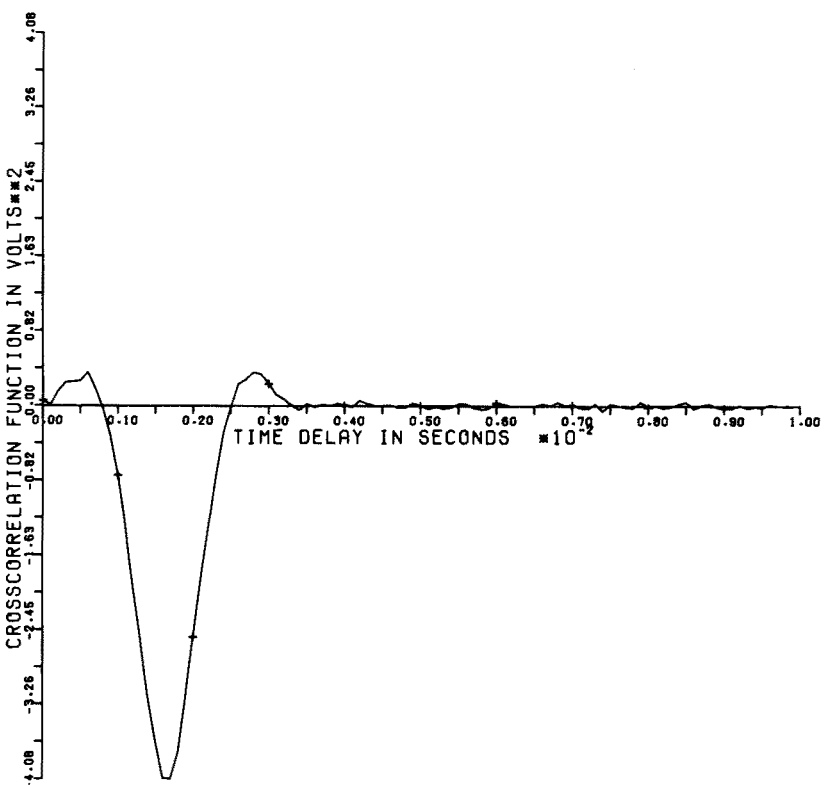

Fig. 7. Impulse response of a higher-order commercial filter, determined as a 100 points c.c.v.f. The c.c.v.f. is the result of averaging 1300 segments. $\Delta\tau = 0.333 \cdot 10^{-3}$ s.

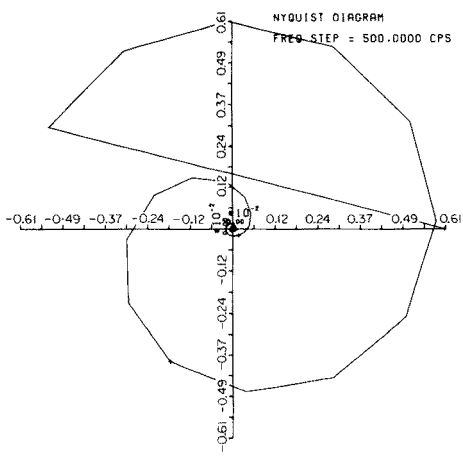

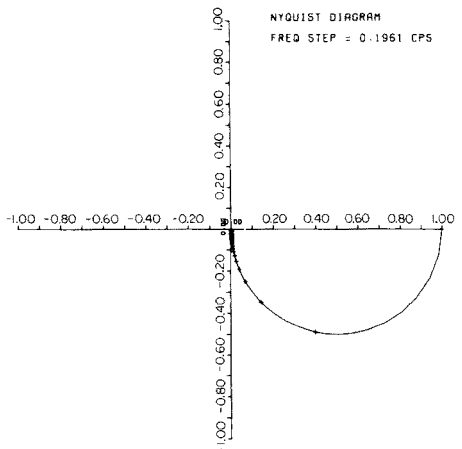

Fig. 8. Complex frequency response of the commercial filter from Fig. 7 in Nyquist representation, obtained by a smoothed transform of the c.c.v.f. from Fig. 7. The skew line is an artefact, caused by the Calcomp polar subroutine.

Fig. 9. Complex frequency response of a linear system in Nyquist representation, obtained by an unsmoothed transform of the time series e^{-t}, representing an impulse response of a first-order system. $\Delta t = 0.1$ s.

The required level of confidence is defined as $100(1-\kappa)\%$. The lower and upper confidence limits for $G_{xx}(k\Delta f)$ can be obtained as multiplication factors, which are, respectively:

$$\frac{\nu}{\chi_\nu^2(1-\kappa/2)} \quad \text{and} \quad \frac{\nu}{\chi_\nu^2(\kappa/2)} \tag{33}$$

Chi-square values are generated in the program by inversion of the cumulative distribution function (c.d.f.), as is normally done in tables [14].

Cross-spectral estimators are smoothed by the same windows, applied however, on both even and odd functions. Under the conditions that are valid for autospectra (flat spectrum over the spectral window, K large or M/N small), the normalized variance of the cross amplitude spectrum can be derived [10]:

$$\frac{\mathrm{Var}[|\bar{C}_{xy}(k\Delta f)|]}{|G_{xy}(k\Delta f)|^2} \approx \frac{1}{K}\,\frac{IM}{N} \tag{34}$$

Again $Z_{xy}(f)$ is distributed according to χ_ν^2, analogously to eqn. (31). This is only valid if the theoretical squared coherency spectrum $\gamma_{12}^2(f)$ equals unity, i.e. in the case of the c.c.v.f. of a linear system. Confidence limits can now be calculated by eqns. (33).

This is the only quantity that can be determined because a good estimation method for the sample squared coherency spectrum is not available in a

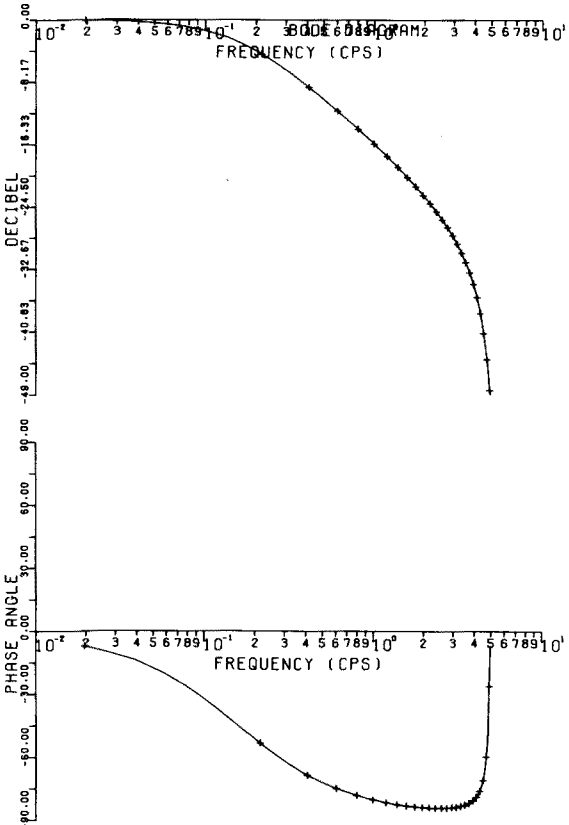

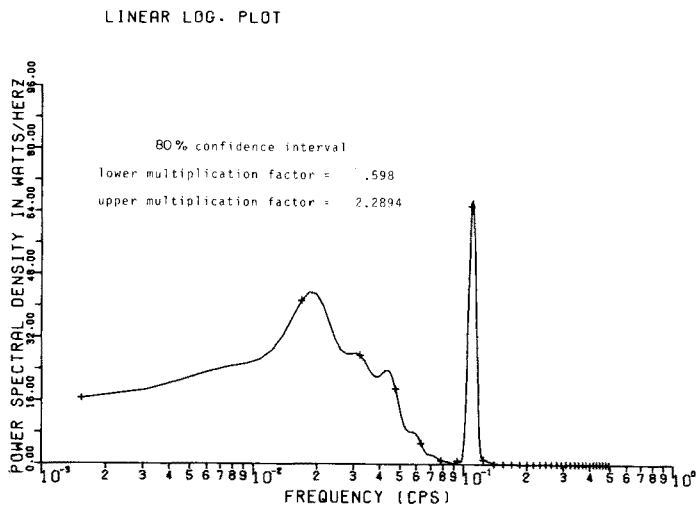

Fig. 10. Complex frequency response of the system described in Fig. 9 in Bode representation.

Fig. 11. Smoothed p.s.d.-plot of a sample noise record with a hidden periodic component. Spectrum obtained by a smoothed time series transform.

single-channel program. In practice, generation of the χ^2 values depends on ν. If $\nu \geqslant 30$, a direct inversion formula is used [15]. If $\nu < 30$, no analytical inversion expression exists and the values are obtained by an iteration scheme involving the numerical integration of the p.d.f. over χ^2.

The total range from $\nu = 1$ to $\nu > 10.000$ for any κ has an accuracy better than 1% on a 16-bit computer.

TESTS AND EXAMPLES FROM PRACTICE

The program has been tested in practice with a variety of deterministic and stochastic signals. The examples selected have been largely chosen to provide an insight into the quality of the Fourier transforms performed. They are intended mainly as a performance test and to a lesser extent as typical examples from analytical practice. Thus the Fourier spectrum to be obtained should be perfectly known and consequently the input data have to be completely specified, a reason for their artificial generation.

Examples of autocovariance functions and the related spectra are shown in Figs. 2—6. The noise properties shown in Figs. 2—6 and 11 are typical of many analytical signal sources. The filter in Figs. 7 and 8 is an electronic filter, often used in an analytical chemical framing.

The response of the linear system of Figs. 8—10 is characteristic of an ideal mixer, but many detectors and electrochemical electrodes behave similarly.

These authors express their appreciation to Mr. J. C. Smit, who collaborated in a part of the software design.

REFERENCES

1 H. C. Smit and H. L. Walg, Chromatographia, 8 (1975) 311.
2 H. C. Smit, Chromatographia, 3 (1970) 515.
3 J. E. Lovelock, J. Chromatogr., 112 (1975) 29.
4 G. D. Bergland, IEEE Spectrum, 6 (1969) 41.
5 J. S. Bendat and A. G. Piersol, Measurements and Analysis of Random Data, New York, Wiley, 1966.
6 W. T. Cochran, et al., IEEE Trans. Audio Electroacoustics, AU-15 (1967) 45.
7 J. W. Cooley, P. A. W. Lewis and P. D. Welch, IEEE Trans. Audio Electroacoustics, AU-15 (1967) 79.
8 C. Bingham, M. D. Godfrey and J. W. Tukey, IEEE Trans. Audio Electroacoustics, AU-15 (1967) 56.
9 R. B. Blackman and J. W. Tukey, The Measurement of Power Spectra, New York, Dover, 1958.
10 G. M. Jenkins and D. G. Watts, Spectral Analysis and its Applications, San Francisco, Holden Day, 1968.
11 R. C. Singleton, IEEE Trans. Audio Electroacoustics, AU-17 (1969) 93.
12 D. E. Newland, An Introduction to Random Vibrations and Spectral Analysis, London, Longman, 1975.
13 P. D. Welch, IEEE Trans. Audio Electrocoustics, AU-15 (1967) 70.
14 P. R. Bevington, Data Reduction and Error Analysis for the Physical Sciences, New York, MacGraw-Hill, 1969.
15 M. Abramowitz and I. A. Stegun, Handbook of Mathematical Functions, New York, Dover, 1965, ch. 26.

Analytica Chimica Acta, 103 (1978) 61—71
Computer Techniques and Optimization
©Elsevier Scientific Publishing Company, Amsterdam — Printed in The Netherlands

COMPUTER-AIDED INTERPRETATION OF STEROID MASS SPECTRA BY PATTERN RECOGNITION METHODS[§]
Part III. Computation of Binary Classifiers by Linear Regression

H. ROTTER and K. VARMUZA*

Institut für Allgemeine Chemie, Technische Universität, Lehargasse 4, A-1060 Vienna (Austria)

(Received 30th August 1977)

SUMMARY

The method of linear regression analysis is used to compute binary linear classifiers which can recognize 17 chemical structures of steroids from given low-resolution mass spectra. Different ways of spectral preprocessing and feature selection are compared. The best classification results are obtained with spectra which are normalized to local ion current and with feature selection based on maximum Fisher ratio. An average predictive ability of 84% was achieved for a spectral sample which was not used for the computation of the classifiers.

Computer-aided interpretation of low-resolution mass spectra by pattern recognition methods is based on the following ideas. A low-resolution mass spectrum can be considered as a pattern vector which can be related to a point in a D-dimensional spectral space (D-dimensional vector space). In the simplest case, the M mass numbers correspond to the D coordinate axes while the peak intensities correspond to the coordinates of the point. It is assumed that spectra of substances with similar chemical structure have similar pattern vectors and therefore form clusters in the spectral space. If a point that represents an unknown spectrum lies near or in such a cluster, it may be assumed that, in all probability, the chemical structure of the unknown is similar to the structures of the members of the cluster.

One possible means of determining the membership of a cluster is to calculate the distances between the unknown point and the centres of gravity of all existing clusters (classification by distance measurement [1]). In many cases, it is convenient to assume that there are only two clusters: cluster 1 contains all spectra of substances with a certain chemical structure (class 1), and cluster 2 comprises all remaining spectra (class 2). For classification by distance measurement, in this case, it is necessary to determine on which side of the symmetry plane between the two centres of gravity the unknown spectrum is situated.

[§] For Part II, see [1].

Undoubtedly, this symmetry plane is not necessarily the best decision plane. If there is any plane which completely separates the two classes, then it can be computed by a training process (learning machine [2—4]), but this iterative procedure fails if the two clusters are not separable completely and linearly.

In this paper, linear regression analysis based on minimization of the sum of squared errors is used to obtain a decision plane. This method allows a well defined, and in some ways optimal, decision plane to be achieved even for overlapping clusters. This "least-squares classification" has been recommended for the discrimination of more than two classes [4, 5]. In the present study, linear regression analysis is used to calculate a number of binary classifiers from a library of steroid mass spectra. With these classifiers some chemical sub-structures can be determined from a low-resolution mass spectrum easily and automatically.

LINEAR REGRESSION ANALYSIS

The aim of regression analysis [3, 6] is to determine the statistical relation between the given pattern vectors of observed values x and a scope value z on which a decision is needed. A function $y = y(\mathbf{x})$ that approximates z as closely as possible is therefore sought. For classifiers, the scope value z defines the class of the unknown: e.g. a value of $z = -1$ can be chosen for all spectra of class 1 and a value of $z = +1$ for all spectra of class 2. The pattern vectors x relate to the N mass spectra in a sample of known class membership.

The decision function y has then to be determined so that the expected value (E) of the squared error $(z - y)^2$ is minimized:

$$E(z-y)^2 = \frac{1}{N}\sum_{n=1}^{N}(z_n - y_n)^2 \rightarrow \text{Minimum} \tag{1}$$

If the problem is restricted to linear classifiers, i.e. the decision surface is a plane, the decision function y has the general form

$$y = y(x_0, x_1, \ldots x_i, \ldots, x_D) = \sum_{i=0}^{D} w_i x_i \tag{2}$$

The components x_i of the pattern vector are given by the peak intensities of the mass spectrum or by a function of these intensities (see Preprocessing and Feature Selection). For simplicity, a component $x_0 = 1$ is added to the pattern vector. Thus, the decision planes obtained always pass through the origin of the coordinate system.

The weight factors w_i of the decision function y form the decision vector w which is perpendicular to the decision plane required. The scalar product of decision vector w and pattern vector x gives the classification result.

By definition, negative values ($z = -1$) refer to class 1 and positive values ($z = +1$) to class 2; nevertheless during the test of the decision vector, a non-zero discriminating value between the two classes may prove more efficient than the boundary $y = 0$.

In order to establish the decision vector **w** (with component $w_0, w_1, \ldots w_j, \ldots, w_D$) which minimizes the sum of the squared errors as in eqn. (1) $E(z - y)^2$ is differentiated with respect to w_j and the derivatives are set equal to zero.

$$\partial E(z - y)^2 / \partial w_j = 0 \quad \text{for all } w_j, \text{ with } j = 0, 1, \ldots D \tag{3}$$

Because z is independent of w_j

$$\partial E(z - y)^2 / \partial w_j = -2E(z(\partial y / \partial w_j)) + 2E(y(\partial y / \partial w_j)) = 0 \tag{4}$$

Substitution of eqn. (2) for y then gives the following relation for the $D + 1$ partial derivatives

$$\partial y / \partial w_j = (\partial / \partial w_j) \sum_{i=0}^{D} w_i x_i = x_j \tag{5}$$

Substitution of eqns. (2) and (5) into eqn. (4) gives

$$E\left(x_j \sum_{i=0}^{D} w_i x_i\right) = E(z x_j) \tag{6}$$

A change of summation and formation of the expected values gives

$$\sum_{i=0}^{D} w_i \, E(x_i x_j) = E(z x_j) \quad \text{for } j = 0, 1, \ldots D \tag{7}$$

Relation (7) defines a system of $(D + 1)$ linear equations for $(D + 1)$ variables $w_0, w_1, \ldots w_D$. Solution of this set of equations gives the desired components of the decision vector **w**. The expected values $E(x_i x_j)$ and $E(z x_j)$ can be estimated from a random sample of N pattern vectors $\mathbf{x}_n$ for which the class membership and thus z_n are known

$$E(x_i x_j) = (1/N) \sum_{n=1}^{N} x_{in} x_{jn} \quad \text{for } i, j = 0, 1, \ldots D \tag{8}$$

$$E(z x_j) = (1/N) \sum_{n=1}^{N} z_n x_{jn} \quad \text{for } j = 0, 1, \ldots D \tag{9}$$

where x_{in} means the i-th component of pattern vector number n.

The expected values obtained from eqns. (8) and (9) have the disadvantage of being dependent on the ratio of spectra in the two classes. The resulting

classifier therefore recognizes the more frequent class well but is unsatisfactory for the other class. For this reason it is useful to construct a fictitious sample where spectra are equally distributed between the two classes. For this purpose, the expected value E is split into two class-dependent parts E_1 (expected value for class 1) and E_2 (for class 2). If $p(1)$ is defined as the probability of class 1 in the sample, then

$$E = p(1)\,E_1 + [1 - p(1)]\,E_2 \tag{10}$$

The expected value for class 1, E_1, is calculated from all N_1 spectra vectors of class 1, and E_2 is calculated from all N_2 spectra vectors of class 2. To obtain the expected value E for a fictitious sample with equal probabilities of both classes, $p(1)$ is given the value 0.5. Instead of eqns. (8) and (9), the following equations are used to determine the coefficients of the set of linear equations (7):

$$E(x_i x_j) = (0.5/N_1) \sum_{n=1}^{N_1} x_{in} x_{jn} + (0.5/N_2) \sum_{r=1}^{N_2} x_{ir} x_{jr} \tag{11}$$

$$E(z x_j) = (0.5/N_1) \sum_{n=1}^{N_1} z_n x_{jn} + (0.5/N_2) \sum_{r=1}^{N_2} z_r x_{jr} \tag{12}$$

(The index n is varied over all spectra in class 1, the index r over all spectra in class 2, and i and j are varied between 0 and D.)

To summarize, the following steps are necessary for the calculation of a classifier by linear regression analysis.

1. Calculation of the coefficients which determine the set of linear equations; see eqns. (7), (11), and (12). The computational effort is proportional to the number of dimensions D and to the number of spectral vectors N.
2. Solution of the set of linear equations by using standard methods of numerical mathematics, e.g. the Gauss algorithm.

Although the computational effort for the calculation of the decision vector is rather high, the application of the classifier to unknown spectra is very quick and simple. The classifier works in exactly the same way as an adaptive classifier (learning machine) or a distance-measuring classifier. It is only necessary to compute the scalar product between spectral vector and decision vector, and to consider the sign of the result, to obtain some evidence about the class of the unknown.

TREATMENT OF SPECTRA

Data and programmes

The spectral file was the same as used previously [1], consisting of 524 low-resolution mass spectra from 524 different steroids [7]. The elemental composition of the steroids was in the range $C_{18-29}\,H_{18-50}\,N_{0-1}\,O_{0-8}\,F_{0-3}\,Si_{0-2}$,

the molecular weights between 256 and 463, and the mass between 39 and 463. Classifiers were calculated for the same 17 chemical structures as previously [1]. Programmes were written in FORTRAN and were run on a Cyber 74 (memory: 98K words, 60 bits) at the Computer Centre, University of Technology in Vienna. Computation of one classifier by linear regression (262 spectra, 100 dimensions) required 16-s CPU-time.

Preprocessing of spectra

Preprocessing may have a great influence on the performance of classifiers, as was shown previously for the classification of steroid mass spectra by distance measurement [1]. The following preprocessing methods which were described in detail earlier [1], were used in this paper:

1. spectra with normalization to the base peak;
2. logarithmic spectra;
3. normalization to total ion current (sum of peak heights);
4. normalization to local ion current with window widths of 3—13 mass units;
5. significant spectra, as discussed by Clerc and Nägeli [8], which only contain the most important peaks;
6. binary encoded spectra with intensity thresholds of 0.05 and 5% of the base peak;
7. reduced spectra with "k largest peaks in mass intervals of length l" ($k = 2$, $l = 14$ and $k = 1$, $l = 7$).

Although preprocessing of spectra sometimes reduces the number of peaks per spectrum, the total number of mass numbers (dimensions) occurring remains almost constant.

Feature selection

The number of dimensions (features, mass numbers) which may be used for the computation of classifiers is restricted. There is the general rule that the number N of pattern vectors (spectra) must be at least 3 times the number D of dimensions, otherwise a decision plane can be found for any arbitrary splitting of the classes. When linear regression is used to calculate classifiers, a set of $D + 1$ equations must be solved for $D + 1$ variables. Thus there are also limits on the number of dimensions to be used for computational reasons. (For the programmes used here the limiting value is $D \leqslant 100$.) Consequently, the "most important" features must be selected before calculation of the classifier is started. This feature selection was always performed after preprocessing of spectra, and two different methods were used.

In the first case, those D mass numbers were selected for which the (transformed) peak heights had maximum variance. The variances v_m at mass numbers m were estimated from all 524 mass spectra ($N = 524$).

$$v_m = [1/(N-1)] \sum_{n=1}^{N} (x_{mn} - \bar{x}_m)^2 \qquad (13)$$

$$\bar{x}_m = 1/N \sum_{n=1}^{N} x_{mn} \tag{14}$$

where x_{mn} means the peak height at mass number m in spectrum n. This algorithm was used to select the same D mass numbers regardless of the chemical structure to be classified.

The second method tries to select those mass numbers which reflect the differences between the two classes best. The Fisher ratio F_m was used as a criterion for these differences [9].

$$F_m = [\bar{x}_m(1) - \bar{x}_m(2)]^2/[v_m(1) + v_m(2)] \tag{15}$$

In this case mean values $\bar{x}_m$ and variances v_m have to be calculated for spectra of class 1 and class 2 separately. The largest values of F_m correspond to the "most important" mass numbers desired.

Comparison and judgement of classifiers

The library of 524 steroid mass spectra with known class membership was randomly divided into two samples of 262 spectra each. One sample was used for the calculation of the classifier (training set), and the other was used for the test (prediction set).

In order to define the quality of the classifiers objectively [10, 11], the following criteria were calculated from the prediction set: the percentage of correctly classified spectra of class 1 and class 2, respectively (predictive abilities P_1 and P_2), and the maximum information I_{max} obtained if a classifier is applied to a sample with the same number of spectra in each class. I_{max} is a function of P_1 and P_2 and ranges from 0 to 1 bit [11]. In order to compare different methods of preprocessing and feature selection, the results for I_{max} were averaged for 14 chemical structures. Three structures, shown in Table 2 as numbers 8, 11, and 12, were not considered for these average values, because these structures gave extremely bad results in all applications of linear regression.

Improper use of pattern recognition methods makes it possible to achieve good classification results even for senseless questions. Thus, for mass spectra of pharmacologically active substances, adaptive linear classifiers could be calculated which recognized very successfully whether the substance was a sedative or a tranquillizer [12]. For the same set of spectra, a classifier was calculated which decided whether the name of the substance had an odd or even number of characters [13]. Normally, such effects occur if the samples are too small, the numbers of spectra in the classes too different, or if the number of spectra in the sample does not exceed the number of dimensions significantly.

For these reasons, it seemed useful to test the quality of the classifiers obtained, on randomly distributed spectra. All 524 steroid mass spectra were assigned randomly to class 1 or class 2. The probability $p(1)$ of class 1

was varied from 0.05 to 0.5. Primarily, calculation and test of the classifier were done with the same set of 524 spectra. Figure 1 shows the "classification results" (I_{max}) for normal spectra (% base peak) and feature selection according to maximum variance; similar results were obtained for the Fisher ratio. A spectral sample with $p(1) = 0.05$ and selection of 100 features yields a classifier with $I_{max} = 0.54$ bit (corresponding to an average percentage of correctly classified spectra of 90%). It can be seen that even a ratio of number of spectra to number of dimensions (N/D) of 5 is inadequate if one class is only weakly represented. The chance of achieving a satisfactory decision plane even for random classes increases if the population of the classes tends to be less uniform and if the ratio N/D decreases.

When calculation and test of the classifiers were carried out with two different samples (262 spectra each), the resulting value of I_{max} was practically zero in all cases (I_{max} is zero if $P_1 + P_2 = 0$ [14]). So, if two different samples are used for training and test, the values for quality criteria of classifiers do not reflect any random effect of the orientation of the decision plane.

RESULTS AND DISCUSSION

Figure 2 shows a comparison of feature selection by maximum variance (eqn. 13) and by maximum Fisher ratio (eqn. 15). The average maximum information $\bar{I}_{max}$ is plotted versus the number D of dimensions (mass numbers) used. The Fisher ratio yielded somewhat better results for 25 to 75 dimensions than did maximum variance. This is not surprising because with the Fisher ratio method, preprocessing was done separately for each chemical structure.

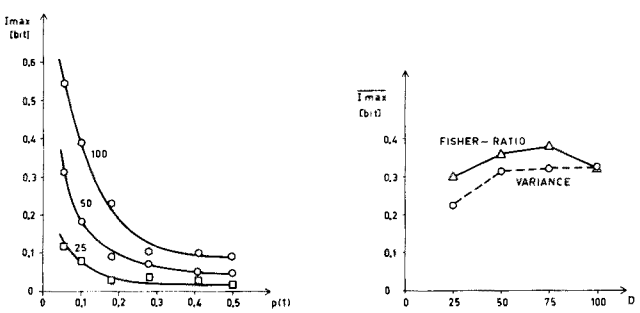

Fig. 1. Maximum information, I_{max}, for randomly selected classes. 524 steroid mass spectra (% base peak) with 25, 50, or 100 mass numbers with maximum variance were used, $p(1)$ means the probability of class 1. Each point is the average of 3 different experiments with different class assignment.

Fig. 2. $\bar{I}_{max}$, the maximum information averaged for 14 chemical structures as a function of the number D of the mass numbers used. D mass numbers were selected with maximum variance or maximum Fisher ratio of peak heights (% base peak). The values given refer to the prediction set.

Although this means greater computational effort during calculation of a classifier, no additional time is required during application of the classifier. The computed decision vector simply contains zero components for all unused mass numbers, and calculation of the scalar product of the decision vector and the pattern vector of the unknown spectrum is accomplished as usual.

The best method, as shown in Fig. 2 (75 dimensions with maximum Fisher ratio) was used to test the different preprocessing methods. The results in Table 1 show that predictive ability is not significantly improved compared to "normal spectra" (I_{max} = 0.379 bit). Preprocessing methods which reduce the number of peaks per spectrum (like significant spectra or spectra with k largest peaks in mass intervals) and binary-encoded spectra produce worse results than normal spectra. Normalization to local ion current with a window width of 13 mass units (m.u.) gave I_{max} = 0.397 bit,

TABLE 1

Classification results
($\bar{P}_1$, $\bar{P}_2$, $\bar{I}_{max}$ are averaged values for 14 chemical structures; $\bar{P}_1$ ($\bar{P}_2$) is the percentage of correctly classified spectra in the prediction set from class 1 (2), and $\bar{I}_{max}$ is maximum information in bit.)

Preprocessing	$\bar{P}_1$	$\bar{P}_2$	$\bar{I}_{max}$
Linear regression			
Normal spectra	0.82	0.85	0.379
Logarithmic spectra	0.79	0.84	0.335
Binary spectra (threshold 0.05% B)	0.73	0.78	0.216
Binary spectra (threshold 5% B)	0.76	0.75	0.210
Norm. to total ion current	0.78	0.86	0.347
Norm. to local ion current (window 3 m.u.)	0.72	0.82	0.250
Norm. to local ion current (window 7 m.u.)	0.83	0.85	0.390
Norm. to local ion current (window 13 m.u.)	0.83	0.85	0.397
Significant spectra (%B)	0.77	0.82	0.291
Significant spectra binary encoded	0.75	0.77	0.235
Significant spectra norm. to local ion current (window 7 m.u.)	0.75	0.80	0.257
2 largest peaks in intervals of 14	0.80	0.84	0.343
1 largest peak in intervals of 7	0.74	0.86	0.290
Other methods			
Distance measurement, norm. to local ion current (window 7 m.u.)[a]	0.87	0.87	0.458
Nearest neighbour, normal spectra[b]	0.79	0.86	0.353
Adaptive linear classifiers (learning machine), normal spectra[c]	0.78	0.78	0.262

[a] Values for the same 14 chemical structures as used in this work, training and test with all 524 spectra, without feature selection [1].
[b] Each of the 524 spectra was treated as unknown and classified with all other spectra by the nearest neighbour [15].
[c] Training and prediction with 2 random samples [16]; feature selection as in [17].

TABLE 2

Detailed classification results for the best method
(Preprocessing: normalization to local ion current, window width 13 m.u. Feature selection: 75 mass numbers with maximum Fisher ratio. Training of the classifiers: linear regression. $p(1)$ is the probability of class 1 (the denoted substructure is present). P_1 (P_2) is the percentage of correctly classified spectra in the prediction set from class 1 (2). I_{max} is the maximum information in bit.)

No.	substructure	$p(1)$	P_1	P_2	I_{max}
1	Double bond C=C	0.45	0.77	0.91	0.373
2	Double bond C-4=C-5	0.25	0.73	0.85	0.263
3	Hydroxysteroid	0.73	0.75	0.74	0.179
4	Ketosteroid	0.73	0.88	0.78	0.347
5	Oestran- or androstan-type	0.56	0.91	0.89	0.529
6	3-Hydroxysteroid	0.39	0.71	0.78	0.178
7	3-Ketosteroid	0.45	0.87	0.82	0.383
8[a]	Oxygen function at C-3	0.91	0.88	0.48	0.115
9	Oxygen function at C-11	0.22	0.85	0.78	0.312
10	Oxygen function at C-17	0.63	0.85	0.85	0.385
11[a]	5α-Steroid	0.38	0.57	0.70	0.054
12[a]	5β-Steroid	0.25	0.55	0.71	0.050
13	OH in side-chain at C-17	0.13	0.64	0.89	0.229
14	CO in side-chain at C-17	0.23	0.95	0.86	0.558
15	20-Ketopregnane	0.23	0.95	0.87	0.572
16	20-Hydroxypregnane	0.06	1.00	0.96	0.888
17	Carboxyl group	0.11	0.71	0.94	0.367

[a]Results for these substructures were not used for the comparison of preprocessing methods (Table 1).

which was the highest average maximum information. Table 2 shows the detailed results for this preprocessing method for all 17 chemical structures. If structures 8, 11, and 12 are discarded as obviously useless, the predictive abilities P_1 and P_2 range from 64% to 100% with a mean value of 84%. $\bar{I}_{max} = 0.397$ corresponds to a classifier with $P_1 = P_2 = 0.85$.

Figure 3 shows the class-dependent probability density functions of the scalar product between decision vector and spectra vectors for the chemical structure 14 of Table 2, obtained by classification of the prediction set. There is little overlapping of the densities, and the scope values −1 and +1 of the regression are achieved fairly well.

For practical applications, classifiers were calculated with all 524 spectra in the training set. The information gain that can be obtained with these classifiers during classification of new unknown spectra should be at least as great as the values in Table 2. This statement involves the assumption that the sample used for calculation of the classifier is representative of the unknown spectra to be classified.

Table 1 also contains several results that were obtained with the same spectra but by other pattern recognition methods. The predictive abilities

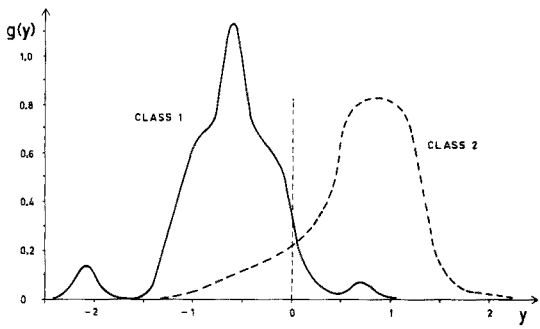

Fig. 3. Probability density functions, g, of the classification result (scalar product), y. Class 1 contains steroids with a CO-group in the side-chain at C-17 (no. 14 in Table 2). Preprocessing: normalization to local ion current, window width 13 m.u. Feature selection: 75 mass numbers with greatest Fisher ratios. The curves were calculated from the prediction set.

of adaptive linear classifiers (learning machine) [16] are significantly worse than the values obtained by linear regression analysis. Values obtained by distance measurement to centres of gravity [1] and by the k-nearest neighbour method (KNN) [15, 18] are not directly comparable with the values for regression. No feature selection was performed for distance measurement, and all 524 spectra were used for calculation and testing of classifiers. For the KNN method, also, no features were selected and each spectrum was considered unknown and classified with all remaining spectra.

Linear regression analysis seems to be a promising method for the calculation of linear classifiers. The position of the decision plane is very satisfactory, and its orientation is not greatly affected by several spectra in extreme positions as can happen with adaptive classifiers. A percentage of more than 80% correct classifications makes this method suitable for assisting human interpretation of steroid mass spectra. Complete replacement of human work and intelligence in the interpretation of spectra cannot be achieved by the current pattern recognition methods.

We thank Prof. Dr. G. Spiteller for the use of his library of steroid mass spectra, Prof. Dr. A. Maschka for his support of this work, and Mr. H. Urban for technical assistance.

REFERENCES

1 Part II: H. Rotter and K. Varmuza, Anal. Chim. Acta, 95 (1977) 25.
2 N. J. Nilsson, Learning Machines, McGraw-Hill, New York, 1965.
3 G. M. Meyer-Brötz and J. Schürmann, Methoden der automatischen Zeichenerkennung, Oldenbourg, München-Wien, 1970.
4 P. C. Jurs and T. L. Isenhour, Chemical Applications of Pattern Recognition, Wiley, New York, 1975.

5 B. R. Kowalski, P. C. Jurs, T. L. Isenhour and C. N. Reilley, Anal. Chem., 41 (1969) 695.
6 C. R. Rao, Lineare statistische Methoden und ihre Anwendungen, Akademie-Verlag, Berlin, 1973.
7 G. Spiteller, Steroid Mass Spectra Library, Göttingen.
8 P. R. Nägeli, Dissertation, ETH Zürich, 1975.
9 W. S. Meisel, Computer-oriented Approaches to Pattern Recognition, Academic Press, New York, 1972.
10 K. Varmuza and H. Rotter, Mh. Chem., 107 (1976) 547.
11 K. Varmuza and H. Rotter, Adv. Mass Spectrom., 7 (1977) in press,
12 Kai-Li H. Ting, R. C. T. Lee, G. W. A. Milne, M. Shapiro and A. M. Guarino, Science, 180 (1973) 417.
13 J. T. Clerc, P. Nägeli and J. Seibl, Chimia, 27 (1973) 639.
14 H. Rotter and K. Varmuza, Org. Mass Spectrom., 10 (1975) 874.
15 K. Varmuza, unpublished (1977).
16 K. Varmuza and H. Buchroithner, unpublished (1977).
17 P. C. Jurs, Anal. Chem., 42 (1970) 1633.
18 K. Varmuza, Fresenius Z. Anal. Chem., 268 (1974) 352.

Analytica Chimica Acta, 103 (1978) 73—108
Computer Techniques and Optimization
©Elsevier Scientific Publishing Company, Amsterdam — Printed in The Netherlands

DECONVOLUTION OF SPECTRA BY LEAST-SQUARES FITTING

GEOFFREY C. ALLEN

Central Electricity Generating Board, Berkeley Nuclear Laboratories, Berkeley, Gloucestershire, GL13 9PB (Gt. Britain)

ROBERT F. McMEEKING

Department of Inorganic Chemistry, The University, Bristol, BS8 1TS (Gt. Britain)

(Received 26th July 1977)

SUMMARY

Spectra of varying complexity appear in several areas of surface studies and analytical chemistry, and computer programs are used to determine the positions and areas of individual spectral bands. The methods used for the deconvolution of spectral data are described together with a computer program which has been developed for this purpose. The application of the program to the analysis of spectral bands obtained from various spectroscopic techniques is discussed.

In chemical research computers find a ready application in two main areas: (i) general computational tasks (off-line operation); and (ii) the acquisition of data from measuring instruments coupled to the computer (on-line operation). Calculation problems in the fields of theoretical chemistry and spectroscopy are usually solved in off-line operation. Since spectra of varying complexity appear in several areas of surface studies and analytical chemistry, computer programs are used to determine the positions and areas of component spectral bands. This paper describes the methods used for the deconvolution of spectral data together with a computer program which has been developed for this purpose. The application of the program to the analysis of the electronic spectra of transition metal compounds is discussed in some detail, but in principle the program is equally applicable to the deconvolution of spectral bands obtained from x-ray photoelectron, Auger, infrared, electronic absorption and electron spin resonance measurements.

GENERAL CONSIDERATIONS

The simplest method applicable to both curve analysis and ligand field parameter fitting is the trial-and-error approach. In this way, ligand-field parameters are varied empirically when calculated transition energies are compared with experimental values. For curve analysis, suitable mathematical

functions are chosen for the component bands, the positional and width parameters are adjusted, and the contour of the composite band envelope is compared graphically with the measured spectrum. Moderately complex band systems have been analysed in this fashion for both vibrational spectra [1] and electronic absorption spectra [2]. A more sophisticated adaptation of this method uses an analog computer to generate the component curves and match the band envelope [3—5]. Electronic devices of this kind are commercially available (Model 310 Curve Resolver, E.I. Du Pont de Nemours and Co., Wilmington, Del.), but greater precision and flexibility can be obtained by digital techniques. In the first part of this paper an attempt is made to outline the basic theory behind, and the limitations of, the more successful algorithms which have been programmed for digital machines.

The usual criterion by which the analysis is judged involves the sum of the squares of the differences between observed and calculated data. The problem then reduces to that of minimizing this sum. Many mathematical techniques are available for the solution of this problem, some of which are outlined in the following section. However, the basic philosophy behind many of these methods is very similar, and they all suffer from the limitation that they converge to a local minimum even when a more satisfactory minimum is present elsewhere in parameter space.

In general, for a minimization procedure an initial estimate is required for the adjustable parameters. This estimate may be derived from previous experience of the system by using a rather similar model function which can be solved analytically, or by sheer guesswork. The parameters are then adjusted stepwise so as to reduce the function and eventually a function minimum is obtained. The problems associated with local minima can best be illustrated by considering a two-argument function corresponding to a landscape in three-dimensional space with a number of depressions. Here, unless the initial estimate for the parameters corresponds to a point on a perfectly flat plateau, one will eventually descend to the lowest point in a depression. But there is no guarantee that this is the deepest depression or the one that corresponds to the most physically realistic parameters. Moreover, for a function of fairly high dimensionality, it is rarely feasible to search even a small region for alternative minima since if each parameter can adopt N discrete values and there are n parameters, N^n function evaluations will be required. This soon becomes prohibitively large for even fairly small values of N and, more dramatically, n.

The more efficient optimization algorithms use some kind of linear search procedure in their main iteration. Thus, instead of simply calculating a correction factor for each parameter, the method uses the correction to define a direction of search. This guarantees that the value of the function will be reduced on each iteration, and ensures final convergence to a minimum. Returning to the example of the three-dimensional landscape, if the point of departure lies at the side of a valley all descending pathways will eventually reach the valley floor, and from there descend to some minimum

point. The degree of meandering permissible along the valley floor will depend on the relative steepness of the valley and the sharpness of its sides. However, for a simple valley all methods based on linear search must descend to the same minimum. The situation becomes less straightforward if the valley divides while descending. Here, the branch eventually followed depends very much on the exact path being pursued. Greater uncertainty is encountered if the point of departure is at the summit of a rounded hill. Any direction pursued will then represent a descending pathway, which may lead to a number of different minima. In higher-dimensional space the possibility of this kind of ambiguity will be proportionally larger.

Clearly, the fitted parameters obtained as a result of a minimization procedure may depend on both the algorithm used and the initial estimate for the parameters. In general, unambiguous results are not obtained for the problem of fitting N ligand field parameters to N transitions. Ambiguities do not occur, however, if there are no off-diagonal elements, since the problem reduces to that of solving N linear equations in N unknowns. It is possible that the presence of off-diagonal elements may not distort the function sufficiently to create new minima.

The problems encountered in spectral deconvolution are more complicated, and numerous fits are often possible. Even for the trivial example of N isolated curves there will be $N!$ fits depending on the curves associated with a given set of parameters. Although each of the possible fittings is essentially the same as any other, problems associated with possible permutations of the component curves may lead to convergence difficulties in the deconvolution of strongly overlapping bands. More important, however, are possible alternative fittings whose differences are more fundamental than a permutation of parameters. Figure 1(a—c) illustrates three possible fittings for standard data. Figure 1(a) shows the two overlapping Gaussian curves from which the data are constructed. For the fit shown in Fig. 1(b) a deliberately poor initial estimate for the Gaussian parameters was chosen, whereas Fig. 1(c) illustrates the use of a Lorentzian curve form.

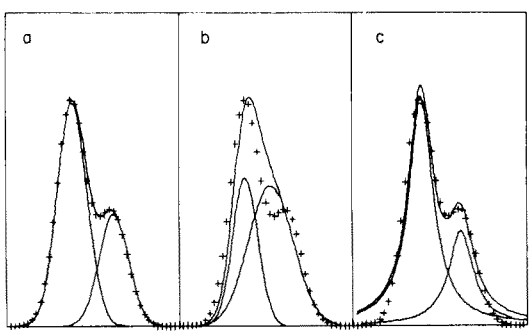

Fig. 1. Alternative fits for standard spectral data. (a) Curves of Gaussian line shape used to generate data. (b) Alternative fitting Gaussian line shapes. (c) Best fit with Lorentzian line shapes.

The fits derived from the curves in Figs. 1(b) and (c) assessed in terms of the squares of the difference between observed and calculated forms are similar. The Gaussian fit, however, smooths out important detail, and the smaller band at the side is reduced to a shoulder. The Lorentzian fit preserves important features of the spectrum and is clearly preferable. Despite the difference in line shape, the Lorentzian curves have very similar lengths and half-weight widths to the Gaussian curves used to construct the spectral data. This important observation helps to justify the use of arbitrary curve shapes in the analysis of spectral data where the true curve form is unknown.

The type of fit illustrated in Fig. 1(b) can be avoided by choosing more reasonable starting parameters. In particular, it is often possible to make a very good estimate of the positions of component peaks from a simple inspection of the spectral data. When the peaks are more closely spaced, they tend to coalesce, and estimating their positions becomes more difficult. Under these circumstances, derivative data can be used as in e.s.r., n.m.r. and Auger electron spectroscopy, where the use of first- and second-derivative presentation is routine. The advantages of displaying Auger spectra in both the N(E) and N′(E) form have been demonstrated quite recently [6], and Olson and Alway [7] have designed an attachment to produce first-derivative ultraviolet spectra. However, for the purposes of spectral analysis, a second-derivative presentation is more useful in the latter application because the positions of component bands can be associated with minima in the spectrum. The band positions obtained by this technique may be slightly inaccurate, but the error in position associated with the overlap of other component bands is less than that for first-derivative data.

To demonstrate the use of the second-derivative method to estimate the positions of component bands, Fig. 2(a—p) shows a series of composite curves in which the components become progressively coincident. However, when two component curves approach each other sufficiently closely, a point is reached where they can no longer be resolved. Smith [8] has shown that for resolution of a Gaussian doublet, the minimum separation, ν_s, required between the maxima is 1.256 $\nu_{\frac{1}{2}}$ ($\nu_{\frac{1}{2}}$ = half width of the function at half intensity) for the second-derivative function. The absorption curve requires 1.698 $\nu_{\frac{1}{2}}$ separation for resolution. The corresponding values for a Lorentzian doublet are 0.650 $\nu_{\frac{1}{2}}$ and 1.114 $\nu_{\frac{1}{2}}$.

For band separation where resolution is still possible, the slight displacement of the second-derivative minimum from the location of the original band maximum is associated with the overlap of the wings of neighbouring bands. The direction and size of the shift will depend on both the separation and line shape of the bands. For symmetrical doublets of Lorentzian functions, it has been found [9] that the displacement is 0.1 $\nu_{\frac{1}{2}}$ unit inwards for a ν_s value of 0.8. Displacements are not apparent for greater separations. For the Gaussian functions, displacements of 1.0 $\nu_{\frac{1}{2}}$ unit inwards are observed [9] for ν_s = 1.40, whilst the values of ν_s, up to 2.50, cause the minima to be displaced outwards by 0.1 $\nu_{\frac{1}{2}}$ unit.

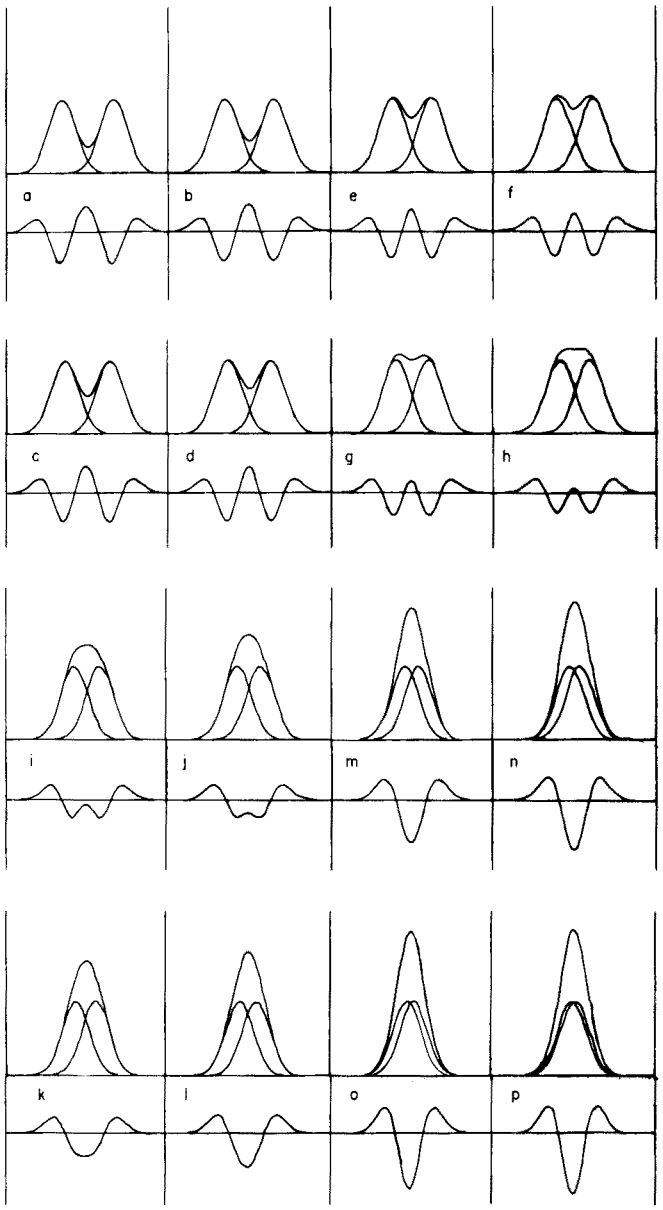

Fig. 2. Composite curves of two equal Gaussian functions (half-height half-width $\nu_{\frac{1}{2}}$) at separations ν_s together with their second derivatives (arbitrary scales). Values for ν_s in units of $\nu_{\frac{1}{2}}$ are: a, 3.2; b, 3.0; c, 2.8; d, 2.6; e, 2.4; f, 2.2; g, 2.0; h, 1.8; i, 1.6; j, 1.4; k, 1.2; l, 1.0; m, 0.8, n, 0.6; o, 0.4; p, 0.2.

In view of the difficulties associated with the direct recording of second-derivative spectra, it is usual to compute them numerically from direct absorption data. Algorithms which perform these calculations are listed by Challice and Clarke [10] and Derflinger and Lishka [11].

Challice and Clarke [9] also discuss the possible use of the shape parameter, ψ, where

$$\psi = \left[\frac{d^2D}{d\nu^2}\right]_{-\min} \Big/ \left[\frac{d^2D}{d\nu^2}\right]_{+\max} \tag{1}$$

as a means of detecting doublet structures in otherwise unresolvable spectral functions. The shape parameter is independent of curve height and half-width, being purely a measure of curve shape. The value of ψ for a Gaussian function is -2.24 and for a Lorentzian function -4.00. For strongly overlapping curves ψ decreases in magnitude with increased separation, expressed in terms of $\nu_{\frac{1}{2}}$ with ψ. This method, however, finds only a limited application in the analysis of experimental spectra, since it depends on a knowledge of actual line shapes. Moreover, the calculated second derivatives may not be exact. The apparent magnitude of ψ decreases as the interval chosen between spectral points is increased.

Analysis of Challice and Clarke's results show that, although the shape parameter for Lorentzian doublets is a sensitive guide to separation for the entire range, Gaussian functions show little variation of ψ for separations up to $0.8\ \nu_{\frac{1}{2}}$. Furthermore, a symmetrical Lorentzian doublet with a value for ν_s just below that required for resolution in the derivative function has a shape parameter which could also indicate the presence of a single spectral line of predominantly Gaussian form, with only a small tendency towards Lorentzian shape.

The problems associated with strongly overlapping doublets are well-illustrated by the fits shown in Figs. 3(a—d) and 4(a—d). Figures 3(a—d) show the best single Gaussian function fits to spectral data generated from two equal Gaussian curves. Figures 4(a—d) show spectral data equivalent to one Gaussian curve fitted by two curves at various separations. If the half-widths of the component bands are known it may be possible to infer their separation from the half-widths of the envelope. Figure 5 shows the half-widths at various heights for Gaussian functions at various separations. Even this approach is limited since, as Fig. 5 shows, near the limit of band coincidence the half-widths of the envelope are very close to those of the component bands and are very insensitive to variation of band separation.

For strongly overlapping doublets of non-equal curves, it is often possible to infer the presence of two bands from the asymmetry of the envelope. However, it is clear from the preceding discussion that even here there will be great ambiguity as to possible fits. Take, for example, two strongly overlapping curves of equal $\nu_{\frac{1}{2}}$ where one has twice the intensity of the other. The larger component can be considered as comprizing two equal parts. One of these parts can then be combined with the smaller of the

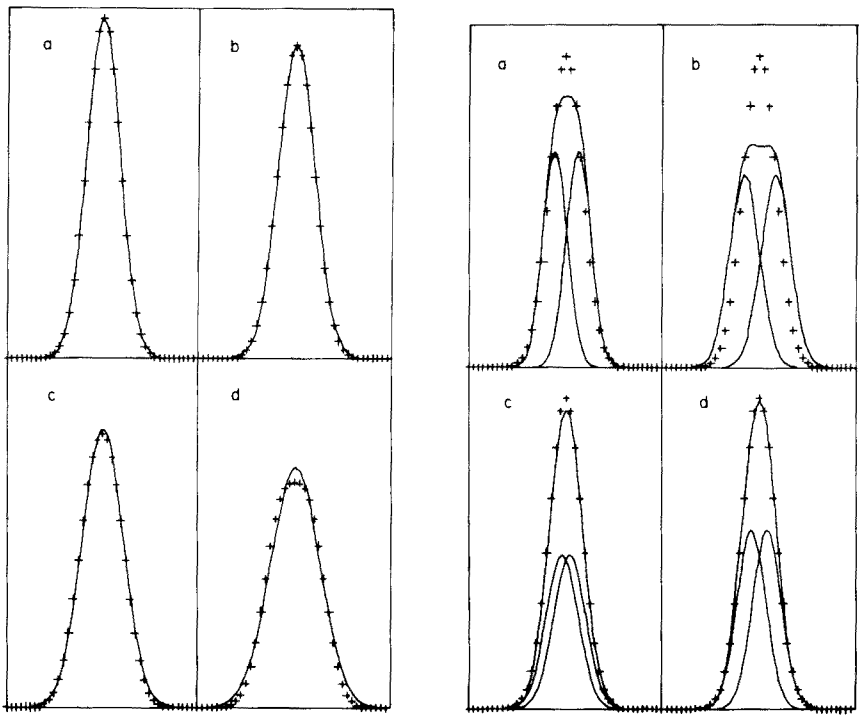

Fig. 3. Data for composite curves of two equal Gaussian functions fitted with a single Gaussian function. (a) Component curves separated by 0.4 $\nu_{\frac{1}{2}}$. (b) Component curves separated by 0.8 $\nu_{\frac{1}{2}}$. (c) Component curves separated by 1.2 $\nu_{\frac{1}{2}}$. (d) Component curves separated by 1.6 $\nu_{\frac{1}{2}}$.

Fig. 4. Data for a single Gaussian function fitted with composite curves of equal Gaussian functions at various separations. (a) Component curves separated by 1.6 $\nu_{\frac{1}{2}}$. (b) Component curves separated by 1.2 $\nu_{\frac{1}{2}}$. (c) Component curves separated by 0.8 $\nu_{\frac{1}{2}}$. (d) Component curves separated by 0.4 $\nu_{\frac{1}{2}}$.

original components, and the resultant curve fitted by a single broad Gaussian curve. Thus an alternative assignment can be readily derived where the ordering of the intensities of the component curves is reversed. Figures 6(a—h) show sets of alternative assignments derived to fit standard spectral data based on these criteria.

By the use of similar arguments it is possible to construct alternative assignments for symmetrical doublets. Where the component bands are too widely separated to permit a reasonable fit with a single Gaussian function, it may be possible to construct a reasonable three-band model. Here the two component bands of the doublet are in turn split into two components, the inner of which are combined. This yields a three-band model consisting of a broad central band with two less intense and narrower satellites (Fig. 7).

Clearly the number of component bands used for analysis of a curve envelope can be increased to any arbitrary number; conversely, satisfactory fits may be obtained with fewer curves than are present in reality.

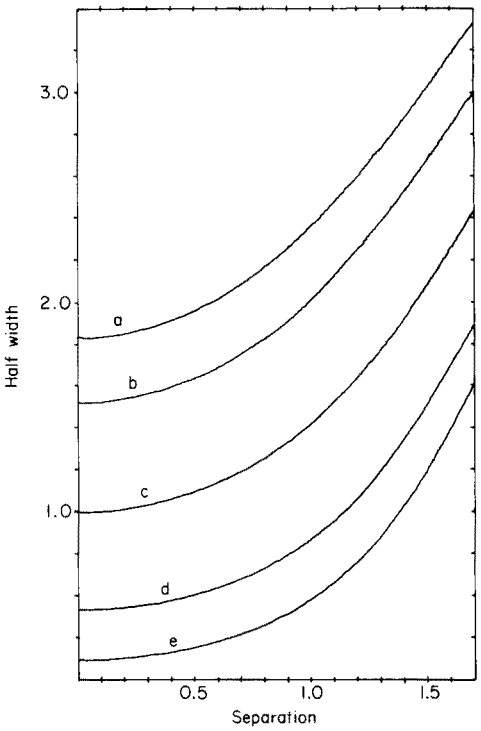

Fig. 5. Half-widths at various heights for a composite curve of equal Gaussian functions plotted against the separation of the component curves (both the half-widths and the separation in units $\nu_{\frac{1}{2}}$). The fractional heights chosen for half-width measurements are: a, 0.75; b, 0.66; c, 0.5; d, 0.33; e, 0.25.

In fact, if vibrational fine structure is included, visible and ultraviolet transitions often consist of a very large number of bands. Derflinger and Lishka [12] have obtained plausible analyses in terms of vibrational components for well-resolved ultraviolet transitions. They did, however, make simplifying assumptions as to the separations and intensities of the components, and it seems unlikely that an unambiguous fit could be obtained by means of an unconstrained optimization method.

SURVEY OF OPTIMIZATION METHODS

There are currently available a wide variety of different optimization methods, and a number of reviews have appeared [13—16]. In this section, the most important basic methods and those of direct relevance to the later discussions are outlined.

Cauchy method

This is a well established method [17]. It corresponds, for an objective two-dimensional function, to finding the direction of steepest descent for

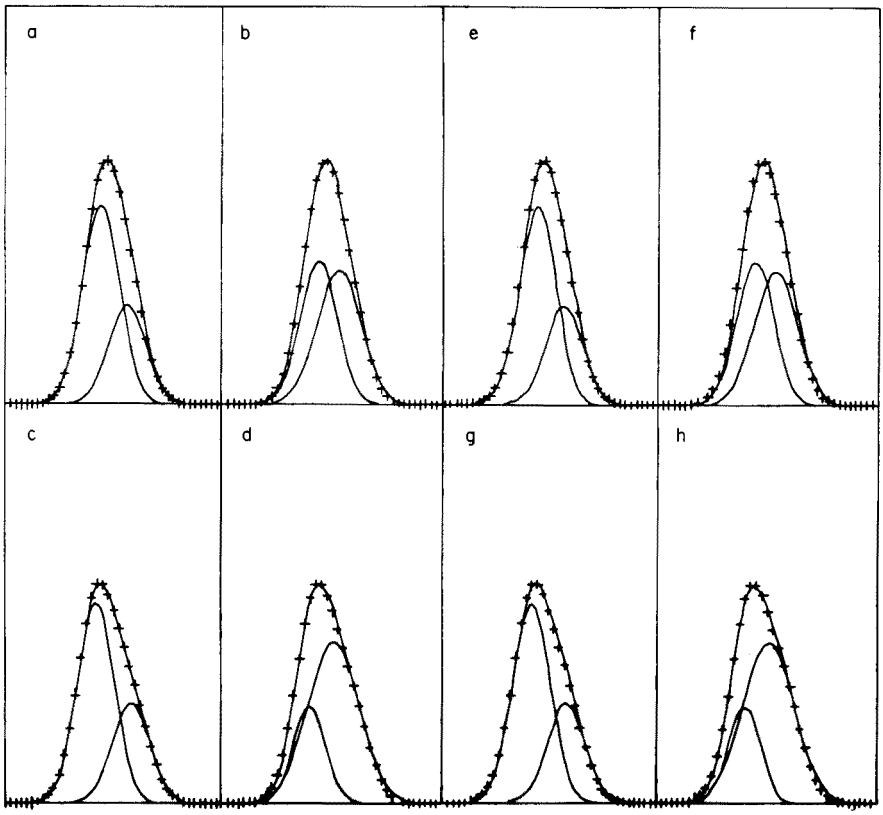

Fig. 6. Alternative fits for standard spectral data based on curves of Gaussian line shape. The spectral data correspond to composite curves of Gaussian functions of equal half-height width and an intensity ratio of two. Standard curves with a separation of 0.4 $\nu\frac{1}{2}$. Alternative fit for the data used in (a). Standard curves with a separation 0.8 $\nu\frac{1}{2}$. Alternative fit for the data used in (c). Standard curves with a separation 1.2 $\nu\frac{1}{2}$. Alternative fit for the data used in (e). Standard curves with a separation 1.6 $\nu\frac{1}{2}$. Alternative fit for the data used in (g).

the surface $z = F(x_1, x_2)$. For a differentiable object function, if one takes a very small step (δ_1, δ_2) from the point (x_1, x_2) one obtains from first-order terms in the Taylor series:

$$F(x_1 + \delta_1, x_2 + \delta_2) - F(x_1, x_2) \simeq \delta_1 \frac{\partial F}{\partial x_1} + \delta_2 \frac{\partial F}{\partial x_2}$$

$$= [\delta_1^2 + \delta_2^2]^{\frac{1}{2}} \left[\left(\frac{\partial F}{\partial x_1}\right)^2 + \left(\frac{\partial F}{\partial x_2}\right)^2\right]^{\frac{1}{2}} \cos\theta \qquad (2)$$

where θ is the angle between the step (δ_1, δ_2) and the gradient vector (g_1, g_2) at (x_1, x_2). The steepest direction is expected to be where $\cos\theta = 1$. Thus (δ_1, δ_2) is set at $(-\lambda g_1, -\lambda g_2)$. The problem in more generalized form is then

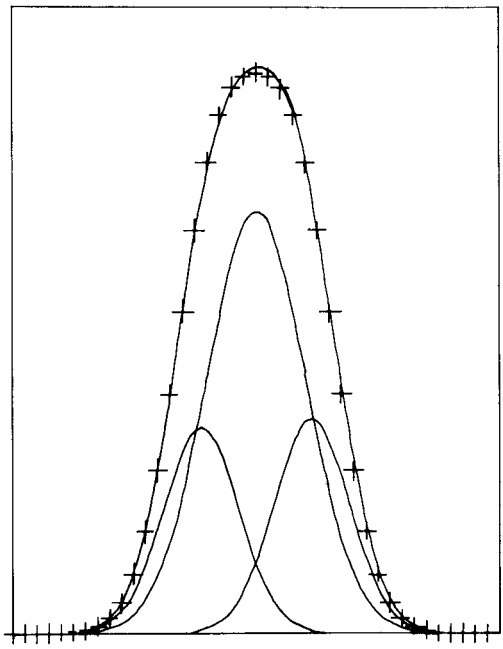

Fig. 7. Data for a composite curve of two equal Gaussian functions with a separation of 1.6 $\nu_{\frac{1}{2}}$ fitted by a three-band model.

to find a value of λ so as to minimize $\phi(\lambda)$:

$$\phi(\lambda) = F(x_1 - \lambda g_1, x_2 - \lambda g_2, \ldots, x_n - \lambda g_n) \tag{3}$$

When this is found, the entire process is repeated until complete convergence is achieved. It is often inefficient to attempt a precise minimization of $\phi(\lambda)$ [13], and some methods deliberately use smaller values for λ than are required to minimize $\phi(\lambda)$ [18].

In general, the Cauchy method can be rigorously proved to lead to convergence for continuous functions with one or more local minima, but it is usually found to be prohibitively slow.

Direct search method

In this method the initial estimate $(x_1, x_2, \ldots. x_n)$ is altered to $(x_1 + \lambda_1, x_2, \ldots, x_n)$, this estimate is altered to $(x_1 + \lambda_1, x_2 + \lambda_2, \ldots, x_n)$, and so on until all the parameters are adjusted. The whole process is then repeated until the correction factor $(\lambda_1, \lambda_2, \ldots \lambda_n)$ becomes sufficiently small. The problem of finding the appropriate value for λ_i is exactly the same as that for minimizing $\phi(\lambda)$ in the Cauchy method.

Because this process decreases $F(x_1, x_2, \ldots, x_n)$ until all gradient components g_i, $i = 1, 2_1 \ldots n_1$ are zero, the convergence properties are like those of the Cauchy method. However, this method can be used where first derivatives are impossible or tedious to calculate.

Newton—Raphson method

For an object function to have a distinct minimum it must curve, i.e. it must have non-zero second derivatives. This is taken into account by the Newton—Raphson method. Thus, instead of just first-order terms as for the Cauchy method, one takes into account second-order terms in the Taylor series. Equation (2) is then expanded, for a generalized function:

$$F(x_1 + \delta_1, x_2 + \delta_2, \ldots, x_n + \delta_n)$$

$$\simeq F(x_1, x_2, \ldots, x_n) + \sum_{i=1}^{n} -\delta_i g_i^{-\frac{1}{2}} \sum_{i=1}^{n} \sum_{j=1}^{n} \delta_i G_{ij} \delta_j \tag{4}$$

where G_{ij} is defined as

$$G_{ij} = \partial^2 F(x_1, x_2, \ldots, x_n)/\partial x_i \partial x_j \tag{5}$$

At the minimum of a differentiable function, all the first derivatives are zero. If it is possible to ignore all derivatives higher than second order, eqn. (5) will hold and

$$g_i + \sum_{j=1}^{n} G_{ij} \delta_j = 0 \quad (i = 1, 2, \ldots, n) \tag{6}$$

Thus evaluation of the components δ_i reduces to the solution of n linear equations in n unknowns, and the method progresses by altering the initial estimate for $(x_1, x_2, \ldots, x_n)$ from these components. The complete cycle is repeated until, hopefully, the function is minimized.

Because the Newton—Raphson method is exact if approximation (4) holds, it may be proved that, if the second-derivative matrix G is positive and definite at the solution, then the iterations have quadratic convergence, provided that the initial estimate $(x_1, x_2, \ldots x_n)$ is sufficiently close to the optimal values for the variables. Therefore, the procedure can be very efficient, but, if the initial estimate is poor, the method often fails to converge. Also convergence may be to a stationary point, since the method only seeks positions where the first derivatives are zero, and does not distinguish between true minima and stationary points.

This problem can be overcome by using the correction $(\delta_1, \delta_2 \ldots, \delta_n)$ as a direction for search. One finds a scaling factor λ in a manner analogous to that of minimizing $\phi(\lambda)$ defined by eqn. (3). In this manner, one obtains an algorithm that has good second-order convergence near the minimum, and will converge from poor starting approximations. It has, however, been shown [19] that there are conditions where convergence is not achieved.

Simplex method

A simplex in n-dimensional space is a solid having plane faces and $n + 1$ vertices. For example, triangles and tetrahedra are simplexes in two and three dimensions. The method, originally developed by Spendley et al. [20], relies on an iterative procedure which moves the simplex near to the

optimal parameter values by reflecting specific points in the hyperplanes formed by the remaining points. Once near the optimum point, the simplex can be contracted in order to determine its position more precisely. This method is somewhat more speculative than those previously described and its progress is influenced less by the immediate landscape. Because of this it is less likely to become trapped by an adjacent "poor" local minimum when there is a better one nearby.

In its original form, the method is suitable for minimizing functions with substantial random errors since its progress depends only on whether certain values of the object function are greater or less than other values. For this reason it is useful for regulating input flows to industrial processes.

The simplex method has been extended by Nelder and Mead [21] to allow reflection or expansion, or contraction of the simplex on each iteration. The method developed is then very efficient for exact, differentiable object functions, but has been shown to become less efficient as the number of variables is increased above 5 [13].

Generalized least-squares method

A most important problem for the present studies is that of fitting, by adjusting the input parameters, predictions from theoretical models to experimental observations. It is usual to formulate this problem as that of minimizing the sum of the squares of the differences between predicted and observed data. Clearly, any of the previous methods can be used to solve this problem. It is useful, however, to have a method which takes into account a specified form of the object function and thus reduces the number of function evaluations required. The "generalized least-squares" method has these properties.

For the least-squares problem the object function has the form of fitting m data points:

$$F(\underline{x}) = \sum_{k=1}^{m} [f^{(k)}(\underline{x})]^2 \quad m \geqslant n \tag{7}$$

$\underline{x}$ is equivalent to the position $x_1, x_2, \ldots x_n$, and $f^{(k)}(\underline{x})$ is defined as

$$f^{(k)}(\underline{x}) = f^{(k)}_{\text{predicted}}(\underline{x}) - f^{(k)}_{\text{observed}}(\underline{x}) \tag{8}$$

where k refers to a particular data point.

If the iteration starts at the point $\underline{\xi}$, an approximation to the position of the minimum and the actual minimum is at $\underline{\xi} + \delta$, then differentiation of eqn. (7) gives

$$\sum_{k=1}^{m} g_i^{(k)}(\underline{\xi} + \underline{\delta}) \cdot F^{(k)}(\underline{\xi} + \underline{\delta}) = 0 \quad i = 1, 2, \ldots, n \tag{9}$$

By approximating the left-hand side of eqn. (9) by the first two terms of the Taylor series, the following equation is obtained:

$$\sum_{k=1}^{m}\left[g_i^{(k)}(\underline{\xi})\cdot f^{(k)}(\underline{\xi})+\sum_{j=1}^{n}\{G_{ij}^{(k)}(\underline{\xi})\,f^{(k)}(\underline{\xi})+g_i^{(k)}(\underline{\xi})\cdot g_j^{(k)}(\underline{\xi})\}\,\delta_j\right]\simeq 0 \quad i=1,2,\ldots,n \tag{10}$$

The least-squares method hinges on the further approximation that the terms of the form $G_{ij}^{(k)}(\underline{\xi})\,f^{(k)}(\underline{\xi})$ can be ignored. In this case, the correction $\underline{\delta}$ can be calculated by solving the linear equations

$$\sum_{j=1}^{n}\left\{\sum_{k=1}^{m}g_i^{(k)}(\underline{\xi})\cdot g_j^{(k)}(\underline{\xi})\right\}\delta_j=-\sum_{k=1}^{m}g_i^{(k)}(\underline{\xi})\cdot f^{(k)}(\underline{\xi}) \quad (i=1,2,\ldots,n.) \tag{11}$$

Oscillatory behaviour or even divergence may be experienced in practical applications of this generalized least-squares method. This may be overcome by applying a damping procedure of the sort outlined by Levenberg [22]. Convergence can be guaranteed by using $\underline{\delta}$ as a direction for search and calculating a scaling factor λ, in a manner analogous to that used in the Newton—Raphson and Cauchy methods.

EXTENSION OF PREVIOUS METHODS

Of the methods described above, the Newton—Raphson method can under the correct conditions give the most efficient convergence. It is, however, possible by means of a suitable transformation producing conjugate variables to achieve similar convergence for the Cauchy and direct-search methods. The required variable change is given by the following equation

$$y_i=\sum_{j=1}^{n}(G^{\frac{1}{2}})\,ij\cdot x_j \tag{12}$$

where G is the second derivative matrix derived from $x_1, x_2, \ldots x_n$. This will be positive and definite at points close to the optimal values for $x_1, x_2, \ldots x_n$. With this transformation of variables the G matrix in eqn. (4) becomes equal to the unit matrix, so that the following equation can be written directly:

$$\delta_i'=-g_i' \quad (i=1,2,\ldots n) \tag{13}$$

where g_i' refers to the first derivative of y_i, and δ_i' is the calculated correction for y_i.

There are a number of successful algorithms based on the generation of conjugate direction. Two of the best known are by Powell [23] and Davidson [24] (cf. Fletcher and Powell [25]).

Powell's conjugate direction method

This is essentially an extended direct-search method, and so avoids the need to calculate derivatives. The method requires an estimate ($x_1^{(k)}$, $x_2^{(k)}, \ldots, xn^{(k)}$) of the position of the optimum, and n independent search

directions, which are usually chosen initially as the co-ordinate directions, defined as $\underline{d}_1^{(k)}, \underline{d}_2^{(k)}, \ldots, \underline{d}_n^{(k)}$.

The basic iteration begins by searching along each of the directions in turn, and thus the estimate for the optimal position is changed by the amount

$$\underline{\delta} = \sum_{i=1}^{n} \lambda_i \underline{d}_i^{(k)} \tag{14}$$

where $\lambda_i = 1, 2, \ldots, n$ is calculated to minimize the object function for the appropriate direction search. The displacement $\underline{\delta}$ defined by eqn. (14) is then used as a search direction and the resultant point $(x_1^{(k+1)}, x_2^{(k+1)}, \ldots x_n^{(k+1)})$ is used as the starting estimate for the next iteration. However, the search directions are replaced by the set

$$\underline{d}_i^{(k+1)} = \underline{d}_{i+1}^{(1)} \quad (i = 1, 2, \ldots, n-1) \text{ and } \underline{d}_n^{(k+1)} = \underline{\delta} \tag{15}$$

If the object function is of quadratic form, it can be proved by induction [23] that after the k^{th} interaction the new direction generated, namely $\underline{d}_1^{(k+1)}, \underline{d}_2^{(k+1)}, \ldots, \underline{d}_n^{(k+1)}$ has the property that the lost k are mutually conjugate.

The algorithm is complicated by the need to avoid generating a set of directions which are linearly dependent. When this is likely, the step indicated by eqn. (15) is omitted.

Davidson's method

This procedure is based on the observation that whereas for the Cauchy method the direction of search is given by:

$$\delta_i = -\sum_{j=n}^{n} I_{ij} \cdot g_j \quad (i = 1, 2, \ldots, n) \tag{16}$$

where I is the unit matrix, and g_j is the jth component of the gradient of the object function, the direction of search for the Newton—Raphson method is

$$\delta_i = -\sum_{j=1}^{n} (G^{-1})_{ij} \cdot g_j \quad (i = 1, 2, \ldots, n) \tag{17}$$

Thus in Davidson's method the k'th iteration will be along the direction given by

$$\delta_i^{(k)} = -\sum_{j=1}^{n} H_{ij}^{(k)} g_j^{(k)} \quad (i = 1, 2, \ldots, n) \tag{18}$$

$H^{(k)}$ is here a positive definite matrix which is usually set initially as the unit matrix. The up-dated matrix $H^{(k+1)}$ is calculated by means of the vectors $\underline{\sigma}^{(k)}$ and $\underline{\gamma}^{(k)}$ where

$$\underline{\sigma}^{(k)} = (x_1^{(k+1)}, x_2^{(k+1)}, \ldots, x_n^{(k+1)}) - (x_1^{(k)}, \ldots, x_2^{(k)})$$

$$\underline{\gamma}^{(k)} = (g_1^{(k+1)}, g_2^{(k+1)}, \ldots, g_n^{(k+1)}) - (g_1^{(k)}, \ldots, g_n^{(k)}) \tag{19}$$

The method used is designed to make $H^{(k+1)}$ as close to the matrix G^{-1} as possible [25], and is based on the assumption of a quadratic object function. This method, unlike the previous one, requires the evaluation of first derivatives, but has been extended by Stewart [26] to approximate those based on differences between function values.

Powell's least-squares method

The generalized least-squares method, as indicated, relies on the simplification that the second-derivative terms can be ignored. Usually this approximation will be valid near the minimum, but may be false for a poor approximation or where the sum of the squares even at the minimum is relatively high. In these cases the scaling procedure outlined is necessary to ensure convergence, and even then the rate of convergence may be slow. Powell's method [27] seeks to eliminate this deficiency by generating conjugate directions to replace initial co-ordinate directions. The procedure employed is very similar to that described for the conjugate direction method. In fact, the first replacement direction is chosen to be the search direction calculated by solving eqn. (11) in the generalized least-squares method. The co-ordinate direction replaced is chosen so as to minimize the possibility of linear dependency amongst the coordinate directions generated.

A most important property of the method is that it requires only eqn. (11) to be set up during the first iteration. In fact, one then obtains the inverse of the A-matrix, where, with reference to eqn. (11):

$$A_{ij} = \sum_{h=1}^{m} g_i^{(k)}(\underline{\xi})\, g_j^{(k)}(\underline{\xi}) \tag{20}$$

The search direction $\underline{\delta}$ is then generated by mutliplying this inverse by the vector $\underline{\sigma}$ defined as

$$\sigma_i = \sum_{k=1}^{m} g_i^{(k)}(\underline{\xi})\, f^{(k)}(\underline{\xi}) \quad (i = 1, 2, \ldots, n) \tag{20a}$$

For each successive iteration one modifies the matrix A^{-1} by replacing the components, $g_1^{(k)}$, $k = 1, 2, \ldots, m$, using derivatives with respect to the search direction $\underline{\delta}$ generated during the previous iteration. An efficient way of doing this without having to set up eqn. (11) and then inverting the A-matrix has been developed by Rosen [28].

The generalized least-squares method requires evaluation of the derivatives for all the components, $f^{(k)}$, $k = 1, 2, \ldots, m$, with respect to all the variables, for each iteration. After the first iteration, the present method only requires derivative evaluation with respect to the direction $\underline{\delta}$, and this can be accomplished by a difference technique. This procedure, therefore, is suitable where function derivatives are difficult or impossible to calculate directly.

AVAILABLE ALGORITHMS

Little work has been published on completely automatic computer fitting of ligand field parameters to spectral data. The use of correlation diagrams [29, 30] is well established, but it is necessary to make basic assumptions about the size of some of the parameters and to assume fixed ratios between others.

A great deal of work has been done however on the analysis of band envelopes [12, 31—46]. This work is not limited to optical spectroscopy [11, 12, 46] and includes the analysis of data in gas chromatography as well as e.s.r. [40—42], n.m.r. [39], i.r. [33, 34, 45] and mass spectrometry [43]. Most of the references listed use some variation on the generalized least-squares procedure implemented by Stone [31] for computerized band analysis. This method has been extended further by Papoušek and Plíva [32] who introduced a damping procedure of the sort originally suggested by Levenberg [22]. Pitha and Jones [45] have tested a number of optimization methods for fitting both natural and synthesized test spectra. They found the most efficient methods [47, 48] to be further modifications of Levenberg's damped least-squares procedure, but suggested, however, that a "moving subspace" modification may be required to maintain efficiency when many parameters are involved. Here only the parameters of a group of adjacent bands are adjusted at one time. The area for variation is then moved systematically to cover the entire range of parameters.

Most references concentrate on the description of the actual optimization procedures and pay little attention to the problem of choosing reasonable starting parameters. This problem is discussed by Anderson et al. [35], as well as the problem of convergence to poor or unrealistic fits for gas chromatography. Pitha and Jones [45] also discuss the problem of ambiguous fits for i.r. spectra with special reference to the problem of component band shape. A remote access computer terminal system which allows intervention by the operator if the rate of convergence is poor or in the event of an unrealistic fit has been described by Schwartz [46].

Derflinger and Lishka [11] have written a program which will generate starting parameters for the analysis of u.v. spectra. Their algorithm involves the derivation of the second-derivative spectrum, which is then analysed to detect component bands. The positions of the peak maxima are taken as the minima in the second-derivative spectrum. The peak heights are equated with spectral intensity, and the width for the assumed band model is calculated from the heights and second derivative at the peak maxima. This method is satisfactory for well-resolved spectra, but equating peak height with spectral intensity is no longer justified for strongly overlapping band envelopes. Because of this, Derflinger and Lishka extended their method to include an iterative procedure which compares calculated intensities and second derivatives with the observed values at positions of peak maximum.

THE DEVELOPMENT OF A PROGRAM FOR THE CURVE ANALYSIS OF SPECTROSCOPIC DATA

Most of the methods described above require calculation of first derivatives with respect to all the parameters for each calculated point. The ease of such calculations depends on the form of presentation of the spectral data, as well as the line shape assumed for the component curves. Calculation of partial derivatives with respect to the parameters defining the component curves is relatively simple for standard functions such as Gaussian or Lorentzian [10]. Greater difficulty is encountered when more complex or experimentally observed line shapes are used. The two commonest ways of presenting transmittance spectral data are in terms of percentage transmittance, T, and absorbance A:

$$A^{(k)} = \log_{10} T^{(k)} \quad (k = 1, 2, \ldots, m) \tag{21}$$

Absorbance is more convenient for curve analysis, because the calculated composite band envelope can be compared directly with observed spectral data. If a percentage transmittance presentation is used, the inverse of eqn. (21) may be used as a conversion function for the composite band envelope. Thus

$$T^{(k)} = 10^{A^{(k)}} \quad (k = 1, 2, \ldots, m) \tag{22}$$

Also the derivative values must be corrected:

$$\frac{\partial T^{(k)}}{\partial P_j} = \frac{\partial A^{(k)}}{\partial P_j} \cdot \frac{\partial T^{(k)}}{\partial A^{(k)}} \quad (k = 1, 2, \ldots, m; j = 1, 2, \ldots, n) \tag{23}$$

where the third partial derivative is

$$\partial T^{(k)}/\partial A^{(k)} = e \cdot T^{(k)} \quad (k = 1, 2, \ldots, m) \tag{24}$$

Reflective data can be treated similarly. Here for spectral results recorded in terms of absorbance, and if the Kubelka—Munk relation [49] holds, the required conversion function is

$$R^{(k)} = 1 - ((1 + F^{(k)})^2 - 1)^{\frac{1}{2}} \quad \text{and} \quad A^{(k)} = -\log_{10} R^{(k)} \quad (k = 1, 2, \ldots, m) \tag{25}$$

The derivative conversion factor will then be

$$\frac{\partial A^{(k)}}{\partial F^{(k)}} = \frac{1 + F^{(k)}}{e \cdot R^{(k)} (1 + F^{(k)2} - 1)^{\frac{1}{2}}} \quad (k = 1, 2, \ldots, n) \tag{26}$$

A standard program [13] has been converted to enable it to handle spectral data in a number of forms. An extra subroutine CONV has been introduced which converts calculated intensities, and adjusts the component partial derivatives. Convergence is often poor if this procedure is followed with poor starting parameters. More satisfactory results are obtained, however, if a preliminary step is introduced. Here the spectral data is converted to the appropriate form (e.g. absorbance for transmission spectra, $F_{(R)}$ units

for reflectance spectra), and a standard optimization is performed. The improved parameters are then used to fit the raw spectral data by the program in its modified form.

In the problem of ligand field parameter fitting, it is difficult to calculate the required partial derivatives*. Similarly, the difficulties of curve fitting increase considerably if non-standard curves are used or the spectral data are expressed in unusual form. Derivatives could be calculated by a differencing technique but this is wasteful. Two approaches were followed, the simplex method and Powell's least-squares method; programming details are discussed below. Both methods gave reasonable rates of convergence, but Powell's method converged more rapidly and reliably near the minimum.

In curve analysis, it was found that Powell's method will converge, giving good fits even for systems of strongly overlapping bands. The exact fit obtained, however, may be strongly dependent on the choice of initial parameters. If poor parameters are chosen, unrealistic fits may be obtained. As indicated above, it is possible to fix the positions of peak maxima with a fair degree of certainty, but even so if the height and width parameter are inaccurate false convergence may still occur. Even the use of parameter improvement [12] may not prevent this. A major deficiency of the method of Derflinger and Lishka [12] is, however, its reliance on the use of quantitative second-derivative data in the calculation of width parameters. The second derivative at the peak maximum for curves of equal height depends on the curve form. If an incorrect curve form is assumed, the results obtained will be highly suspect. Also, calculated values for second derivatives are subject to errors related to the interval used in the spectral data from which they have been derived [10].

A fruitful approach to the improvement of initial parameters that has been used is to perform an optimization procedure in which all positioned parameters are held constant. The assumption of constant half-width for all component bands eliminates the possibility of unrealistic fits of the kind illustrated in Fig. 1(b). It has also often been found advantageous to assign the initial values of half-width parameters either with reference to known analogous systems or to use estimates applicable to outer or particularly well-resolved bands.

The use of a complete optimization technique is in many ways wasteful for the improvement of initial parameters. In fact, once the peak positions have been assigned with some certainty, the calculated band envelope can be reasonably fitted to a limited set of important spectral points. The points most sensitive to peak heights are those nearest the peak maxima. Those strongly affected by peak width and position are at points equidistant between peak maxima. If the assumptions about peak positions are correct, because of the rather smooth nature inherent in any sum of component curves, spectral variation between these points will not be dramatic. For

*It is not impossible, however. An algorithm has been devised (see below) but has not been coded.

this reason, a resonable fit to this limited set must be satisfactory for the complete spectrum.

In the case where perfect fitting is impossible (e.g. incorrect line shape is assumed for the component curves), a minimum in the squares of the residues is likely to be better defined for the smaller set of spectral points. Because of this, convergence will be easier, and there is less likelihood of being diverted to a spurious minimum. Employing a limited set of spectral points also allows the use of more straightforward techniques for the optimization of parameters. A program embodying these principles has been written; a fuller description is given below.

EXAMPLES OF ANALYSIS OF EXPERIMENTAL SPECTROSCOPIC DATA

It may not be possible to fit unambiguously a set of strongly overlapping curves to a poorly resolved spectrum, but if certain reasonable assumptions are made concerning the nature of the component curves, the range of possible fits may be greatly reduced. Also, fits which are similar in terms of some general test, such as the root mean-square deviation of calculated values from observed values, may be differentiated according to the nature of the divergence from the experimental curve at important parts of the spectrum. Examples of the analysis of experimental spectra are given below to illustrate these points.

Figure 8 shows the reflectance spectrum of the compound $Ag^{II}SnF_6$ in the range 400—2000 nm. This spectrum was fitted by taking points from 500 to 1800 nm at intervals of 20 nm. The choice of line used for the analysis must be, to some extent, arbitrary. There are, however, theoretical reasons for assuming the following curve form to be reasonable [50].

$$e = e_0 \nu e^{-(\nu-\nu_0)/b^2} \qquad (27)$$

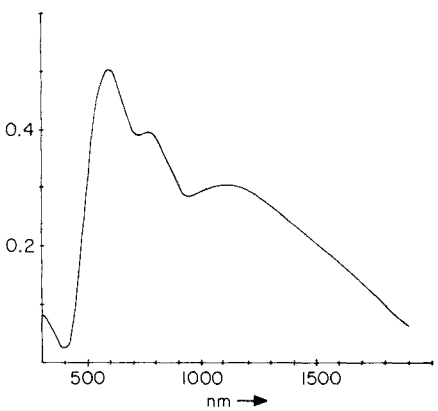

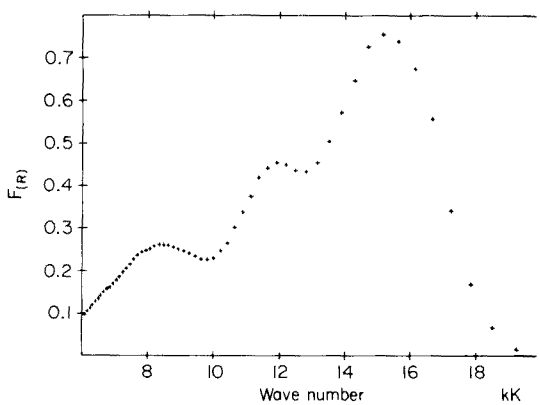

Fig. 8. Diffuse reflectance spectrum of $Ag^{II}SnF_6$ in terms of absorbance against nm.

Fig. 9. Diffuse reflectance spectrum of $Ag^{II}SnF_6$ in terms of $F_{(R)}$ against kK.

This model will be used in all the following examples. However, very similar results are obtained if a simple Gaussian function is used. The quantities ν and ν_0 refer to an energy scale expressed in terms of cm^{-1}. The spectrum shown in Fig. 8 is not in a suitable form for direct analysis into component curves. The required form is in terms of the Kubelka—Munk function, $F(R)$. Figure 9 shows experimental points chosen from the spectrum in terms of $F(R)$ against wave number; this form of presentation is, as discussed above, useful in the initial optimization of parameters. However, in the examples chosen here, the envelope of the component curves was converted to the absorbance form by eqn. (25). In all the examples below, reasonably good parameters were chosen, and the final convergence was achieved by Powell's least-squares method, which does not require direct calculation of derivatives. However, in methods that do require this, the relation shown in eqn. (26) must be used when reflectance spectra expressed in terms of absorbance are fitted directly. For any meaningful illustration of the nature of the component curves, reflectance spectra must, however, be drawn in terms of $F(R)$, and this form will be used in all diagrams.

The three resolved peaks in the reflectance spectrum of $AgSnF_6$ can be reasonably assigned to *d—d* transitions for the tetragonal $(Ag^{II}F_6)^{4-}$ grouping representing in increasing energy: $^2B_{1g} \rightarrow {}^2A_{1g}$, $^2B_{1g} \rightarrow {}^2B_{2g}$ and $^2B_{1g} \rightarrow {}^2E_g$ transitions [51]. A more detailed analysis shows that the $^2B_{1g} \rightarrow {}^2E_g$ transition should be split by spin—orbit effects [52]. The splitting can, to a first approximation, be equated with the spin—orbit coupling constant, λ. Thus a splitting of ca. 1.6 kK might be expected for the high-energy transition. Moreover, the two components of the high-energy transition are expected to have approximately equal intensity.

With this information, it is possible to construct sets of reasonable starting parameters, which should converge to a unique fit, but do not do so. If fairly poor starting parameters are used, unreasonable fits may be produced, as shown in Fig. 10. Although such fits are easily discounted, it is possible to obtain fits which appear reasonable but which require unacceptable parameter values, and the nature of fit obtained may be related to the actual optimization method used. Thus for Powell's least-squares method there was a tendency for one of the high-energy peaks to grow at the expense of the other (see Fig. 11). This problem could be overcome by applying a preliminary optimization where the higher-energy bands were held at a constant ratio, but even so the fits obtained depended on the starting parameters and the precise details of the optimization procedure. Moreover, although the fitted parameters obtained were strongly dependent on the starting values, no precise correlation between the two could be discerned.

A systematic analysis of the range of reasonable fits is thus not possible by just feeding in a number of limiting starting parameters. In a relatively simple case such as that under consideration it is possible to consider the spectrum in terms of two portions. The low-energy portion, below 12 kK is essentially unaffected by the nature of the two high-energy bands. For

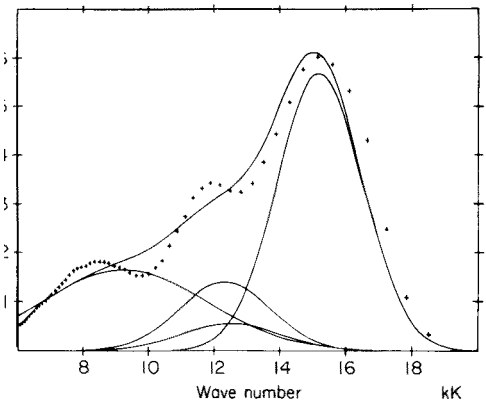

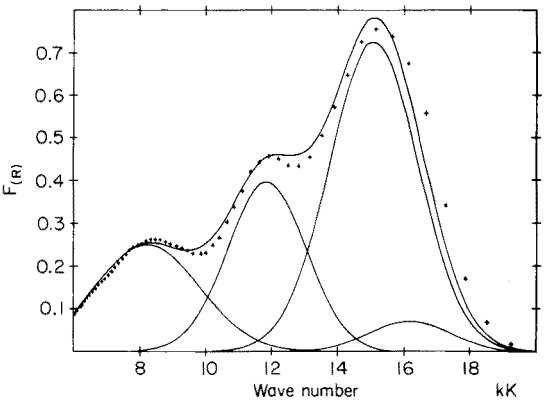

Fig. 10. Very poor deconvolution of $Ag^{II}SnF_6$ reflectance spectrum.

Fig. 11. Deconvolution of $Ag^{II}SnF_6$ spectrum by Powell's least-squares method.

this portion of the spectrum, only a fairly narrow range for the parameters specifying the low-energy bands was possible, and this depended to some extent on the base-line correction assumed for the spectrum. Two extreme parameter values used in further analysis of the spectrum are listed in Table 1.

The analysis obtained for the high-energy part of the spectrum depended on the form of the middle transition; that is, the asymmetry of the envelope to be fitted, on subtracting the low-energy peaks from the spectrum and hence the relative intensities and widths of its two components, depended markedly on the position and width of the middle peak. As shown above, it is not usually possible to obtain unambiguous two-band analyses for asymmetrical band envelopes. There will be a range of peak positions and relative intensities depending on the ratio of widths assumed for the component bands. However, for the spectrum under consideration, the fit obtained, assuming specific values for the low-energy bands and given ratios of widths for the high-energy bands, appears to be unique where reasonable fits can be obtained. Fits based on specific width ratios are illustrated in Figs. 12—15, and the parameters are listed in Table 1.

As can be seen from Table 1, the higher-energy position of the middle component requires a smaller separation between the high-energy components. With the low-energy middle peak, the separation between the higher-energy components varies very little, despite variation in their relative intensities and the position of their centres of gravity. Moreover, the variation in these quantities follows regular trends. Hence a fairly systematic presentation of the range of possible fits is possible for this spectrum. In an attempt to discover a suitable criterion for choosing between the various analyses, crystal field parameters were calculated corresponding to specific sets of transition energies. Fits were obtained by using Powell's least-squares method, both high and low starting values for the spin—orbit parameter, λ, being assumed.

TABLE 1

Fitting parameters for the $Ag^{II}SnF_6$ spectrum illustrated in Figs. 12—15

Set of low-energy curves[a]	Parameters for high-energy curves[b]						Ratio of half-widths	Figure
A	0.367	13.898	1.464	0.477	15.657	1.464	1/1	12
A	0.417	14.066	1.559	0.414	15.794	1.417	1.1/1	13a
A	0.463	14.224	1.645	0.348	15.925	1.371	1.2/1	13b
A	0.498	14.350	1.723	0.287	16.027	1.326	1.3/1	13c
A	0.576	14.548	1.815	0.147	16.237	1.296	1.4/1	13d
A	0.319	13.743	1.382	0.523	15.531	1.521	1/1.1	13e
A	0.277	13.622	1.309	0.554	15.424	1.571	1/1.2	13f
A	0.222	13.470	1.252	0.588	15.301	1.627	1/1.3	13g
A	0.212	13.420	1.179	0.595	15.264	1.650	1/1.4	13h
B	0.549	14.609	1.705	0.325	15.909	1.705	1/1	14
B	0.695	14.852	1.809	0.143	16.29	1.640	1.1/1	15a
B	0.618	14.909	1.926	0.140	15.92	1.605	1.2/1	15b
B	0.745	15.000	1.969	0.014	15.894	1.515	1.3/1	15c
B	0.658	15.012	2.017	0.012	15.257	1.440	1.4/1	15d
B	0.360	14.365	1.625	0.507	15.560	1.788	1/1.1	15e
B	0.226	14.202	1.538	0.617	15.359	1.846	1/1.2	15f
B	0.168	14.091	1.436	0.667	15.278	1.867	1/1.3	15g
B	0.0236	14.974	1.403	0.739	15.067	1.964	1/1.4	15h

[a]Set A has the parameters: 0.176 8.096 1.464 0.288 11.543 1.311, with a baseline correction of —0.05 applied to experimental points. Set B has the parameters 0.246 7.917 2.264 0.394 11.722 1.689, with zero baseline correction applied to experimental points.

[b]Throughout the Table, parameters should be considered in groups of three defining the component curves. For a particular group (a_1, a_2, a_3) the corresponding curve is defined:

$e = a_1 \cdot \nu/a_2 \cdot e^{-(a_2-\nu)^2/a_3^2}$ where ν is in kK.

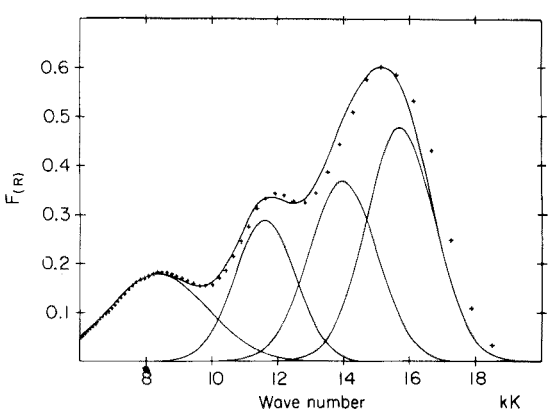

Fig. 12. Deconvolution of $Ag^{II}SnF_6$ spectrum using parameters given in Table 2.

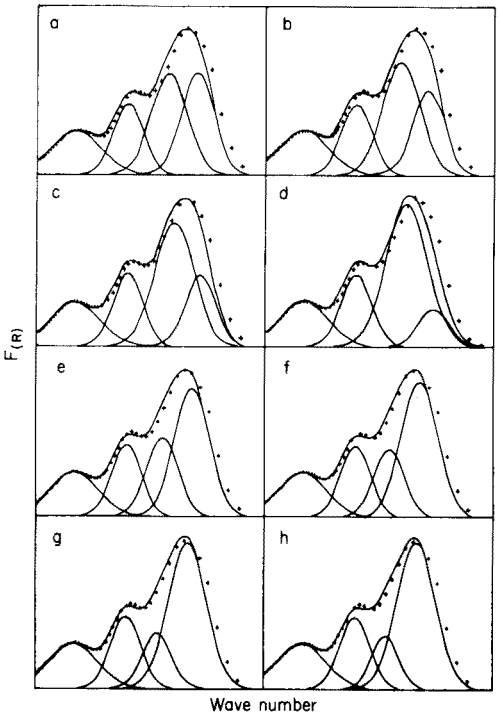

Fig. 13(a—h). Deconvolution of $Ag^{II}SnF_6$ spectrum using the parameters listed in Table 2.

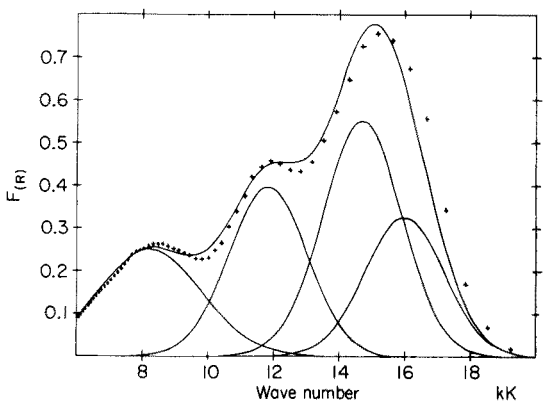

Fig. 14. Deconvolution of $Ag^{II}SnF_6$ spectrum using parameters listed in Table 2.

When this procedure was followed, a number of interesting features emerged. A sample of fitted parameters is listed in Table 2. In those cases with small assumed separation between the high-energy transitions, two possible parameters fits were possible. Where large separations were assumed, exact fits could not be obtained on the basis of a simple tetragonal model.

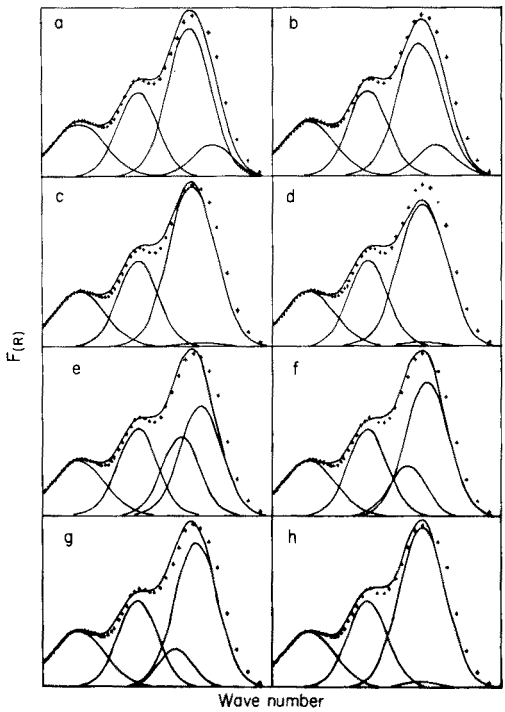

Fig. 15 (a—h). Deconvolution of $Ag^{II}SnF_6$ spectrum using parameters listed in Table 2.

The range of ligand field parameters*, excepting λ, is not very great, and none of the fits could be excluded on this basis. The analyses showed, however, that the assumption of a simple first-order splitting of the ^2E_g level by spin—orbit coupling may not be valid, and considerable mixing is possible between the $^2B_{2g}$ level and the lower component of the ^2E_g level. This will upset any simple assumptions as to the relative intensities of the two components of ^2E_g level. Even so it would be unreasonable to expect vast differences in intensities. This, together with the assumption that the high-energy bands will display reasonably uniform half-widths, reduces markedly the range of fits to be considered. Two typical examples are provided by the fits shown in Figs. 12 and 14. Although both analyses are similar in terms of the root-mean-square deviation of calculated from observed spectral values, fine detail of spectral shape is reproduced more faithfully in the former. This is true in general for all the analyses, if the lower-energy assignment is assumed for the $^2B_{1g} \rightarrow {}^2B_{2g}$ transition. In all these cases, however, exact fits could not be obtained for crystal field parameters on the assumption of a tetragonal crystal field model. This difficulty can be rationalized if it is remembered that the large splitting of the ^2E_g level assumed in these fits

*In those cases where no exact fits could be obtained, parameter values corresponding to the best obtainable fits are considered.

TABLE 2

Crystal field parameters and transition energies for the $Ag^{II}SnF_6$ spectrum in Figs. 12—15

Figure showing assumed transition energies	Fitted parameters (cm^{-1}) Dq, Bs, Ft, λ				Fitted transition energies (kK) if exact fits could not be obtained			
12	−1180	1486	475	−1567	8.06	11.49	14.23	15.48
13a	−1177	1511	455	−1609	8.06	11.49	14.36	15.67
13b	−1180	1520	457	−1657	8.09	11.51	14.44	15.78
13c	−1176	1537	443	−1714	8.08	11.49	14.55	15.95
13d	−1176	1560	433	−1774	8.11	11.50	14.68	16.14
13e	−1181	1474	480	−1502	8.05	11.51	14.14	15.33
13f	−1180	1460	489	−1474	8.04	11.49	14.05	15.21
13g	−1183	1452	502	−1431	8.08	11.51	13.97	15.09
14	−1200	1491	439	−1623				
14	−1208	1464	464	−1706				
15a	−1172	1619	306	−1057				
15b	−1268	1336	597	−1978				
15c	−1170	1636	287	−908				
15d	−1286	1298	633—	−2020				
15e	−1200	1463	457	−1492				
15f	−1204	1447	469	−1538				
15g	−1196	1453	461	−1391				
15h	−1196	1455	458	−1396				

requires a large value of λ. Increasing λ, however, mixes the $^2B_{2g}$ level with the lower ^2E_g component, raising its energy and tending to counteract the overall splitting of the ^2E_g level.

A possible mechanism for further splitting of the ^2E_g level is reduction of the symmetry of the $(AgF_6)^{4-}$ grouping to say C_{2v}. This will remove the centre of the symmetry of the system so that *d—d* transitions are no longer strictly Laporte-forbidden. Although x-ray powder data are available for these compounds [53], the exact symmetry of the $(AgF_6)^{4-}$ grouping is not known. The spectral transitions in $AgSnF_6$ are relatively weak. The isomorphous compound $AgPbF_6$ has greater intensity, while $AgHfF_6$ and $AgZrF_6$ show even stronger *d—d* bands consistent with the removal of the centre of symmetry. A small distortion of this kind might then be reasonably expected in $AgSnF_6$. This example shows that for even a relatively simple system an unambiguous fit may not be possible. It is conceivable that a unique fit could be obtained if account were taken of the relative intensities of the various transitions. This would require a sophisticated model involving the calculation of eigenvectors of all component states. To be realistic the model must allow for possible reduction in the symmetry of the system to C_{2v}, either by a static or vibronic mechanism. Here possible *d—p* or d—(charge transfer) mixing must be considered. Such a procedure is hardly justifiable for the kind of spectral information available from reflectance studies. Where intensity data are relatively easily extracted from the appropriate

theoretical model (e.g., n.m.r. or Mössbauer studies) it should be possible to discount certain regions of fit on this basis, even though a unique fit may be unattainable, except under exceptional circumstances.

The literature contains many examples of apparently unique fits for the analysis of quite complicated spectra. It is probable in many cases that these fits reflect the prejudices (either conscious or unconscious) of the author, or merely the first successful fit obtained. Where line shapes and relative positions of the component bands are known with some certainty, however (e.g., in certain kinetic studies and possibly in the analysis of gas chromatograms), complicated systems may be analysed and a unique fit obtained. Even where this is not possible, curve analysis in conjunction with other parameter-fitting procedures may provide a basis for either rejection or further refinement of a theoretical model for a physical system.

COMPUTER PROGRAMS

This section outlines the methods used in a number of computer programs written by the authors. The programs were written in FORTRAN IV for use on an ICL 4-75 computer. Detail of the actual programming techniques involved is kept to a minimum, because it is probably of limited interest and tends to obscure the basic principles behind the programming methods. The mathematical operations performed in the various subroutines are, however, discussed and the main iterative processes outlined.

The background theory presented should provide a basis for the routine use of the programs, and necessary extensions or modifications. Listings of actual programs are available on request.

Powell's least-squares method

The main program based on this method reads in the variable parameters, and experimental data such as spectral points. The exact form of the main program depends on the particular object function being used. A subroutine VALUE is used to calculate the actual values for the object function, and similarly can be modified depending on the exact application. The remaining subroutines are standard.

The main iteration of the program is performed in subroutine POWELL, which in turn calls five subroutines: MATRIX, LIMTST, MINSET, ROSEN and FORM. The function of these routines and those they call is outlined in the following text and a flow diagram is given in Fig. 16.

Subroutine MATRIX has the function of setting up and solving the linear eqns. (11). The form of this equation is, however, altered in the manner recommended by Powell [27]. Instead of using the derivative $g_j^{(k)}(\underline{x})$, $j = 1, 2, \ldots, n$, with respect to the parameters x_1, $i = 1, 2, \ldots, n$ derivatives, $\gamma^{(k)}(i)$, $i = 1, 2, \ldots, n$, $k = 1, 2, \ldots, m$, are used with respect to vectorial directions $\underline{d}(i)$, $i = 1, 2, \ldots, n$. These are defined as

$$\gamma^{(k)}(i) = \sum_{j=1}^{n} g_j^{(k)} \cdot d_j(i) \quad i = 1, 2, \ldots, n, \; k = 1, 2, \ldots, m \tag{28}$$

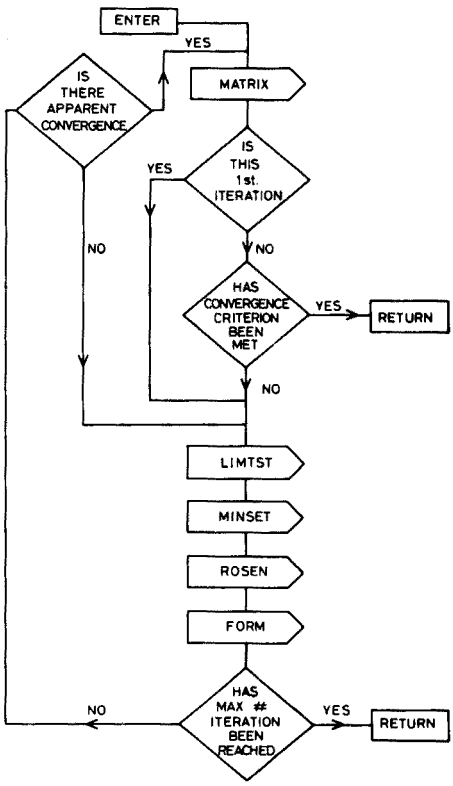

Fig. 16. Flow chart for the POWELL program.

Also the direction vectors are scaled so that

$$\sum_{k=1}^{m} [\gamma^{(k)}(i)]^2 = 1, \quad i = 1, 2, \ldots, n \tag{29}$$

Equation (11) can then be rewritten as:

$$\sum_{j=1}^{n} \left\{ \sum_{k=1}^{m} \gamma^{(k)}(i)\, \gamma^{(k)}(j) \right\} q(j) = p(i); \quad i = 1, 2, \ldots, n \tag{30}$$

$$p(i) = -\sum_{k=1}^{m} \gamma^{(k)}(i)\, \mathrm{f}^{(k)}(\underline{\xi}) \tag{31}$$

The corrections to the parameters, δ_i, $i = 1, 2, \ldots, n$, are then calculated by substituting in the equation

$$\delta_i = \sum_{j=1}^{n} q(j) \cdot d_i(j); \quad i = 1, 2, \ldots, n \tag{32}$$

Solution of the linear eqn. (30) is accomplished by defining a matrix A, such that

$$A_{ij} = \sum_{k=1}^{m} \gamma^{(k)}(i) \cdot \gamma^{(k)}(j) \tag{33}$$

Inversion of this matrix and multiplication of the inverse by the p-vector, defined in eqn. (31), generates the q-vector, which can be used to calculate parameter corrections. The scaling of the direction vectors introduced in eqn. (29) ensures that the A-matrix has all its diagonal elements equal to one. This reduces the computer round-off errors in the matrix inversion, and multiplication processes.

MATRIX calls four subroutines; ABLF2, ABLF3, INVERT and GDELTA. ABLF2 is called by MATRIX only during the first iteration in POWELL. It has the function of calculating the derivatives $\gamma^{(k)}(i)$, $i = 1, 2, \ldots n$, defined by eqn. (29) along the vectors corresponding to the parameter directions. Instead of calculating derivatives at the initial parameter estimate $\underline{\xi}$, a direct search method is employed. Derivatives are then calculated at the point of function minimum along each direction of search. Subroutine ABLF2 generates the search directions and calls LIMTST and MINSET. Both these subroutines are also called by POWELL. LIMTST calculates the limits and step size for the linear search. MINSET performs the linear search itself and calculates derivatives at the function minimum. This is a most important subroutine and will be described in greater detail below. ABLF3 performs a similar function to ABLF2 but uses the vectorial search directions generated by POWELL after the first iteration. The A-matrix and p-vector are set-up in subroutine MATRIX itself. Matrix inversion is performed by INVERT, and calculation of the parameter corrections, δ_i, $i = 1, 2, \ldots, n$, in GDELTA.

The correction vector $\underline{\delta}$ is returned to subroutine POWELL. Linear search and derivative evaluations are then performed by LIMTST and POWELL. This linear search procedure is most important and provides a theoretical guarantee for convergence.

Another crucial step in the method is the modification of the inverted A-matrix by replacement of the components, $\gamma^{(k)}(i)$, $k = 1, 2, \ldots, m$, with derivatives taken along the search direction, $\underline{\delta}$. The approach used is applied in subroutine ROSEN. An algorithm is set out quite clearly in the literature [27] and was closely followed in writing the subroutine. However, the method was modified to allow replacement of any set of components, $\gamma^{(k)}(i)$, $k = 1, 2, \ldots, m$, and is not restricted to $i = 1$.

The modified inverse A-matrix can then be used to generate new search directions, $\underline{\delta}$, and this gives the basic for the iteration. Search directions are calculated in subroutine FORM, which simply generates the p-vector and calls GDELTA which multiplies by the inverted A-matrix. GDELTA also has the function of deciding which derivative components are to be replaced in subroutine ROSEN during the next iteration. The criterion used by Powell [27] was to choose i such that

$$|p(i) \cdot q(i)| = \max. \tag{34}$$

This was, however, modified so that the same direction cannot be replaced twice during n iterations.

Subroutine MATRIX is not called after the first iteration except when there is apparent convergence. The linear search procedure used in ABLF3 then provides a check on whether the convergence is real or arises from corruption of the inverted A-matrix.

As mentioned above, subroutine MINSET plays a most important role in ensuring convergence for Powell's least-squares procedure. The algorithm on which it is based is closely related to that used in this conjugate direction method [22]. This approach hinges on the approximation that the form of the object function near the minimum, along a linear search direction, can be taken to be parabolic. Powell worked out function values at positions a, b and c along the search direction and predicted the turning value to be at position d where

$$d = \tfrac{1}{2} \cdot [(b^2-c^2)\,f_a + (c^2-a^2)\,f_b + (a^2-b^2)\,f_c]/[(b-c)\,f_a + (c-a)\,f_b + (a-b)\,f_c] \tag{35}$$

This method is, however, rather unsatisfactory in so far as (1) d may represent a maximum rather than a minimum; (2) the denominator may be a very small number or even zero, and the value calculated for d subject to a very large computational error.

The method adopted for use in MINSET is to choose step lengths and limits along the search direction (achieved in subroutine LIMTST), and evaluate the object function one step from the origin. If the function at this position is less than at the origin, a function evaluation is made at two steps from the origin, if greater at one step in the opposite direction. The objective is to create a set of three points such that the middle has the lowest function value. If this condition is not met by the set created initially, the point with the highest function value is moved to a position one step outside that with the lowest value, and the process is repeated until the desired configuration is achieved. If the object is reasonably well-behaved, there will be no local maxima between the outer two points, and a parabolic form can be assumed. Three parameters are required to define a parabola, and these can be readily derived, if three function values and position along the search direction are known, by setting up and solving three linear equations. Because of the form chosen for the points used, the parabola so defined must have a minimum whose position is between the outer points. The range of the set of points can then be reduced by moving one of the outer points to the position calculated for the parabolic minimum. The particular point is chosen so as to retain the condition of the lowest function value at the middle position. Convergence is achieved when the range of the points generated is sufficiently small.

Derivatives at the function minimum are calculated by a differencing technique by using the equation

$$\frac{\partial}{\partial\lambda} f^{(k)}(\underline{\xi} + \lambda\underline{\delta}) \simeq [f^{(k)}(\underline{\xi} + \lambda_1\underline{\delta}) - f^{(k)}(\underline{\xi} + \lambda_2\underline{\delta})]/(\lambda_1 - \lambda_2) = u^{(k)}(\underline{\delta}) \tag{36}$$

Clearly the approximation in eqn. (36) will be minimized by reducing the value of $(\lambda_1 - \lambda_2)$. However, this may drastically increase the computer round-off error in the calculated derivatives. Because of this, Powell's basic method was extended to allow for this, and, if necessary, increase $(\lambda_1 - \lambda_2)$. The approximation is improved by

$$\gamma^{(k)}(\underline{\delta}) = u^{(k)}(\underline{\delta}) - \mu f^{(k)}(\underline{\xi} + \lambda_m \underline{\delta}) \tag{37}$$

where

$$\mu = \sum_{k=1}^{m} [\mu^{(k)}(\underline{\delta}) \cdot f^{(k)}(\underline{\xi} + \lambda_m \underline{\delta})] / \sum_{k=1}^{m} [f^{(k)}(\underline{\xi} + \lambda_n \underline{\delta})]^2 \tag{38}$$

because it is known that the derivative of $F(\underline{x})$ along $\underline{\delta}$ at $\underline{\xi} + \lambda_m \underline{\delta}$, the minimum point, must be zero. Finally $\gamma^{(k)}(\underline{\delta})$ and $(\underline{\delta})$ are scaled so that the conditions required to fulfil eqn. (29) are met.

Simplex method

A program based on Nelder and Mead's modification [21] of the simplex method was written. All routines are standard except the main program, which reads in data, and subroutine CALC, which calculates function values.

The main iteration of the program takes place in subroutine NELDER. Before commencing the iterative procedure, NELDER calls subroutines SIMPLEX and DIFCAL. These respectively set up and calculate function values for the initial simplex.

The actual techniques of programming for the main iteration are illustrated in Fig. 17. The numbers in parentheses refer to the actual CONTINUE statements used in the program. Here $P_0, P_l, \ldots, P_n$ are the $(n + 1)$ points in n-dimensional space defining the current simplex. The function value at P_i is written y_i. The suffixes h (for high) and l (for low) are defined such that

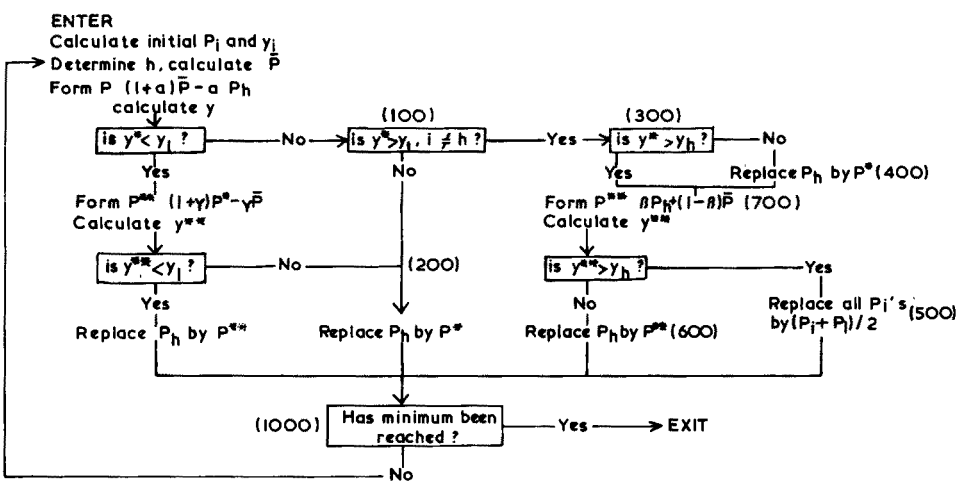

Fig. 17. Flow chart of simplex algorithm.

$$y_h = \max_i (y_i) \text{ and } y_l = \min_i (y_i) \tag{39}$$

$\bar{P}$ is defined as the centroid of all points with $i \neq h$, and $[P_iP_j]$ is the distance from P_i to P_j. At each stage in the process, P_h is replaced by a new point; three operations are used — reflection, contraction and expansion. These are defined as follows: the reflection of P_h is denoted by P^* and its co-ordinates are defined by the relation

$$P = (1 + \alpha)\bar{P} - \alpha P_h \tag{40}$$

where α is a positive constant, the reflection coefficient. Thus P^* is on the line joining P_h and $\bar{P}$, on the far side of $\bar{P}$ from P_h with $[P^*\bar{P}] = \alpha[P_h\bar{P}]$. If y^* lies between y_h and y_l, then P_h is replaced by P^* and the process continued with the new simplex.

If $y^* < y_l$, P^* is expanded to P^{**} by using the relation

$$P^{**} = \gamma P^* + (1 - \gamma)\bar{P} \tag{41}$$

The expansion coefficient γ, which is greater than unity, is the ratio of the distance $[P^{**}\bar{P}]$ to $[P^*P]$. If $y^{**} < y_l$, P_h is replaced by P^{**} and the process is restarted; but if $y^{**} > y_l$, P_h is replaced by P^* before the iteration is restarted.

If, on reflecting P to P^*, it is found that $y^* > y_i$ for all $i \neq h$, a new P_h is defined to be the old P_h or P^*, whichever has the lower y value. A contraction process is then carried out, producing P^{**} where

$$P^{**} = \beta P_h + (1 - \beta)\bar{P} \tag{42}$$

The contraction coefficient β lies between 0 and 1 and is the ratio of the distance $[P^{**}\bar{P}]$ to $[P\bar{P}]$. P_h is then replaced by P^{**} unless $y^{**} > y_h$. For such a failed contraction all the P_i's are replaced by $(P_i + P_l)/2$ and the process restarted.

The coefficients α, β and γ can be fed in as variable parameters, but for convenience the values found most efficient by Nelder and Mead are used, namely $\alpha = 1$, $\beta = 0.5$, $\gamma = 2$.

Approximate curve-fitting method

When Gaussian or other theoretical curve forms are fitted to spectral data, a reasonable overall fit can be obtained by optimizing a limited number of data points, namely those nearest and those half way between the predicted peak positions. A program embodying this approximation was used to improve poor starting approximations for parameters obtained by analysis of the second-derivative spectrum, or from other theoretical considerations. The improved parameters can then be used as starting parameters for a full least-squares or simplex treatment.

The beginning of the program is concerned with reading in spectral data and converting it to a usable form. For instance, if reflectance data are used,

they are converted to F(R) units, and wavelength data in nm may be converted to kilokaysers. The approximate parameters corresponding to N component curves are then read in, together with their lower and upper limits, which may be read in specifically or calculated from a permissible percentage deviation for all the parameters. Two sets of spectral points are then chosen:

(1) N points at positions close to the peak maxima;

(2) $N + 1$ points; $N - 1$ at positions between the points of set (1), together with two points outside the points of set (1).

The main iteration of the program can be reduced to three basic steps.

Step (a). This step varies the heights of the component curves, to optimize spectral points in set (1). The optimization conditions can be expressed in terms of the following equations

$$y_i = c_{i1}\, e_1 + c_{i2}\, e_2 + \ldots + c_{in} \cdot e_n \quad i = 1, 2, \ldots, n \tag{43}$$

where y_i is the observed value for the ith spectral point, e_j is the height of the jth component curve, and c_{ij} is the fractional height coefficient at the ith spectral point for the jth component curve.

This then represents a set of n linear equations in n unknowns, and the values e_i, $i = 1, 2, \ldots, n$ can be readily evaluated by a Gaussian elimination method, unless eqn. (43) are linearly dependent. In this case, or if the parameters obtained are clearly unphysical (i.e. correspond to negative curves) an alternative procedure is adopted. Here, for the first iteration e_i, $i = 1, 2, \ldots, n$ are assigned the same values as y_i, $= 1, 2, \ldots, n$. For successive iterations where values from the solution of eqn. (43) cannot be used all the height parameters are reduced by 5% from their existing values.

Step (b). This step varies the half-width parameters of the component curves so as to optimize spectral points in set (2); n points are chosen from the set, with the first and last omitted on alternate iterations.

The method used to obtain corrections for the parameters makes use of the approximation, where second and higher derivatives are ignored:

$$\Delta y_i \frac{\partial H_i}{\partial P_1} \times \Delta P_1 + \frac{\partial H_i}{\partial P_2} \times \Delta P_2 + \ldots \frac{\partial H_i}{\partial P_n} \times \Delta P_m \quad i = 1, 2, \ldots, n \tag{44}$$

Δy_i equals $(y_i - H_i)$ where y_i and H_i are the observed and calculated values for the ith spectral points; Pi represents the half-width for the ith spectral point.

Solution of eqn. (44) in a manner analogous to that used for eqn. (43) will yield the corrections, ΔP_i, $i = 1, 2, \ldots, n$, for the half-width parameters. Because of the approximations inherent in eqn. (44) the correction parameters will not be exact. They are, therefore, not applied directly but used to define the direction vector for a linear search. The search procedure is carried out in subroutine MINSET2. This subroutine uses the same method as MINSET, described for the Powell program, but partial derivatives are not

required. As mentioned above, the allowed limits for the parameters are either fed in as data or calculated at the beginning of the program.

Step (c). Here the position parameters for the component parameters are modified to optimize spectral points in set (2). The method is completely analogous to that used in step (b). The algorithm as described in its present form will often converge to give parameters fitting well both spectral points (1) and (2). However, this is not always so, and non-convergent behaviour may occur where parameters oscillate between two well-defined values over a number of complete oscillations. The problem can be overcome by modifying steps (a) and (b) so that linear search procedures fit points from both sets (1) and (2). Step (a) is modified so that, after the first iteration, it also makes use of such a search procedure. The search direction for the jth iteration is defined:

$$\Delta e_i(j) = e_i - e_i'(j-1) \quad i = 1, 2, \ldots, n \tag{45}$$

e_i is the height parameter for the ith component curve, obtained from solving eqns. (43); $e_i'(j-1)$ is the height parameter obtained after a linear search during the $(j-1)^{\text{th}}$ iteration.

These modifications overcome the problem of oscillation encountered in the simplex method, because each step fits the same set of spectral points. Also the fit, expressed as the sum of the squares of differences between observed and calculated spectral values, must improve with each iteration until final convergence is achieved. In fact, no improvement of the sum of squares can be used as a criterion of convergence. This is not necessarily true for the method in its simpler form.

The program described uses the modified method, and exhibits good convergence properties. After the height parameters are set during the first iteration, however, all the parameters are altered by using linear search methods. This ensures convergence to a local minimum, which will probably be the same minimum as would be obtained by an extended least-squares method. It is possible that the unmodified method would, under certain circumstances, converge to a better minimum. Also the oscillatory behaviour sometimes observed for the simple method may well be related to the occurrence of more than one minimum in a local vicinity. In view of these observations, a logical extension of the present work would be to develop a program which employs the unmodified method initially, but converts to the modified method if oscillatory behaviour is detected. An algorithm to search for alternative local minima should also be included.

An algorithm for the calculation of first and second derivatives of calculated eigenvalues with respect to ligand field parameters

The calculation of partial derivatives required in ligand field fitting presents a number of difficulties (see above). It is not, in general, possible to write explicit equations for the partial derivatives of the eigenvalues for secular matrices with respect to the parameters which define the matrix elements.

In Powell's least-squares method, derivatives with respect to all the parameters are required only once, at the beginning, for setting up the initial A-matrix; in this case, the use of a differencing technique is reasonable. Other methods, however, may require more frequent calculation of derivatives and, for completeness, a possible algorithm to perform the task is included.

The method hinges on the important property of Hermitian matrices that it is possible to perform similarity transformations which will convert them to diagonal form

$$D = U^{-1} H U \tag{46}$$

where H refers to the untransformed Hermitian matrix, and D is the corresponding matrix in diagonal form; U is the appropriate unitary matrix for the transformation with U^{-1} as its inverse. The columns of matrix U correspond to the eigenvectors of H found by solving the associated secular equations. There are a number of computational methods for diagonalizing matrices and calculating eigenvectors. Which is the most efficient will depend to some extent on the size of H and how close it is to being diagonal.

The matrix H can be considered as a sum of a number of matrices

$$H = H'_1 p_1 + H'_2 p_2 + \ldots H'_n p_n \tag{47}$$

where p_i refers to the values of the ith parameter, and H'_i its matrix of coefficients required to make up the original Hermitian matrix. The similarity transformation expressed in eqn. (46) can be applied to each of the component matrices H'_i. The diagonals of these transformed matrices will then represent the coefficients of the parameters p_j for each of various eigenvalues E_i:

$$E_i = c_{i1} p_1 + c_{i2} p_2 + \ldots c_{in} p_n \quad (i = 1, 2, \ldots m) \tag{48}$$

The derivative $\partial E_i / \partial p_j$ is then given by c_{ij}. In general, the value of the c_{ij} will vary with the parameters p_i ($i = 1, n$). Thus non-zero second derivatives are possible, and will be given by

$$\partial^2 E_i / \partial p_k \cdot \partial p_j = \partial^2 E_i / \partial p_j \cdot \partial p_k = c_{ij} \cdot \partial c_{ij} / \partial p_k \tag{49}$$

Such second derivatives are required in the Newton—Raphson method and its modifications. The partial derivatives $\partial c_{ik} / \partial p_j$ can be found from the relation:

$$\partial c_{ik} / \partial p_j = \left[\sum_{\substack{t \\ t \neq 1}} m_{itj} / (E_t - E_i) \right] c_{tk} \tag{50}$$

where m_{itj} refers to the appropriate off-diagonal elements in the matrix H'_j after a similarity transformation with the unitary matrix U.

This paper is published by permission of the Central Electricity Generating Board. We thank the SRC for the award of a studentship to R. F. M.

REFERENCES

1 R. N. Jones, Spectrochim. Acta, 9 (1957) 235.
2 C. Sandorfy and R. N. Jones, Can. J. Chem., 34 (1956) 88.
3 F. W. Noble, J. E. Hayes Jr., and M. Eden, Proc. Inst. Radio Engrs., 47 (1959) 1952.
4 I. M. Sarosohn and S. Dal Nogare, Pittsburgh Conference on Analytical Chemistry and Applied Spectroscopy Abstracts, (1966) 143.
5 F. W. Noble and J. E. Hayes, Ann. N.Y. Acad. Sci., 115 (1964) 644.
6 G. C. Allen, P. M. Tucker and R. K. Wild, Surf. Sci., 68 (1977) 469.
7 E. C. Olson and C. D. Alway, Anal. Chem., 32 (1960) 370.
8 R. C. Smith, Rev. Sci. Instrum., 34 (1963) 296.
9 J. S. Challice and G. M. Clarke, Spectrochim. Acta, 22 (1966) 63.
10 J. S. Challice and G. M. Clarke, Spectrochim. Acta, 21 (1965) 791.
11 G. Derflinger and H. Lishka, Monatsh. Chem., 99 (1968) 1851.
12 G. Derflinger and H. Lishka, Monatsh. Chem., 99 (1968) 2450.
13 M. J. Box, Comput. J., 9 (1966) 67.
14 R. Fletcher, Comput. J., 8 (1965) 33.
15 H. A. Spang III, S.I.A.M. Rev., 4 (1962) 343.
16 M. J. D. Powell, S.I.A.M. Rev., 12 (1970) 79.
17 A. Cauchy, C.R. Acad. Sci., 25 (1847) 536.
18 A. D. Booth, Numerical Methods, Butterworths, London, 1957.
19 M. J. D. Powell, in J. Walsh (Ed.), Numerical Analysis: An Introduction, Academic Press, London, 1966.
20 W. Spendley, G. R. Hext and F. R. Himsworth, Technometrics, 4 (1962) 441.
21 J. A. Nelder and R. Mead, Comput. J., 7 (1965) 308.
22 K. Levenberg, Q. Appl. Math., 2 (1944) 164.
23 M. J. D. Powell, Comput. J., 7 (1964) 155.
24 W. C. Davidson, A. E. C., Research and Development Rep. ANL-5990 (rev), (1959).
25 R. Fletcher and M. J. D. Powell, Comput. J., 7 (1964) 149.
26 G. W. Stewart III, J. Assoc. Comput. Mach., 14 (1967) 72.
27 M. J. D. Powell, Comput. J., 7 (1964) 303.
28 J. B. Rosen, J. Soc. Ind. Appl. Math., 8 (1960) 181.
29 Y. Tanabe and S. Sugano, J. Phys. Soc. Jpn., 9 (1954) 753.
30 J. R. Perumareddi, J. Phys. Chem., 71 (1967) 3155.
31 H. Stone, J. Opt. Soc. Am., 52 (1962) 998.
32 D. Papoušek and J. Plíva, Collect. Czech. Chem. Commun., 30 (1965) 3007.
33 J. Pitha and R. N. Jones, Can. Spectrosc., 11 (1966) 14.
34 J. T. Bell and R. E. Biggers, J. Mol. Spectrosc., 18 (1965) 247.
35 A. H. Anderson, T. C. Gibb and A. B. Littlewood, Anal. Chem., 42 (1970) 434.
36 A. B. Littlewood, A. H. Anderson and T. C. Gibb, in C. L. A. Harbourn (Ed.), Gas Chromatography, 1968, Proc. Seventh Int. Symp., Institute of Petroleum, London, Eng., 1969, p. 297.
37 R. D. B. Fraser and E. Suzuki, Anal. Chem., 38 (1956) 1130.
38 A. H. Anderson, T. C. Gibb and A. B. Littlewood, Chromatographia, 2 (1969) 466.
39 W. D. Keller, T. R. Lusebrink and C. H. Sederholm, J. Chem. Phys., 44 (1966) 782.
40 J. A. Ibers and J. D. Swalen, Phys. Rev., 127 (1962) 1914.
41 D. W. Marguardt, R. G. Bennett and E. J. Burrell, J. Mol. Spectrosc., 7 (1961) 269.
42 T. S. Johnston and H. G. Hecht, J. Mol. Spectrosc., 17 (1965) 98.
43 D. C. Luenberger and V. E. Dennis, Anal. Chem., 38 (1966) 715.
44 J. P. Carver, E. Schechter and E. R. Blout, J. Am. Chem. Soc., 88 (1966) 2550.
45 J. Pitha and R. N. Jones, Can. J. Chem., 44 (1966) 3031; 45 (1967) 2347.
46 L. M. Schwartz, Anal. Chem., 43 (1971) 1336.
47 D. W. Marguardt, J. Soc. Ind. Appl. Math., 11 (1963) 431.
48 J. Meiron, J. Opt. Soc. Am., 55 (1965) 1105.

49 P. Kubelka and F. Munk, Z. Techn. Physik., 12 (1931) 593.
50 C. K. Jørgensen, Absorption Spectra and Chemical Bonding in Complexes, Pergamon Press, London, 1962.
51 G. C. Allen, R. F. McMeeking, R. Hoppe and B. Müller, J. Chem. Soc. Chem. Commun., (1972) 291.
52 G. C. Allen and R. F. McMeeking, J. Chem. Soc. Dalton Trans., (1976) 1063.
53 R. Hoppe and B. Müller, Naturwissenschaften, 56 (1969) 35.

Dictionary of Data Processing

Including Applications in Industry, Administration and Business

3rd revised and enlarged edition

in English, German and French

compiled by A. WITTMANN *and* J. KLOS, *members of the staff of the German Patent Office.*

Since the first edition of this dictionary appeared, the number of terms in the field of data processing has steadily increased due to the fact that each new 'computer generation' brings with it many new terms describing components, functions or procedures. The great interest with which the second edition of the Dictionary of Data Processing was received has made a new edition necessary sooner than expected.

This third revised and enlarged edition contains over 6,000 terms in the field of data processing, including 150 new terms. The revision has been further improved by the deletion of obsolete terms.

The compilers have selected the most important and most frequently used English terms and their equivalents in French and German and correlated them with examples where necessary. This selection includes additional terms used in the fields of application of data processing which were considered relevant. The main section of this dictionary consists of a numbered list of English terms in alphabetical order together with the equivalents in the other languages. The German and French alphabetical indexes follow the main section.

This dictionary will be useful to all those involved in the field of data processing, including systems engineers, computer scientists, technicians, translators, interpreters, and information scientists.

August 1977 xvi + 348 pages US $54.95/Dfl. 135.00 ISBN 0-444-99823-3

Distributor for the German language area: R. Oldenbourg Verlag, München

ELSEVIER

P.O. Box 211, Amsterdam
The Netherlands
52 Vanderbilt Ave
New York, N.Y. 10017

The Dutch guilder price is definitive. US $ prices are subject to exchange rate fluctuations.

7055

VOL. 103, No. 1 ANALYTICA CHIMICA ACTA March 15, 1978

(Computer Techniques and Optimization, Vol. 2, No. 1)

CONTENTS

© Elsevier Scientific Publishing Company, 1978.
All rights reserved. No part of this publication may be reproduced, stored in a retrieval system or transmitted in any form or by any means, electronic, mechanical, photocopying, recording or otherwise, without the prior written permission of the publisher, Elsevier Scientific Publishing Company, P.O. Box 330, Amsterdam, The Netherlands.

Submission to this journal of a paper entails the author's irrevocable and exclusive authorization of the publisher to collect any sums or considerations for copying or reproduction payable by third parties (as mentioned in article 17 paragraph 2 of the Dutch Copyright Act of 1912 and in the Royal Decree of June 20, 1974 (S. 351) pursuant to article 16 b of the Dutch Copyright Act of 1912) and/or to act in or out of Court in connection therewith.

Submission of an article for publication implies the transfer of the copyright from the author to the publisher and is also understood to imply that the article is not being considered for publication elsewhere.

Printed in The Netherlands